ABSTRACT

MONTALVO, SOFIA MARGARITA. Statistical and Dynamic Downscaling of Hurricanes Affecting the Southeast US Coast. (Under the direction of committee chair Dr. Lian Xie).

Tropical storm and hurricane landfalls affect the southeast coast more than any other part of the United States. Downscaling techniques need to be improved and focused on the coastal zone. To improve downscaling of hurricanes in the coastal zone, a combined statistical and dynamic technique is developed. First, dynamic downscaling is conducted with the Weather Research and Forecasting model for 12 hurricane seasons with Global Forecast System Final Analysis data and 3 hurricane seasons with Climate Forecast System Reanalysis data. A detection and tracking algorithm is used to find the storms and hurricanes created by the dynamic model. Several bias corrections are conducted to correct the number detected and the intensity of the storms. Next, statistical downscaling is done to choose the correlated climatic predictors for the coastal zone. Lastly, three combined statistical and dynamic downscaling models are formulated using backwards stepwise regression and log-linear regression for total storm, hurricane, and major hurricane numbers. Dynamic downscaling after bias and intensity corrections resulted in 2.733 mean absolute error for total storms numbers, 2.667 mean absolute error for hurricane numbers, and 1.6 mean absolute error for major hurricane numbers. Statistical regression chose several predictors affecting coastal zone frequency. Finally the combined statistical and dynamic downscaling models reduced the mean absolute error by 2.1905 for total storms, 2.1175 for hurricanes, and 0.6476 for major hurricanes. These replicated the observations very well. The combined method for downscaling performed the best and is most skillful in replicating the frequency

in the coastal zone. Improvements to dynamic downscaling and adding more years will add robustness to the models.

Statistical and Dynamic Downscaling of Hurricanes Affecting the Southeast US Coast

by
Sofia Margarita Montalvo

A thesis submitted to the Graduate Faculty of
North Carolina State University
in partial fulfillment of the
requirements for the degree of
Master of Science

Marine, Earth, and Atmospheric Science

Raleigh, North Carolina

2014

APPROVED BY:

_____	_____
Lian Xie, PhD. Committee Chair	Frederick Semazzi, PhD.
_____	
Bin Liu, PhD.	

DEDICATION

To my parents, sisters, and late grandfather.

BIOGRAPHY

Sofia Montalvo was born in the small town of Bradenton on the west coast of Florida. She was the third of four sisters and was encouraged to be herself and study whatever she liked. She loved playing the piano, tennis, and sailing with her father in the Gulf of Mexico and Caribbean, which sparked her interest in weather and climate. She got her undergraduate degree from the University of Miami Rosenstiel School for Marine and Atmospheric Science in meteorology and mathematics. While in Miami, she received the opportunity to be a SCEP intern at the National Hurricane Center. She trained at the Surface Analysis desk, shadowed hurricane specialists, and conducted research on the accuracy of the Automated Microwave Sounding Unit in measuring hurricane wind radii. This sparked her interest in hurricane research and brought her to NCSU for her master's study on downscaling hurricanes that affect the Southeast USA.

ACKNOWLEDGMENTS

I would like to thank my advisor, Dr. Lian Xie, for teaching me so much and supporting me throughout my master's study. I would like to thank Dr. Bin Liu and Dr. Fredrick Semazzi for being on my committee. Also, Dr. Bin Liu thank you for helping me in every aspect of my research. Thank you to NOAA Climate Program Office for funding this research; Coastal Fluid Dynamics Lab group for supporting me in the research process and helping with supplementing the missing aspects; Tim LaRow for supplying us with the Detection and Tracking algorithm integral to the research; Dr. Brian Kirtman for hosting me at UM RSMAS the summer of 2013 and helping me with understanding statistical regression and GrADS; Michael Angus for helping me with writing MATLAB scripts and editing my thesis; Rowan Argent and Allison Michaelis for the support, sanity, chocolate treats, and the editing; Marcela Cordoba for helping me with statistical regression; Dr. Consuelo Arellano for helping me in my initial understanding of statistical bias correction; and James Rohal for keeping me and my pets fed during this process.

TABLE OF CONTENTS

LIST OF TABLES

LIST OF FIGURES

Chapter 1: Introduction

1.1 Motivation

From June 1st to November 30th every year, the US looks to the oceans. This six month period brings hurricanes to the coasts and with it strong winds, large amounts of rain, and storm surge. With climate change becoming a hot topic in today's society and within the scientific community, we are sensitive to the extremes. Landfalling hurricanes pose a great threat to the Southeast US in particular. High population densities on the coast have the risk of loss of life and property during the hurricane season. According to Zandbergen (2009), three states in the southeast US contain the top ten coastal counties with the highest recurrence of hurricane landfalls, the most being in Florida and North Carolina. Florida Office of Economic and Demographic Research Project reported a 27% population growth by 2030, and North Carolina Office of State Budget and Management Project reported a 20% population growth by 2030. Therefore, research focusing on this region is a natural choice.

Tropical cyclones (TC) are warm core low pressure systems that occur in the tropical to sub-tropical oceans with closed cyclonic circulations. Energy for the storm is derived from sensible and latent heat flux from the surface and concentrated in the strong convection of the eyewall (Landsea, et al. 1999). The strongest winds are in the eyewall and decrease radially outward. The maximum wind speed during the lifetime of the storm determines the classification and category the storm falls in. Tropical storms have wind speed of 17m/s to 32m/s, hurricanes have wind speeds of 33 m/s or greater and major hurricanes have wind

speeds of 50m/s or greater. The first two categories of hurricane strength are minor hurricanes, and the last three categories of hurricane strength are major or intense hurricanes.

The Intergovernmental Panel on Climate Change Assessment Report compiled the current research on tropical cyclones, with the 4th Assessment report for 2007 being the most recent. According to this report, on average, 90 tropical cyclones occur globally each year. Currently it is challenging to detect historical trends through lack of observations; consequently there is still worry about possible upward trends in intensity in the future, with more intense storms forming in a warmer climate. With these international worries in mind, there is a need to look at the literature that expands upon the research.

1.2 Climatology

In early research on hurricane climatology, William Gray (1968) studied the tropical storm formation and what environmental aspects affected it. He examined the average time of year when and the latitudes where the most development occurs. For the Northern hemisphere, the time of year for the peak of formation was found to be September and 65% of formation occurs between 10N and 20N. However, there are slight differences for the North Atlantic. To create this climatology, he used data from the early 1900's. He mentions that for the year 1914, 1925 and1930, there were a total of 5 tropical cyclones detected. This might be from the monthly and seasonal variation that he mentions, but may also be a result of the lack of reliable observations before the technological improvements later in the century.

Hurricanes create large amounts of damage for coastal communities at landfall, and it

is a topic of current research that there have been more intense and more frequent hurricanes forming and making landfall in recent decades, consequently, creating more damage in association with climate change. Changes in inflation, coastal population, and property wealth up to the year 1995 (Pielke and Landsea 1998) showed that there was not an increase of hurricane damages for the period 1925-1995. This normalization allows the researchers to see the damages caused by each storm in that 71 year period as if it made landfall in 1995. They found only 21% of those storms were major hurricanes, but they caused 83% of the damages. Another study by Weinkle et al. (2012) focused on the number of minor and major hurricane landfalls for the period 1944-2010 to have the most reliable observations with the start of aircraft reconnaissance. They saw an upward trend in the past several decades (1970-2010), but extending further into the past showed no trend at all in the landfalls. Both these studies debunk the thought that there has been an increase in economic losses, only the increase in coastal populations could result in that. With possibilities of even more people moving to the coasts, future projections are required for the safety of the future citizens.

Pielke and Landsea (1998) and Weinkle et al. (2012) both acknowledged the existence of a multidecadal oscillation. Goldenberg et al. (2001) found that sea surface temperature variation creates the multidecadal oscillation of the North Atlantic Ocean. They found that the years 1953-1970 and 1995-2000 showed the positive phase with more active hurricanes seasons and warmer sea surface temperatures and the years 1971-1994 had less active hurricanes seasons. They also found correlation with US east coast landfalls; 1903-1925 and 1971-1994 did not have many landfalls and yet 1926-1970 and 1995-2000 did see many landfalls. Commenting on the positive phase of the multidecadal oscillation, many

years are expected to be hyperactive, some to be average and few being below average in terms of number of hurricanes. While Goldenberg et al. (2001) looked at a long term history of hurricane activity, Kishtawal et al. (2012) focused on the satellite era (1986-2010). This time has been found by Goldenberg to have more reliable observations than previous years. They found that the North Atlantic sea surface temperatures (SST) have a strong warming rate. However, focusing on this small time frame does not show if this has happened in the past. Going even further into the past and applying more environmental factors, Klotzbach and Gray (2008) found a strong correlation between North Atlantic sea level pressure (SLP) and the further North Atlantic SSTs being multidecadally oscillatory. They found major hurricane numbers to have the greatest variation between the positive and negative phases and that landfalls on the Florida peninsula and the US east coast to be 3 times more frequent in the positive phase. Xie et al. (2002) found, in the years 1887-1999, four modes of oscillation in NATL hurricane activity: interannual, quasi-decadal and two multidecadal modes. Much of the natural variability of tropical cyclones still needs to be understood, including the possibility of relative changes in the next century of hurricane seasons.

1.3 Dynamical Downscaling

Present and future changes in climatology can be further understood through dynamical downscaling. Previous studies discussed above generally use course resolution global models, but to understand the finer scale dynamics of tropical cyclones, higher resolution simulations are needed. Krishnamurti et al. (1989) uses a global spectral model for hurricane prediction tests, and increases the resolution through several tests. The resolution

increases from T21 to T106, and as it gets higher the simulations shows more realistic hurricane data. The finest resolution in the study resolves 35-40m/s winds, which corresponds to category 1 storms, and 975-980mb pressure, approximately indicating category 2 storms. The higher winds speeds and lower central pressures can be resolved in smaller grid spacing models. Using 50km grid spacing with a global model, Zhao et al. (2009) found the general trends and pattern of tropical cyclone frequency. These simulations produce storms no stronger than 50m/s and too many storms with 30m/s peak winds. Sugi et al. (2009) conducted a similar study of tropical cyclone frequency simulation focusing solely on the future. Both studies use changes in SSTs, but Sugi et al. (2009) uses 60km and 20km mesh models. Each of these studies found systematic biases in their simulations. To improve these biases, downscaling these resolutions further to regional models is needed.

Regional model dynamical downscaling seems to be a fairly young tropical cyclone research technique when related to climate change. As stated in Camargo et al. (2007), downscaling to limited area allows increased resolution for a global climate model efficiently. Knutson et al. (1998) uses GFDL (Geophysical Fluid Dynamic Lab) R30 model (2.25 degree x 3.75 degree) to simulate storms and downscaled each to 18 km (1/6 degree) in the high resolution GFDL Hurricane Prediction system. This downscaling creates realistic evolution of tropical cyclone intensity, but still underestimates the strongest storm's wind speed. Camargo et al. (2007) downscaled the ECHAM4.5 atmospheric global climate model with about 2.8 degrees spatial resolution to 50km spatial resolution with the NCEP RSM (Regional Spectral Model) in a one-way nesting method instead of just using the global model and the lateral boundary conditions. Only simulating two seasons, the study does not

produce the frequency very well, but many other aspects of tropical cyclone internal dynamics are simulated well. Feser and von Storch (2008) downscaled NCEP/NCAR Reanalysis to 50km and a double nest to 18km spatial resolution with the domains focusing on Southeast Asia and a small area where case study typhoon Winnie made landfall. This study uses reanalysis data that captured the storm, and used the regional models to further develop it. This allowed the storm to strengthen and deepen similarly to observations. All these studies further improve the ability of the models to simulate tropical cyclone intensity, frequency and inner dynamics.

Recent studies Caron et al. (2011) tested three resolutions downscaling from the one above, 2 degrees, 1 degree and 0.3 degree. The increase of resolution increases the realism of storm numbers. Downscaling of the ERA-40 (40 year ECMWF ReAnalysis) and the 2 and 1 degree model data both became more realistic than keeping it at the courser data, also because the large scale features are kept the same through spectral nudging. However, the intensity is too low in the wind speed only producing category 1 and pressure going to category 3. Xu and Yang (2012) developed a new downscaling method, by improving the global climate model data with bias correction before being downscaled. Many recent studies improve the technology of global models, by raising the resolution for global simulations. Chen et al. (2013) simulated global storm frequency with 25 km spatial resolution, but focused on one region specifically for the coastal community.

Knutson et al. (2010) stated that confidence can be raised by improved downscaling techniques in hindcasting with higher spatial resolutions. With that, they conclude while total tropical cyclone frequency will likely stay the same or decrease, stronger storms will more

likely than not increase. A previous study by Pielke et al. (2005) found a lack of theory for future frequency changes and it was premature to link hurricanes with global warming. However, previously, Henderson-Sellers et al. (1998) stated that there is practical importance for looking into possible future changes. Therefore, while population vulnerability changes will outweigh any changes to the tropical cyclones themselves, improving climate change modeling in order to evaluate what could happen in the future, needs to be advanced for safety reason.

1.3.1 Track and Detection

To determine tropical cyclone activity changes, there first needs to be a way to determine objectively how many storms were simulated by the model. Vitart and Stockdale (2001) created an algorithm to detect and track storms in the simulations, at a 1.865 degree resolution, according to certain criteria. The criteria were determined by tropical cyclone climatology and model resolution. Thresholds were set for local maximum relative vorticity at 850hPa to find the center with the closest minimum sea level pressure, largest average temperature between 500 and 200 hPa levels, and maximum thickness between 1000 to 200 mb. All the thresholds detected need to be within 2 degrees of each other. The detection happens at each time output and the tracks are created by a second algorithm, connecting the snap shots within a distance of 800 km with more than two day track duration. Their model tracked storms with max winds more than 17 m/s at the 850 hPa levels. The minimum intensity cannot be as restrictive as observations because it is a very coarse resolution. Warm core is a necessary threshold to limit the number of non-observation storms detected. TC

frequency is affected by SST drift in the model. Detection is also resolution sensitive.

Camargo and Zebiak (2002) used a detection algorithm based on similar dynamic and thermodynamic criteria thresholds, but these were basin dependent and calculated using statistical properties, i.e. standard deviation. The resolution of their model is 1.235 degrees, and the model bias was taken into account. The criteria was relaxed after the first location detection points. The tracking was based solely on vorticity locations. No tracks created had a curvature, but any storms counted as two were found and combined. While improvements were made for the algorithm, the biases of the results are created through model physics and resolution. This algorithm also used three different temperature anomaly criteria. Each study uses different criteria threshold values, which were determined by model resolution and additional criteria to improve it further.

At 18 km, Knutson et al. (2007) still felt the resolution was too coarse to determine any storms over tropical storm strength. An important point brought up is that hindecasting is downscaling and 'successful downscaling should be a prerequisite for meaningful prediction.' Main Development Region (MDR) formation rate is realistic, but excessive off of the US east coast. Additionally, hurricane rates were too low in the MDR and too high in the north showing a log of spurious storms. Weaker intensities and the basic wind and pressure relationship deficiencies can be seen. It is easier to simulate genesis than landfall as that is dependent on steering and trajectories.

Walsh et al. (2007) compiled all the different criteria thresholds being used in studies (Table 1.1). They tested and adjusted the criteria for different resolutions to test sensitivity. The study found that for limited horizontal resolution wind speed should be lower than the

observed, as the model does not capture the realistic values. Warm core thresholds were found to be important for reducing the number of systems detected based only on the wind speed. The wind speed to resolution relationship is shown to be semi-linear.

LaRow et al. (2008) also conducted a global model resolution study and found that much of the TC frequency issues with the detection algorithm is in the physics more than the resolution. The resolution affects the number of higher intensity storms that are simulated. Also some spurious storms can be caused by polar lows that satisfy criteria, including the warm core.

1.3.2 Intensity

Hurricane intensity is affected by many different factors. Emanuel (1987) tested the changes in thermodynamic efficiency and relative humidity and their effect on intensity. Model resolution was very coarse. Intensity is measured by maximum wind speed and lowest central sea level pressure, and these measures are related by the square root. Tropical cyclone wind increases with SST increase, and Emanuel measured a significant pressure drop. Emanuel (1987) expects the average intensity to increase with the maximum intensity increase. Knutson et al. (1998) found more cases of high wind speed in the higher CO2 environment. Knutson and Tuleya (1999) focused on the NW Pacific, where the warming appeared to increase the radial extent of the hurricane force winds.

Tropical cyclone intensity and climate change studies tend to focus of the frequency changes of the most intense storms compared to the general frequency. Oouchi et al. (2006) found that global frequency decreased, but the north Atlantic TC frequency increases with

the intensity, as wind speed increases by 8.7m/s. Hoyos et al. (2006) found that the higher number of the most intense storms is related to the modeled reduction of the vertical wind shear. Bengtsson et al. (1996) found a reduction of overall strength of the most intense storms, and also a relationship between coarser model resolution and the fewer number storms simulated. In a follow up study, Bengtsson et al. (2007) expanded this relationship with a study that increased model resolution. They found a significant increase in intensity with this increase. They still found an overall frequency reduction with reduced tropical circulation and increase in water vapor, and did not find any significant change in overall intensity. The number of the intense storms did, however, increase.

1.4 Statistical Modeling

Another tool to understand tropical cyclones is statistical modeling. Elsner and Villarini (2011) explains that a statistical model is used to find the average behavior of a group, to quantify the regularity and assign uncertainty. This study is a starter kit for tropical cyclone activity statistical modeling. Poisson regression is commonly used to estimate rate of hurricane activity, and log-linear regression is used to estimate counts of hurricanes. Choosing predictors should reduce the bias of the model while not sacrificing the variance too much. Elsner and Villarini (2011) also importantly explain that stepwise regression is not a model but a procedure to select a model, and highly cross correlated predictors should only be both kept if the literature proves they are both important to predicting tropical cyclone activity.

Elsner et al. (2008) uses a log-linear regression to find trends in TC activity and

intensity frequency during the satellite era, approximately 1970 to today. The model uses the lifetime of maximum wind speeds as the response variables and estimates the trends with quantile regression. It found an upward trend of the strongest storms. Villarini et al. (2010) uses Poisson-linear regression to model TC counts. The study states there is no overall best statistical model. This study tested SST, North Atlantic Oscillation (NAO), and Southern Oscillation Index (SOI) as predictors in the model, and to avoid overfitting, stepwise selection is used, which removed NAO. Gray et al. (1992) used a least absolute deviation regression model to conduct a seasonal prediction of TC numbers using upper level wind (QBO) and Sahel rainfall as predictors. This seasonal prediction is conducted 6-11 months before season, while most seasonal predictions are done 2-4 months before season starts. Gombos and Hoffman et al. (2012) uses an ensemble of multivariate statistical models, not for tropical cyclone counts, but to understand the dynamics of the environment. They predict 500hPa geopotential height using 1000hPa potential vorticity.

1.4.1 Climate indices affecting track and number

Statistical models use other variables related to the variable trying to be predicted. These variables are known as predictors. The predictors are generally from climatology factors. El Niño-Southern Oscillation (ENSO) has been observed to affect the recurrence rate of hurricanes on the southeast United States coast (Muller and Stone 2001). Bengtsson et al. (2006) found that future storm changes may be affected by a general El Nino-like warm Pacific sea surface temperature. Warming of the SST in the Pacific increases the vertical wind shear over the North Atlantic by changing the atmospheric circulation. Wang and Lee

(2008) found this caused a reduction in TC activity and intensity in the MDR of the North Atlantic. The geographic location of tracks also changed similar to an El Nino event. Another climate predictor is discussed by Wang et al. (2011). The Atlantic warm pool affects landfalls, genesis locations, and the location of the North Atlantic Subtropical High. Changes in these factors affect the likelihood of TC entering the coastal zone. Gray et al. (1992) tested two predictors, Quasi-biennial Oscillation (QBO) and West African Rainfall. QBO when in the westerly mode allows for more intense storms. The wet phases of the West African Rainfall also allows for more intense and active seasons. Villarini et al. (2011) conducted a study comparing a statistical model and a dynamical models, and found that using both Atlantic SST and global tropical SSTs as predictors allows the two types of models to agree fairly well. There are many more predictors one can use, including factors directly related to tropical cyclone climatology and output from dynamical models.

1.5 Statistical-Dynamical Downscaling

Multiple linear regression is often used to adjust model data with model output variables as predictors, creating Model Output Statistics (MOS). Ghosh (2007) explains the value of multiple linear regression and describes different statistical methods, and how to evaluate them. Here Ghosh includes stepwise regression as a regression model evaluation tool. The evaluation tools are for variable selection, which also include hypothesis testing, cross validation, coefficient of determination R^2, C_p, and information criteria. MOS is just another way of thinking of hybrid statistical and dynamical downscaling. Hybrid downscaling is being developed by many people for tropical cyclone modeling, predictions,

and projections.

To improve Western North Pacific tropical cyclone activity dynamical forecasts, Li et al. (2013) creates a dynamical-statistical forecast model. The model is based on 30 years of observations and uses variables from the Climate Forecast System Version 2 (CFSv2) dynamical forecast as predictors. This uses "leave one out cross validation" and mean square skill score. The best predictor combinations for this study are 500 mb height, North Atlantic SSTs and West Pacific vertical wind shear, West Pacific vertical wind shear and 500 mb height, and 850 mb zonal wind and 500 mb height, in four linear models. Lee (2011) uses a hybrid model to improve seasonal forecast of tropical cyclones for a small region, focusing on Hong Kong. El Nino/Southern Oscillation is a predictor in a Poisson regression. LaRow et al. (2013), for CLIVAR program, is developing a hybrid model that uses interannual variability of tropical cyclones, SST and vertical wind shear from CFS model hindcasts. The findings and implications show that the hybrid was found to be more skillful in seasonal forecasts than just statistical models. Knutson et al. (2010) hopes for higher resolution models combined with statistical models in order to improve and develop results, therefore giving confidence in future projections. New techniques for downscaling using hybrid models will help avoid the intensity simulation limitations of dynamical models and downscaling.

Four different types of downscaling for both dynamical and statistical models are described in Castro et al. (2005). However, the statistical downscaling that the article describes is a combination between dynamical and statistical for each type. The uncertainty

grows with each type: (1) regression using observations and dynamical downscaling of limited area and short term hindcast using observations as initial conditions; (2) regression using observations and dynamical downscaling using regional climate model simulation based on global model lateral boundary conditions; (3) regression using seasonal predictions; and (4) regression based on future global climate prediction based on the empirical relationships of the present climate not changing. This thesis hopes to develop type 2 statistical downscaling in order to be able to use it with confidence for type 4 in future work.

1.6 Hypothesis

The main research questions this thesis aims to answer are as follows. Does the model simulate the observed past climate hurricane frequency and intensity well? What combination of predictors will create the most accurate statistical regression model to get the correct frequency and intensity for past climate? Will this allow us to have confidence in the model to simulate hurricanes for a future climate? Using Scale Selective Data Assimilation and a combined statistical and dynamical regression model, the tropical cyclone frequency and intensity produced by the model for the coastal zone are a skillful match to observations. This allows for confidence in the model to simulate future climate hurricanes affecting the Southeast United States.

1.7 Thesis outline

This thesis is broken down into 4 parts. In chapter 2, the preliminary methods are presented. Chapter 3 has the dynamical downscaling results and the error fixes pertaining to

it. Chapter 4 presents the statistical downscaling with dynamical input. Last the conclusions and future work are presented in Chapter 5.

Table 1.1 Table 1 from Walsh et al. (2006). Listing many criteria used in resolution dependent cyclone detection studies

TABLE 1. Minimum threshold detection criteria for tropical cyclones employed by modeling studies. Here, "V" refers to wind speed and "T" to temperature anomaly vs the surrounding environment, at the pressure levels (hPa).

Study	Model horizontal resolution (km)	Wind speed ($m\ s^{-1}$)	Vorticity (s^{-1})	Warm core temperature anomaly (K)	Structure or location	Duration (days)
Bengtsson et al. (1982)	~200	25 at 850 hPa	7×10^{-5} at 850 hPa	—	<30° latitude	—
Broccoli and Manabe (1990)	~300 (R30)	17 at surface	—	—	<30° latitude	—
Haarsma et al. (1993)	~300	—	3.5×10^{-5} at 850 hPa	T250 > 0.5 T500 > −0.5 T250 − T850 > −1	—	3
Bengtsson et al. (1995)	~125 (T106)	15	3.5×10^{-5} at 850 hPa	T700 + T500 + T300 > 3	T300 > T850 V850 > V300	1.5
Tsutsui and Kasahara (1996)	~300 (T42)	$V900 > 17.2$	Cyclonic at 900 hPa	Thickness criterion	V200 < 10	2
Walsh and Watterson (1997)	125	6 and 10 at 10 m (area average)	2.0×10^{-5} at 850 hPa	T700 + T500 + T300 > 0	T300 > T850 V850 > V300	2
Krishnamurti et al. (1998)	~300 (T42)	15 at 850 hPa	3.5×10^{-5} at 850 hPa	T700 + T500 + T300 > 3	V850 > V300	1
Vitart et al. (1997)	~300 (T42)	17	3.5×10^{-5} at 850 hPa	$T_{200-500} > 0.5$ Thickness criterion	—	2
Vitart et al. (1999)	~300 (T42)	17	3.5×10^{-5} at 850 hPa	$T_{200-500} > 0.5$ Thickness criterion	—	2
Walsh and Katzfey (2000)	125	5 at 10 m (area average)	1×10^{-5} at 850 hPa	T700 + T500 + T300 > 0	T300 > T850 V850 > V300	1
Vitart and Anderson (2001)	~300 (T42)	17	3.5×10^{-5} at 850 hPa	$T_{200-500} > 0.5$ Thickness criterion	—	2
Nguyen and Walsh (2001)	125	5 at 10 m (area average)	1×10^{-5} at 850 hPa	T700 + T500 + T300 > 0	T300 > T850 V850 > V300	1
Sugi et al. (2002)	~125 (T106)	15 at 850 hPa	3.5×10^{-5} at 850 hPa	Mean of (T850 + T700 + T500 + T300) > 3	V850 > V300	2
Tsutsui (2002)	~300 (T42)	—	—	Thickness condition between 200 and 700 hPa	<40° latitude	—
Camargo and Zebiak (2002)	~300 (T42)	Basin dependent	Basin dependent			
Walsh et al. (2004)	30	17 at 10 m	1×10^{-5} at 850 hPa	T700 + T500 + T300 > 0	T300 > T850 V850 > V300	1
McDonald et al. (2005)	~300 and ~120	—	5×10^{-5} at 850 hPa	—	<30° latitude	—
Oouchi et al. (2006)	~20	17 at 850 hPa	3.5×10^{-5} at 850 hPa	T700 + T500 + T300 > 1.5	V300−V850 <3 ms^{-1} or <35° latitude	1.5

Chapter 2: Description of Model and Data

2.1 Model setup

To complete the objectives of this thesis, a dynamical model is used for the preliminary simulations. We use the Weather Research and Forecasting Model (WRF) version 3.2 with the Advanced Research WRF (ARW) core. The WRF model is a nonhydrostatic, fully compressible atmospheric model. It consists of a core of equations for prediction in Euler Flux form, using the Runge-Kutta integration scheme (Skamarock et al 2008).

The domain covers the entire Southeast United States, from Mexico to central North Atlantic Ocean including the Gulf of Mexico and Caribbean Sea, 100˚W to 60˚W and 8˚N to 48˚N (Fig. 2.1). To have realistic simulations at relatively coarse resolutions, parameters representing processes not resolved by the model need to be set. The parameters are set in the input namelist of WRF, which call schemes that solve equations for the physical processes. The main physical processes that require parameters are microphysics, convection, surface layer, land surface, planetary boundary layer (PBL), short wave and long wave radiation. Microphysics schemes resolve water vapor, cloud and precipitation processes as an adjustment process. Convection or cumulus schemes represent vertical fluxes: from unresolved up and down drafts to compensating motion outside the cloud. The surface layer scheme calculates the friction velocities and exchange coefficients and enables calculations in the land surface model and planetary boundary layer scheme. The land surface model

(LSM) uses information from all the other schemes and provides heat and moisture fluxes as a lower bound condition for the vertical transport in the PBL scheme. The PBL scheme provides vertical sub grid scale fluxes from eddy transports and mixing, along with the temperature and moisture momentum over the column. The atmospheric radiation provides atmospheric heating due to radiative fluxes and surface longwave and shortwave radiation for the ground heat budget. A preliminary sensitivity study is conducted to optimize the parameter choices to best represent the domain. The physics parameters chosen are as follows. WRF Single-Moment 5 (WSM-5) Microphysics scheme adds mixed phase processes and super cooled water. The Kain-Fritsch (KF) Cumulus/Convective Scheme has deep and shallow convection from the subgrid scales using flux approach with downdrafts. The Unified Noah (NCEP/NCAR/AFWA) Land Surface Model has soil temperature and moisture in four layers, fractional snow cover, and frozen soil physics. A Surface Layer scheme associated with Unified Noah LSM is used. The Yonsei University (YSU) Planetary Boundary Layer Scheme uses a nonlocal K scheme with explicit entrainment layer and parabolic K profiles in the unstable mixed layer. The Community Atmospheric Model V. 5 (CAM) Atmospheric Shortwave and Longwave Radiation schemes allow for aerosols and trace gases and use yearly carbon dioxide and constant N_2O and CH_4.

A preliminary sensitivity study for resolution effect on hurricane structure and computational efficiency was conducted. The resolutions tested were 108 km, 36 km, 12 km and 4 km grid spacing. Five days, with hurricane Wilma in the Gulf of Mexico 2005, are simulated using each spacing. Using NCAR Computing Language (NCL), images of the 500

hPa absolute vorticity, 10m winds, sea level pressure and total precipitation were created. With the 108 km grid spacing, the hurricane has a very symmetric basic structure with a minimum sea level pressure (MSLP) of 996 hPa (Fig. 2.2). The 36 km grid spacing shows more asymmetrical structure and a MSLP of 977 hPa, but the vorticity is still symmetrical to the center of the storm. (Fig. 2.2). The 12 km shows much more asymmetric structure with the rainbands spiraling off with vorticity spikes and a MSLP of about 968 hPa (Fig. 2.2). The 4 km grid spacing (Fig. 2.2) shows many more small details in the rainbands of vorticity, but takes more computational power and time to efficiently finish a 6 month hurricane season simulation. The 12 km spacing is found to be the optimal resolution, showing a detailed hurricane, while not being computationally expensive, covering 379x316 grid boxes. Another interesting feature to note in these simulations is the precipitation over southeast Florida. The 108km has precipitation over the entire SE quadrant of the FL peninsula, while 36km has more detail for coastal rainfall. In the higher resolution, the 12km precipitation is confined to the coast and extends down to the FL Keys, but 4km precipitation is confined to a very small area near the central east coast of FL (Figs. 2.3).

2.1.1 Data Description

The National Centers for Environmental Prediction (NCEP) Global Forecasting System (GFS) 6 hourly final analysis data was used as the base global data to downscale. GFS data is in GRIB or Gridded Binary format (WMO GRIB1) and covers the entire globe, 0 E to 359 E and 90 S to 90 N, with 1 degree by 1 degree horizontal grid spacing. The final analysis data is created 6 hours after the original GFS forecast with the addition of in situ

observations. The vertical levels covered are the surface and 26 pressure levels from 1000 mb to 10 mb or sigma levels 0-30. It includes the surface boundary layer and tropopause. The variables available are surface pressure, sea level pressure, geopotential height, temperature, sea surface temperature, soil values, ice cover, relative humidity, zonal wind, meridional wind, vertical wind, vorticity, and ozone. The data for June 1 to December 2, 2001 to 2012 was downloaded from the Computational and Information Systems Laboratory Research Data Archive (CISL RDA), managed by the Data Support Section (DSS) of the National Center for Atmospheric Research (NCAR).

GFS 6 hourly Final analysis data is only archived since July 1999. To extend the simulation data for statistical significance, NCEP Climate Forecast System Reanalysis (CFSR) data is used for the initial and boundary conditions of the model. The archive has data for 33 years starting with 1979. CFSR uses observational data and the same atmospheric model as GFS to create the data, but it also includes coupled ocean-land model and surface-sea ice system (Saha et al. 2010).

CFSR data comes as two separate GRIB2 files to run WRF, 6-hourly 3D pressure data and surface flux data, in the data archive (rda.ucar.edu, Saha et al. 2010). The 3D pressure data has half degree resolution, containing pressure, relative humidity, temperature, geopotential height, u-component wind, and v-component wind, all at 38 pressure levels. The surface flux data has 0.3 degree resolution, containing pressure, specific humidity, temperature, geopotential height, ice cover, land cover, u-component of wind, v-component wind, volumetric soil moisture content, and water equivalent of accumulated snow depth.

WPS ungrib has to be run twice for this data. These data are archived with analysis and 00-06 and 09 forecast hour data. In this study, 06 forecast hour CFSR data is used for the years 1998, 1999, and 2000. This may cause an error, as analysis data was meant to be used, to be consistent with the GFS analysis data. The comparison between the 6 hour forecast data and the analysis data is forthcoming, as is the comparison with the GFS data. Season long simulations should not be affected by the data-type difference, but a shorter time simulation may.

2.1.2 Scale Selective Data Assimilation Configuration

The basic set up of WRF applies the global data for the initial and boundary conditions, nudging the large and small scale dynamics to the global scale data. The Scale Selective Data Assimilation (SSDA) technique, originally applied by Peng et al. 2010, modifies WRF to improve regional climate modeling and does not include the unnecessary, unphysical nudging terms. SSDA is optimized to develop the small scale flows, important tropical cyclones, in the regional model, where they can be resolved.

This SSDA procedure was developed by the Coastal Fluid Dynamics Lab at North Carolina State University. The SSDA method uses a low pass filter on the global data to extract the large scale components, and a low pass filter on the regional model to separate large and small scale components. Three dimensional variational (3DVAR) data assimilation of the large scale components from the global data into the regional model correct the large scale circulation, and finally the small components from the regional model are combined with the large components from the global data in the model to obtain full scale circulation.

These steps can be visualized with figure 2.4. Integration is continued in the regional model until the next SSDA cycle, restarting every 2 simulation days (Peng et al. 2010, Xie et al. 2010).

The confidence in the benefits of using SSDA procedure over the basic configuration of WRF, referred to as control, has been built up over four studies. The first study found the control had large errors in the upper level winds which represent the large scale steering flows that affect tropical cyclone tracks. The global resolution data resolves these winds, and the SSDA runs match the upper level patterns in the global data, with the scale selection process (Peng et al. 2010). Xie et al. 2010 used SSDA to improve tropical cyclone track simulations compared to WRF, and found having the large scale flows correct improved the tropical cyclone tracks. The control's track error increased with simulation hours, whereas the SSDA error was much less. The third study tested real time forecasting to see if SSDA improved TC track and intensity forecasts. Liu and Xie 2012 found SSDA reduced the control track error by 40%. The SSDA improved long term intensity forecast was correlated to the improved track forecast, showing that the control missed the intensity development pattern of their case study. SSDA getting the environmental features simulated correctly is instrumental in these tropical cyclone forecast improvements. Lastly, Costa 2012 dedicated a thesis chapter to build confidence in SSDA's ability to simulate high wind events. In this study, SSDA improved the wind speed error by 4 m/s and matched the observations better. These findings show that SSDA gives the best simulation of tropical cyclone tracks and intensity.

SSDA configuration of WRF is used to simulate the hurricane seasons of 2001 to 2012 using GFS data and 1998 to 2000 using CFSR data. The simulation output netCDF files are put through ARWpost (post processing system), which concatenates all the data into a useful Grid Analysis and Display System (GrADS) format. This format has a binary data file and a control file that describes the data file. The control file lists the latitudes and longitudes that the data covers, the number of time steps in the data, the vertical levels required, and the number and names of the variables needed. The two CFSR data files useful for this research have geopotential height, temperature, zonal and meridional rotated winds, all at 850, 700, 600, 500, 400, 300, 200 hPa vertical pressure levels, sea level pressure, zonal and meridional winds at 10 meter height, and relative vorticity at the 850 hPa vertical level. Vorticity is calculated with a GrADS script by taking the curl of the zonal and meridional rotated winds (hcurl(umet,vmet)) at the 850 hPa pressure level. GrADS is also used to display the data to view the vortices developed by the model in the domain for the two configurations, including filled and lined contours of wind, wind barbs, 850 hPa vorticity, sea level pressure contours, and 500-200 hPa temperature.

2.2 Detection Algorithm

To determine the number of storms the model created for each past season, a detection algorithm was required. The detection algorithm came from and is described by LaRow et al. (2008), a study on seasonal hurricane simulations for the entire Atlantic Basin. Modifications were needed for it to be compatible with the domain size and model resolution used in this study. The algorithm uses certain criteria to identify hurricanes and tropical

storms in the seasonal simulation data. The criteria chosen to detect the storms were 850 hPa maximum vorticity, maximum warm core temperature anomaly, maximum thickness of warm core between 500 and 200 hPa, limited degree separation of the location of mean sea level pressure from maximum vorticity, and limited degree separation of the location of warm core from the center. The algorithm detects all the vortices in each 6 hour time step. The temperature must decrease by 6 degrees Celcius (˚C) in all directions away from the center of the storm within a distance of 4 degrees (LaRow et al. 2008), and the minimum sea level pressure must be within 2˚ radius of the maximum vorticity. The values of the criteria chosen originally were $2.4x10^{-4}$ s^{-1}, 1.6 K, 30 km, 4˚ from vorticity maxima, and 4˚ from determined center of storm respectively. These values were chosen based on Knutson et al. (2007) because of a similar model resolution of 18 km. These criteria values were preliminary and only analyzed with one year of simulation, 2005, the most active year. The expanded criteria testing will be discussed in the subsequent chapter.

The second step of the algorithm is the tracking scheme. This connects the vorticies into a trajectory for storms that last more than 2 days with the winds 17 m/s or more and with locations within an 8˚ radius from the previous location. The tracking scheme also applies the intensity category for the particular trajectories based on the Saffir-Simpson scale, allowing for good comparison with observed numbers from HURDAT (Table 2.1). After these steps were completed, track location files were created. These track location files were combined into one map for the year in pdf format using the NCL Create_Track script. These are then easy to visually compare with the Best Track maps from the National Hurricane Center (nhc.noaa.gov/data/). Colleague and committee member Dr. Bin Liu followed the same

procedure for the 36 km resolution model that covers the entire Atlantic basin. This was done for a sensitivity study of the storm detection algorithm to model resolution.

2.2.1 Global and regional detection

To thoroughly test the detection algorithm, its sensitivity to model resolution needs to be determined. The test resolutions are 12 km, 36 km and global 1˚ by 1˚ grid spacings. The 12km grid spacing preliminary tracks being created are described previously. The 36km grid spacing tracks for the entire ocean needed to be counted again for the smaller regional domain to be comparable. Tracks for the global resolution are created using GFS FNL data slightly modified into WRF observation input data. This input data from GFS is then put through the ARWpost process for comparable data files. The data is displayed to aid in determining the correct global resolution criteria for vortex detection. Walsh et al. (2007) compiled a table of all the criteria used by most of the tropical cyclone detection research articles, which was useful to compare the criteria used by global models (Table 1.1). The global resolution post processed data is then put through the detection and tracking algorithms. With the tracks and frequencies compiled, we could then determine the sensitivity, which will be discussed in the subsequent chapter.

Table 2.1 Observed storm counts for each category in the domain from HURDAT Best Track data

Best Track Obs	2001	2002	2003	2004	2005	2006	2007	2008	2009	2010	total
total storm	10	9	7	9	16	4	8	10	3	12	88
TropStorm	6	6	5	3	6	3	4	4	1	5	43
total H	4	3	2	6	10	1	4	6	2	7	45
total mH	2	1	1	1	4	1	2	3	1	5	21
Cat1	1	0	1	1	4	1	2	2		3	15
Cat2	1	1	0	0	0	0	0	1	1	2	6
total MH	2	2	1	5	6	0	2	3	1	2	24
Cat3	0	1	0	2	1	0	0	0	1	1	6
Cat4	2	1	0	2	1	0	0	3	0	1	10
Cat5	0	0	1	1	4	0	2	0	0	0	8

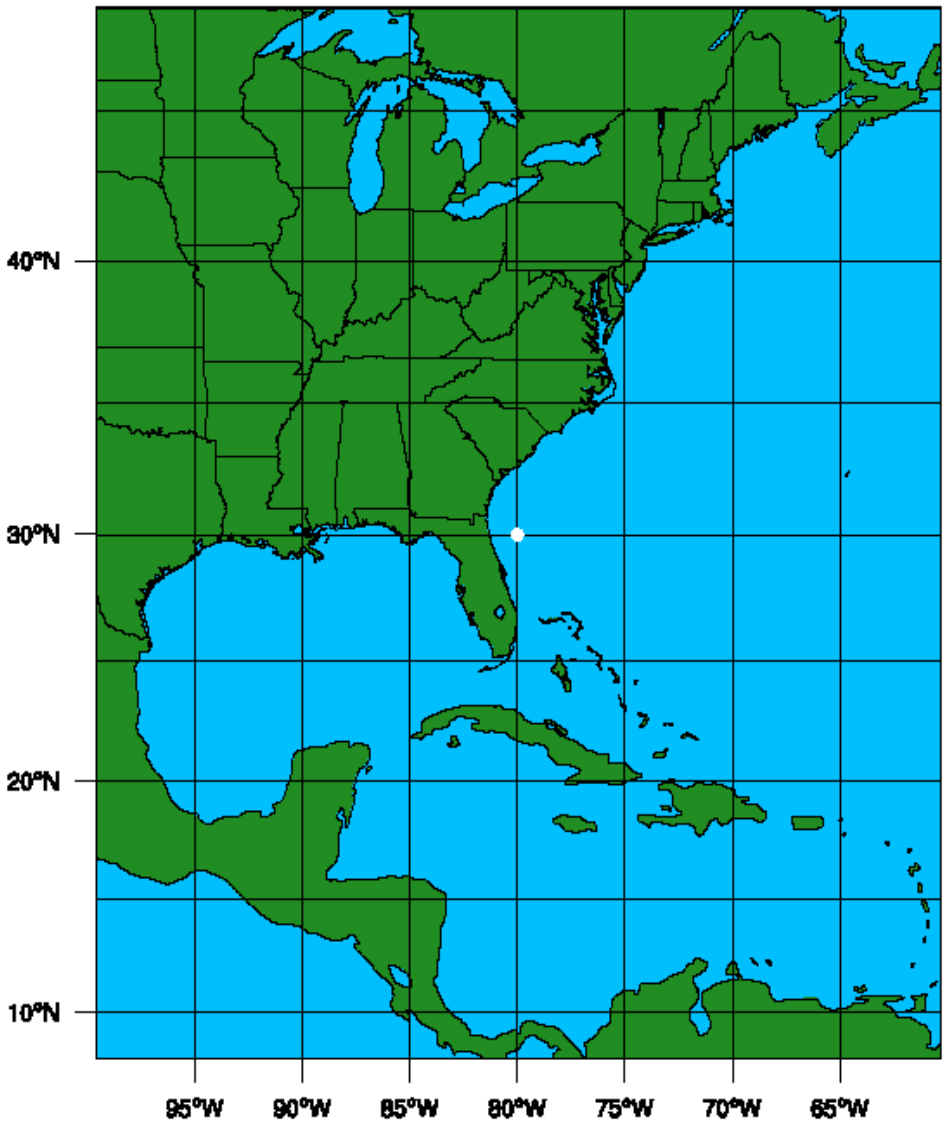

Figure 2.1 Domain extent

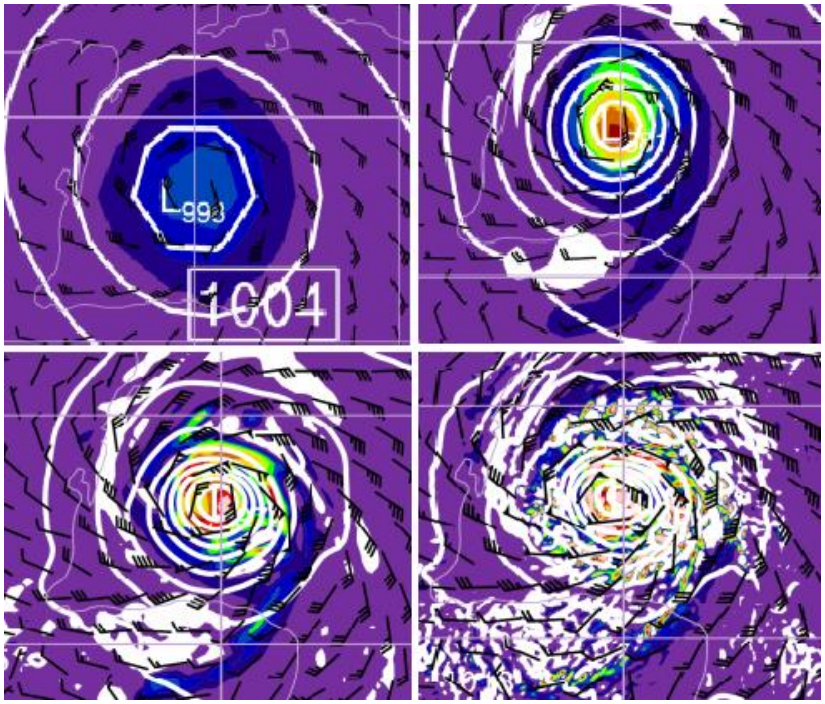

Figure 2.2 Wilma 2005 case study; top left panel with 108 km grid spacing, MSLP is 998 hPa and maximum wind is 45 kts; top right panel with 36 km grid spacing, MSLP is 981 mb and maximum wind is 70 kts; bottom left penel with 12 km grid spacing, MSLP is 972 mb and maximum wind speed is 75 kts; bottom right panel with 4 km grid spacing, MSLP is 968 mb and maximum wind speed is 85 kts.

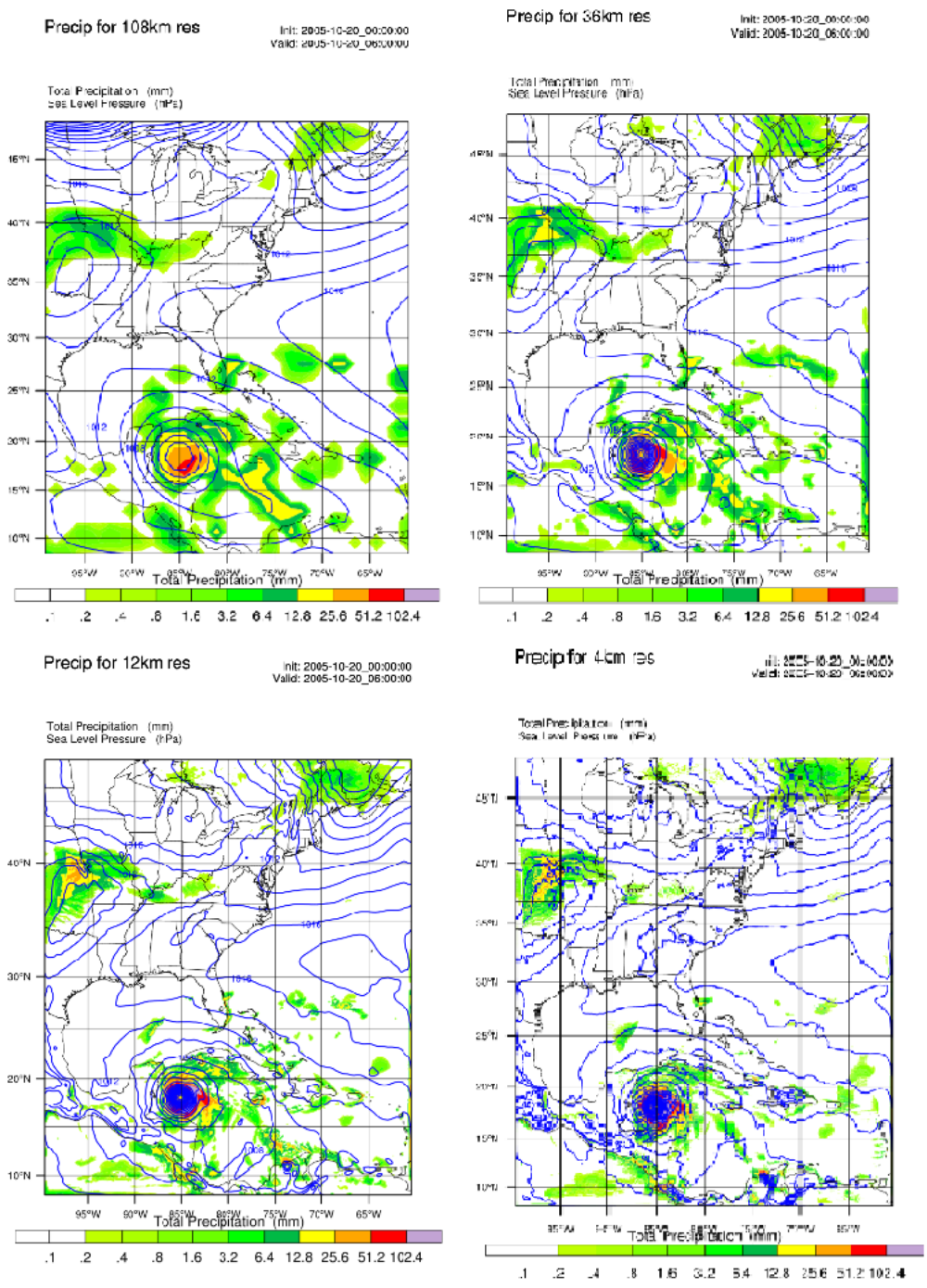

Figure 2.3 Precipitation resolved at 108 km grid spacing, at 36 km grid spacing, at 12 km grid spacing, and at 4 km grid spacing

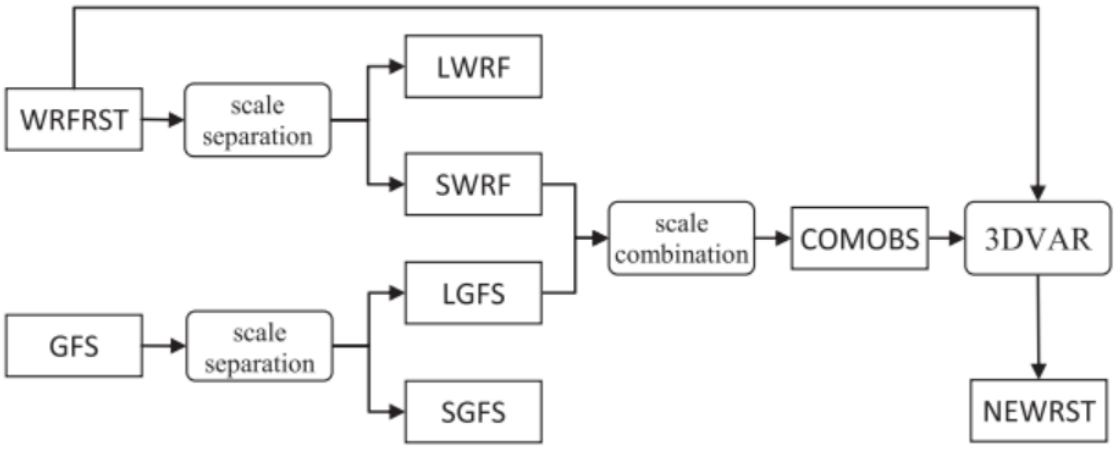

FIG. 1. Procedures of an SSDA cycle.

Figure 2.4 SSDA cycle from Liu and Xie (2012)

Chapter 3: Results from Dynamical Downscaling

3.1 Original Set

3.1.1 First simulation results SSDA

As stated in Chapter 2, a detection and tracking algorithm takes the post-processed simulation data to find storms that fit the set criteria thresholds. This was done for the Scale Selective data assimilation (SSDA) run data. This first set of criteria is only optimized for 2001 and an over active 2005 seasons. The number of storms detected and tracked for each year in the SSDA run are 10, 9, 9, 10, 23, 12, 12, 15, 6, and 22, for the year 2001-2012 respectively. For the extra 5 years of simulation, the first detection created 8, 18, 6, 16, and 12 storms for 1998-2000 and 2011-12 respectively (Fig. 3.1). The numbers for all 15 years detected total storms, hurricanes and major hurricanes and for each category are in table 3.1.

The mean absolute error (MAE) of the 15 years of data is to 4.4 for total number of storms detected. For hurricanes (Fig. 3.2), the MAE for the 15 years is 4.667. For major hurricanes (Fig. 3.3), the MAE is 1.733 for the 15 years. The SSDA storm numbers follow the general trend of the observations, except for the large reduction in storm number of 2006. The SSDA total storms and hurricanes have more spread from the means than the observations. The major hurricane spread is much less than the observed number. Standard deviation of the detected number of storms is more than the standard deviation of the observations by 2.02. Hurricane standard deviation of detection is more than observations by 3.16. Major hurricane standard deviation of detection is less than the observations 0.46. The

actual values of the standard deviations and MAE are in table 3.2.

3.1.2 Tracks and Landfall risk

Track maps were created for this set of detected storms. The SSDA storms, looking at timing and location, seem very spurious. With these tracking maps, the landfall rate can be determined. This is important for the coastal zone and consequently the simulation of risk. The storms that come within 2 degrees of the coast are counted for that region and state. Also, the locations of the storms are determined for different parts of the basin, the Caribbean, Gulf of Mexico and the NW Atlantic. They are counted for that region if the storm passes through. The results are shown in table 3.3. Figures 3.4.1-15 show the track locations detected for each year.

When considering the results and the landfall risk of this data set, there appears to be significant error. These tracks do not match well with the observations. Despite long lived storms being represented well, the landfall risks for hurricane and major hurricane strength is not represented well at all.

3.2 Sensitivity of the Detection Algorithm to resolution

3.2.1 Global detection

To further test the accuracy of the detection algorithm, the sensitivity to model resolution needs to be determined. This sensitivity study was only conducted for the original 10 years of simulations. The resolutions to test are global 1 degree by 1 degree, 36 km, and 12km. The

36 km detection numbers are from a basin wide simulation conducted with SSDA technique by colleague Dr. Bin Liu. The global resolution data is the GFS reanalysis data. Some processing of the GFS data is done to have it in the correct format to be detected. The data is put through WRF preprocessing system and then converted to WRF input data from observation files with WRF real. The end results are then put through ARWpost to concatenate the correct data for detection. The detection and tracking algorithm are then applied as before. The criteria values are changed as the original 12km criteria thresholds are not fully resolved in the global data. The criteria used are 0.5 K warm core temperature anomaly, 10 m maximum thickness, $1*10^{-5}s^{-1}$ 850 hPa relative vorticity, within 8 degrees of the center, 10m/s wind speed and 48 duration.

3.2.2 Comparing to observations

The global detection produced too few storm numbers for each year meeting all the criteria. The duration is the most problematic since GFS reanalysis should have the initial storm location. The majority of the storms in the global data more than likely lasts less than 2 days and therefore no longer fit the criteria specified. The mean absolute error is 4.2 storms. The global hurricane numbers are very low with zero for 3 years. The global runs cannot spin up the storms enough to make the storms hurricanes. The mean absolute error for global hurricane numbers is 3.3.

The 36 km detection algorithm is optimized for all 10 years for the entire basin for every year. To see the storm numbers for only the coastal domain, the track maps are used for the new count. The storm subset is fairly accurate for all seasons for both storm numbers

and hurricane numbers for SSDA, with MAE's no greater than 2.1 (Table 3.4).

3.2.3 Resolution comparison

A yearly performance comparison results are as follows. The 12km SSDA gave better results than the 36km SSDA over 5 years only for tropical storm numbers (Fig. 3.5.1). For hurricane numbers (Fig. 3.5.2), 36 km SSDA has better counts for every year when compared to the 12km counts. The GFS storm counts tie with 12km SSDA for 2 years, improves for 5 years and does worse for 5 years. For hurricane counts, while the GFS is close to zero for most of the counts, it does better than the 12 km SSDA for 8 years, ties for 1 and worse for 1.

While the yearly comparison produces interesting results, the sensitivity study should only be considered with respect to overall error. Compared to the storms detected from the GFS data, the original detection of the 12km SSDA data performs similarly. Compared to the 36km downscaled data detected storm in the smaller region does best, the 12 km downscaled data actually does slightly worse, and for hurricane numbers, much worse. The errors is shown in Table 3.4.

The sensitivity study was predicted to show that GFS has the fewest storms and hurricanes and does the worst, the 36 km improves the GFS counts, and the 12 km counts are the best. The last expectation did not occur, and the hurricane numbers are far from the observations. These errors for 12km SSDA show many things need to be improved. The detection algorithm for the small resolution needs to be optimized to all the years to decrease the error. Also, a bias correction will correct the distribution of intensity counts, since SSDA 12km seems to spin up too many tropical storms to hurricane strength and yet has too few

major hurricanes.

3.3 Sensitivity to criteria for detection

3.3.1 Methods

The problems with the SSDA data and the sensitivity study can be fixed with changing criteria thresholds to detect the number of storms closer to the observed amount. The criteria to test are 850 hPa relative vorticity maxima and the tracked wind speed as storms are found to be most sensitive to these criteria. 22 vorticity values and 15 wind speed thresholds are tested, from 1.6 to 7 x10-4 s-1 and 13-27 m/s respectively. At first only 10 values of each are tested. The MAE and standard deviation (STDEV) are calculated. The MAE contour is shown in figure 3.6.1, and STDEV in contour shown in figure 3.7.1 and 2. The criteria testing is done with only the original 10 years of simulation data.

3.3.1.1 Most sensitive criteria: lowest error to observations

The most noticeable feature in the contour plots is the nearly linear decrease with increasing wind speed. The vorticity effect on error is much less pronounced. While the wind speed has the greatest effect, the highest wind speed and the highest vorticity, the top corner of the MAE figure, has the lowest error. The test values are extended following the lowest value until the error starts increasing again.

The values of criteria increase until a string of combinations are all the same error along the majority of the vorticity values and two wind speeds (Fig. 3.6.2). The lowest error

compared to the observations is chosen out of one of the wind speed and vorticity. The wind speed and vorticity chosen for the least error to observation (LEOB) is 3.6*10-4 s-1 and 25 m/s. This new set of criteria shows that this wind speed is very high and rules out many tropical storms. The error reduces to 2.3, for the total number of storms. The error for only tropical storm strength number increased from 3 to 4.2, but all the other error for hurricane numbers decreased (Table 3.5).

3.3.2 Model bias and recount

The error of the original detection may be caused by bias within the model. Using GrADs, the wind vector and magnitude, sea level pressure, warm core level temperature, and vorticity are displayed over the entire season for every year with the SSDA data. The images are used for an intellectual detection or manual count of the storms created by the model. The initial storm location needs to be south of 30N. The vorticity must exceed 2.4*10-4 s-1. The temperature must be greater than the environment. Lastly the wind speed must exceed 17 m/s. This intellectual detection is only done for total storm numbers. The manual count produces 11, 10, 9, 10, 23, 12, 12, 15, 6 and 22 for the 10 years.

3.3.2.1 New sets

The criteria tested numbers are then compare to this new set of numbers and a new low error point is chosen (Fig. 3.8.1 and 3.8.2). The error is slightly more random in the contour plot for the original 100 criteria combinations. The chosen criteria with the lowest error to the new set of counts are 2.6*10-4 s-1 and 17 m/s, to set the correct tropical storm

wind speed threshold. The error to observation is the same as the original criteria, but the error to the manual count is 1.2. MAE for tropical storm numbers is improved compared to the LEOB set. The LEOB set has an MAE of 2.5 to the manual count. The detection numbers for the criteria set with lowest error to manual count and the error to observations for each category is shown in table 3.6.

3.3.3 New numbers with 15 years data

LEOB and LEMAN criteria are used to detect the extended years of simulation. The MAE and standard deviation of the LEOB are improved over the improved values from the original detection. LEMAN does not improve over the original MAE or standard deviation, except for major hurricanes. LEOB and LEMAN performed comparatively for major hurricane numbers (Fig. 3.11), but the five extended years have no storms above category 1 detected. Overall, LEOB brought many of the detected numbers closer to the observed values (Figs. 3.9.1-3, 3.10).

3.4 Hurricane intensity bias correction

3.4.1 Methods

The next step to fix the model bias is a correction of intensity counts. The intensity correction is applied to both minimum sea level pressure and wind speed for each 6 hourly data output from SSDA LEOB and SSDA LEMAN separately. The first step to intensity correction is to calculate of mean and scatter the observation values and model data (Figs.

3.12, 3.16.1-2). The correction offers three different methods. Method one is to adjust the 5th and 95th percentiles towards the observations. Another method is to adjust the mean and percentile. The third method to test fits the larger values. All three methods are tested to see which will produce the correct range of wind speeds and minimum sea level pressures. Several figures are produced in comparing the methods.

3.4.1.1 Picking the best method

Testing each data set to be corrected shows that for both the MSLP and wind speeds, the first method, fitting the percentiles, performs the best (Figs. 3.13.1-2, 3.17.1-3). The scatter plots show the second method creates values that far exceed the observed maxima (Figs. 3.14, 3.18.1-2), and the third method created values that are lower and still not major hurricane strength (Figs. 3.15.1-4, 3.19.1-2). This is true for each data set, with LEMAN intensity correction shown in figures 3.20.1-9. The first method meets the correct values at both end of the spectrum. Now with the best method, the MSLP and wind speeds are fitted together following Atkinson and Holliday (1977). This creates the new values of both, and consequently these intensities for each storm can be analyzed for each year.

3.4.2 LEOB vs. LEMAN

The focus here are the two SSDA data sets corrections after the intensity correction. Both are compared to observations for an improvement in intensity related error. The total number of storms has not changed. All the errors for both have improved except for total number of major hurricanes due to a small error increase in category 3 hurricanes.

Comparing the two to each other, LEOB now has better intensity numbers than LEMAN. All error is less except at category 2, 4, and 5. The overall improvement of LEOB error for all categories is greater than the LEMAN (Figs. 3.21.1-3). These corrections are originally done with only 10 years of data, but the LEOB is expanded for 15 years. The only differences are in the hurricane and major hurricane numbers (Figs. 3.22.1-2).

3.4.3 Wind-pressure relationship

Atkinson and Holliday (1977) developed an equation representing the relationship between wind and pressure to represent the Northwest Pacific. It has been applied to much of the other basins as well. Figure 3.23 shows the resulting line of best fit from Atkinson and Holliday (1977). Figure 3.24 shows the scatter of wind versus pressure from the LEOB data before intensity correction, LEOB data after intensity correction and the observed wind and pressure. Before intensity correction values do not cover the entire range of wind-pressure values covered by the observations. After intensity correction, the data covers the entire range and seems to follow the non-linear line from figure 3.23, but the observations have a more linear relationship and more spread than the corrected data. However, for this study, the benefit of having the data match the maximum intensity outweighs the other aspects of the relationship from the observations.

Table 3.1 15 years SSDA detected number of storms for each category

Original Detection	1998	1999	2000	2001	2002	2003	2004	2005	2006	2007	2008	2009	2010	2011	2012
Total Storms	8	18	6	10	9	6	10	20	14	16	13	4	21	16	12
TS	4	14	4	3	0	1	0	1	0	3	0	1	4	11	7
H	4	4	2	7	9	5	10	19	14	13	13	3	17	5	5
minor H	4	4	2	6	7	4	8	18	13	13	9	3	16	5	5
H1	4	4	2	2	2	3	1	10	9	8	4	3	9	5	5
H2	0	0	0	4	5	1	7	8	4	5	5	0	7	0	0
Major H	0	0	0	1	2	1	2	1	1	0	4	0	1	0	0
H3	0	0	0	1	2	1	2	1	1	0	4	0	1	0	0
H4	0	0	0	0	0	0	0	0	0	0	0	0	0	0	0
H5	0	0	0	0	0	0	0	0	0	0	0	0	0	0	0

Table 3.2 Mean absolute error and standard deviation for original detection against observations

Original detection	MAE	STDEV
TS	4.4	5.25357
tsobs		3.233751
tsdiff		2.0198
H	4.666667	5.394
hobs		2.231805
hdiff		3.1622
MH	1.733333	1.125463
mhobs		1.58865
mhdiff		-0.4632

Table 3.3 Landfall risk values for Caribbean coast, Gulf coast of Mexico, Gulf coast of US, Southeast Atlantic coast of US, Florida, North Carolina, the Greater Antilles, and the Bahamas for 15 years

Total	Best Track	BT H	BT MH	SSDA	S H	S MH
Counts						
open ATLC	85	39	14	98	83	0
Carib	59	30	18	93	74	0
Gulf of Mex	72	32	12	84	65	0
NATLC	142	71	36	177	129	0
Landfalls						
CentAm y-v	27	11	6	56	30	0
Gulf coast mex	13	3	2	32	11	0
Gulf coast US	45	16	7	64	36	0
SE US	24	10	2	53	26	0
Big Islands	38	17	8	62	36	0
Bahamas	14	8	5	46	19	0
FL	27	8	4	40	20	0
NC	10	4	1	10	5	0

Table 3.4 Detection sensitivity to resolution storm numbers and MAE for global, 36km, and 12km

	2001	2002	2003	2004	2005	2006	2007	2008	2009	2010	
TS											
Obs	10	9	7	9	16	4	8	10	3	12	MA Err
GFS	5	3	3	6	8	4	2	7	2	6	4.2
36kmSSDA	9	8	9	6	15	7	13	9	6	13	2.1
12kmSSDA	11	12	9	10	24	15	16	16	6	21	5.2
H											
Obs	4	3	2	6	10	1	4	6	2	7	
GFS	1	0	2	2	3	0	0	1	1	2	3.3
36kmSSDA	3	6	3	5	8	5	8	6	2	6	1.6
12kmSSDA	7	9	5	10	19	14	13	13	3	17	6.5

Table 3.5 Least error to observations (LEOB) criteria detected storm numbers and the MAE for original 10 years

LEOB	2001	2002	2003	2004	2005	2006	2007	2008	2009	2010	MAE
No. of NS	7	11	7	9	16	12	12	13	4	15	2.4
No. of TS	0	0	1	0	0	0	0	0	0	0	4.2
No. of HR	7	11	6	9	15	12	12	13	3	14	5.7
minor hr	5	10	3	6	11	11	10	7	3	12	5.7
No. of H1	3	4	1	1	7	6	5	3	3	4	2.2
No. of H2	2	6	2	5	4	5	5	4	0	8	3.7
major hr	2	1	3	3	4	1	2	6	0	2	1.2
No. of H3	1	1	1	2	1	1	1	5	0	0	1.1
No. of H4	0	0	0	0	0	0	0	0	0	0	1
No. of H5	1	0	2	1	3	0	1	1	0	2	0.7

Table 3.6 Least error to manual count (LEMAN) criteria detected storm numbers and MAE for original 10 years

LEMAN	2001	2002	2003	2004	2005	2006	2007	2008	2009	2010	MAE
No. of NS	11	2	9	10	24	16	16	16	6	21	4.7
No. of TS	1	1	2	0	2	1	2	0	1	2	3.1
No. of HR	6	12	7	9	21	15	12	15	5	17	7.4
minor hr	4	10	4	6	16	14	9	9	5	14	7
No. of H1	2	4	2	1	11	9	5	5	4	5	3.3
No. of H2	2	6	2	5	5	5	4	4	1	9	3.7
major hr	2	2	3	3	5	1	3	6	0	3	1.2
No. of H3	1	1	1	3	1	1	1	4	0	0	1.1
No. of H4	0	0	0	0	0	0	0	1	0	0	0.9
No. of H5	1	1	2	0	4	0	2	1	0	3	0.8

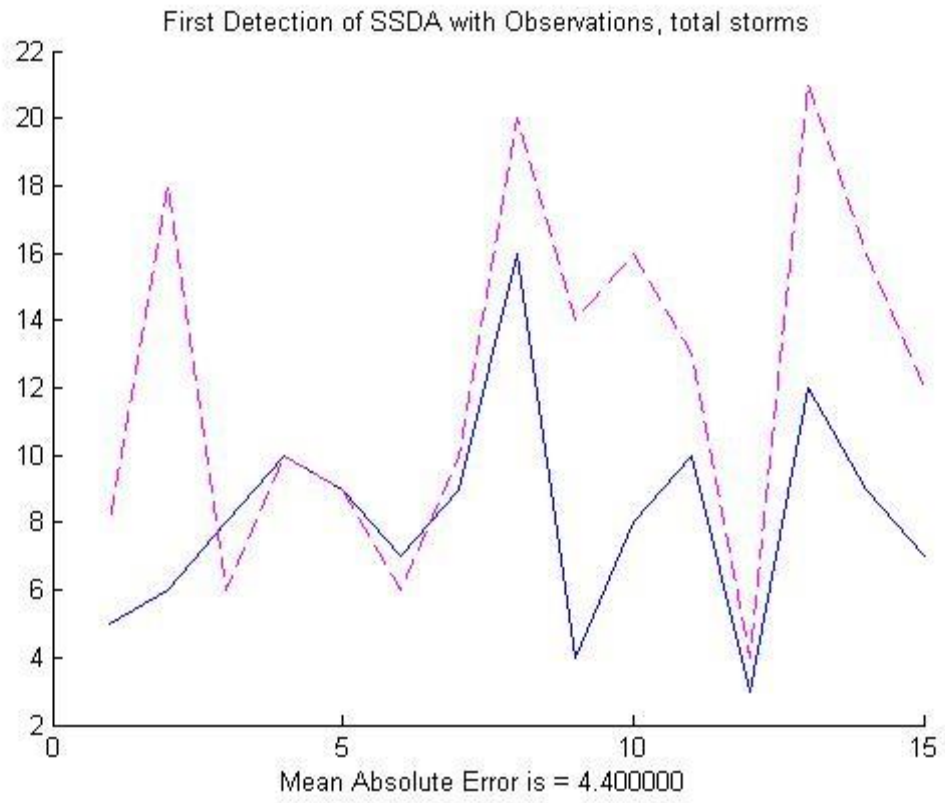

Figure 3.1 SSDA original detection total storm numbers compared with observed number of storms

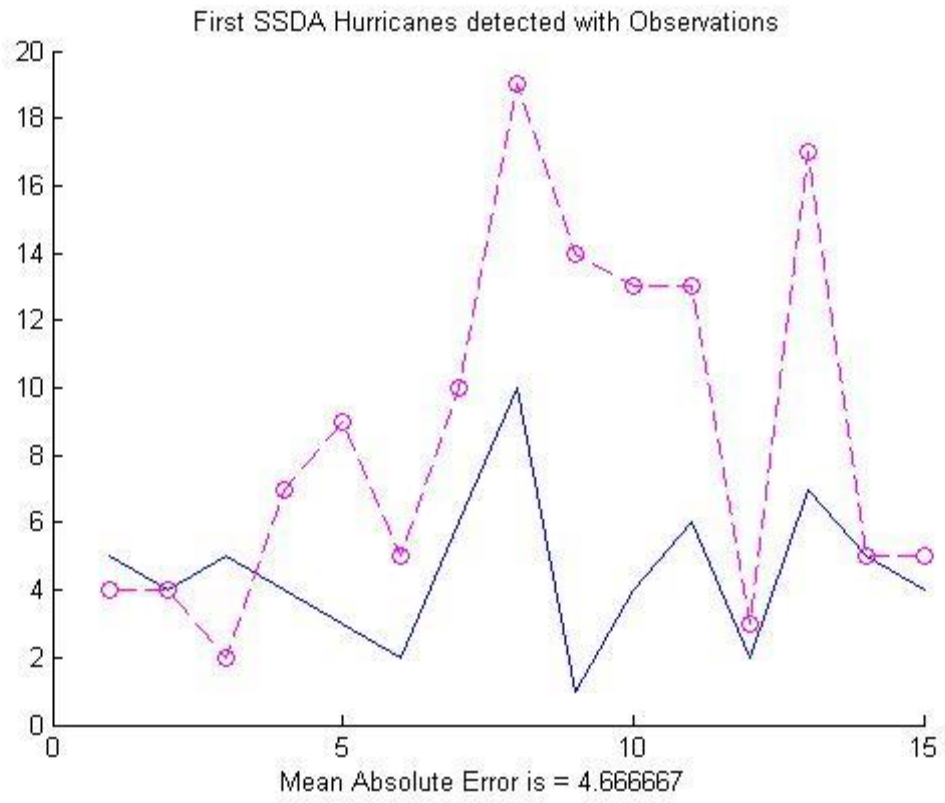

Figure 3.2 SSDA original detection hurricane numbers compared with observations

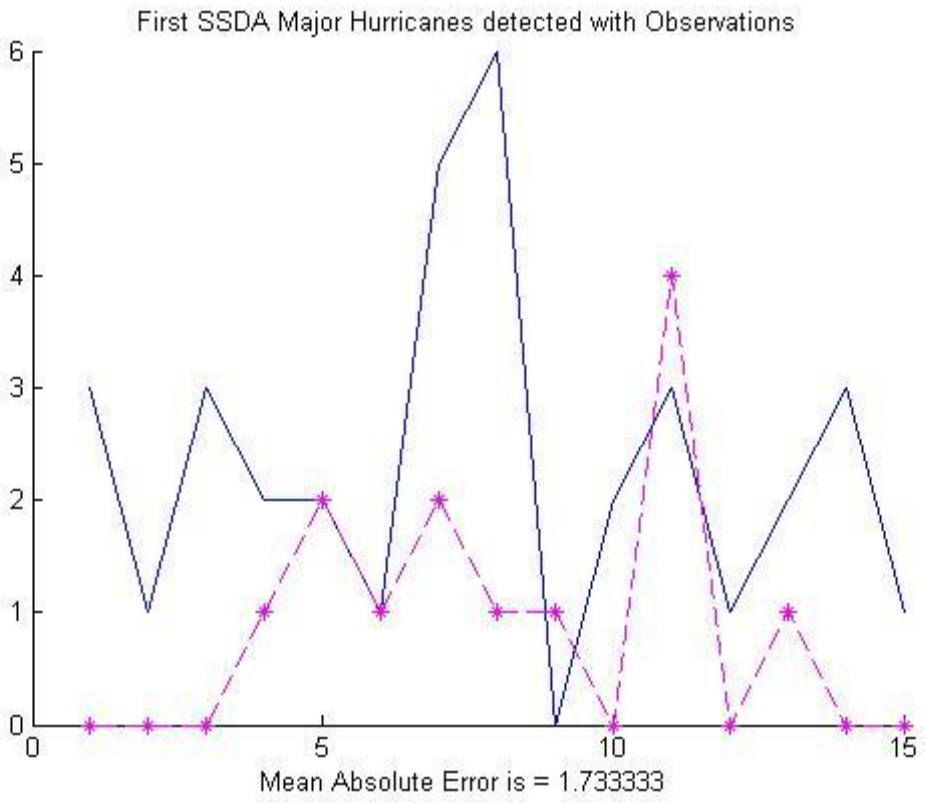

Figure 3.3 SSDA original detection major hurricane numbers compared with observations

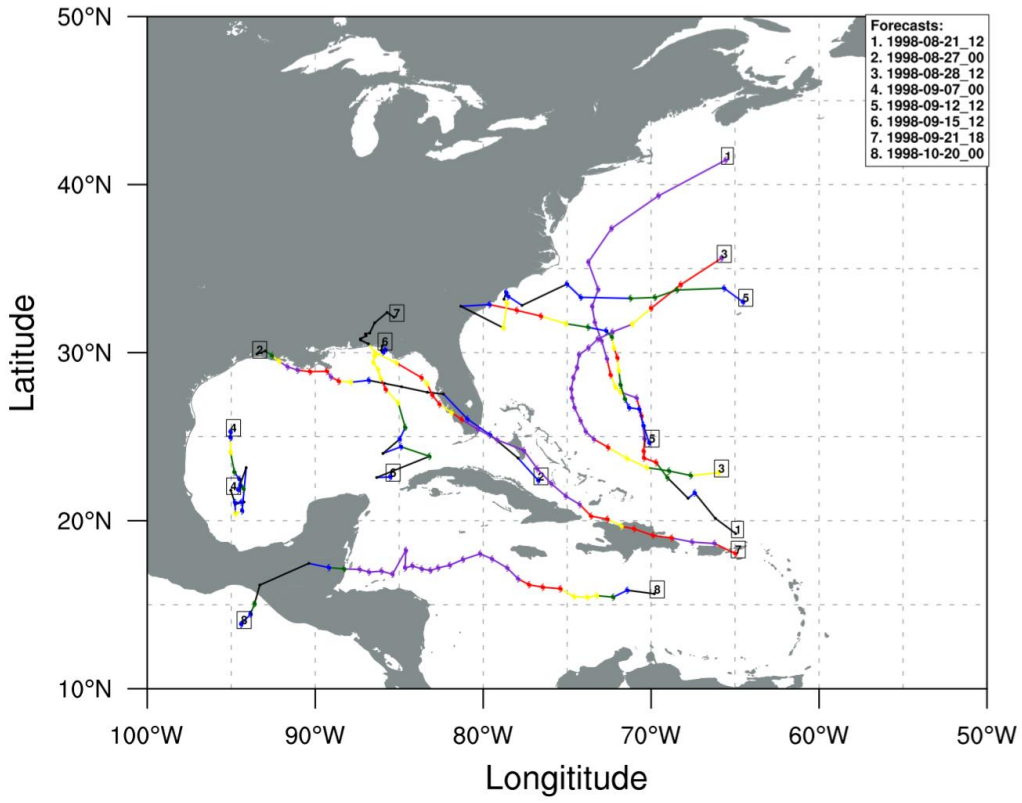

Figure 3.4.1 SSDA original detected tracks for 1998

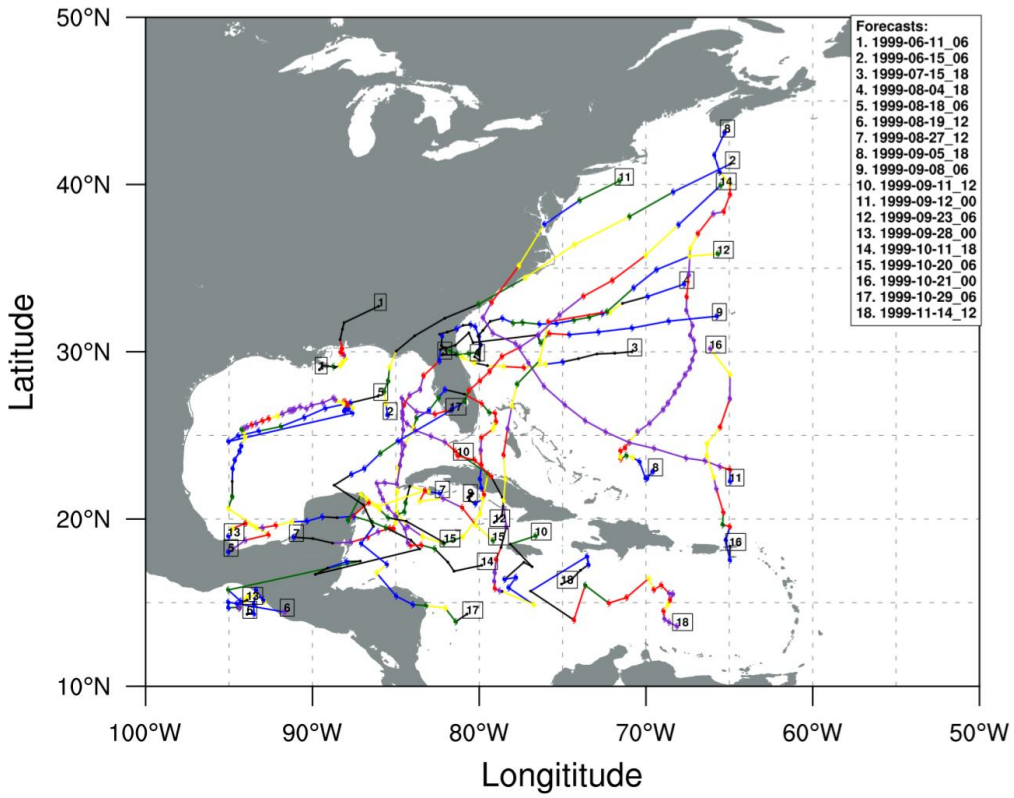

Figure 3.4.2 SSDA track map 1999

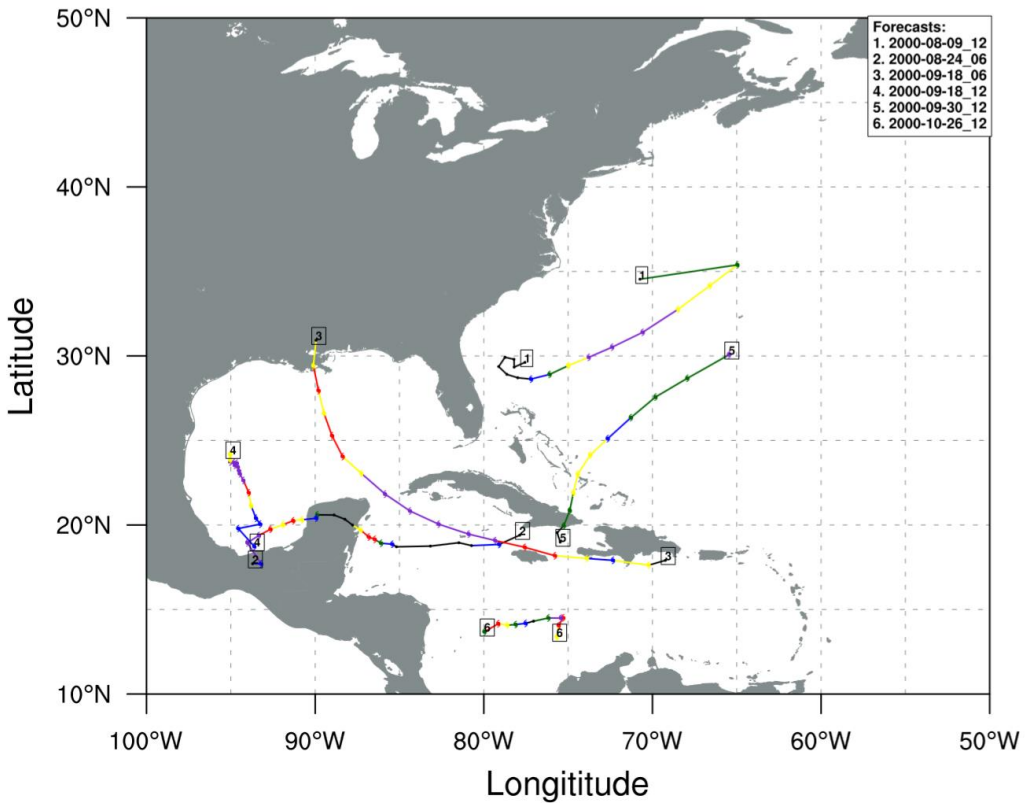

Figure 3.4.3 SSDA track map 2000

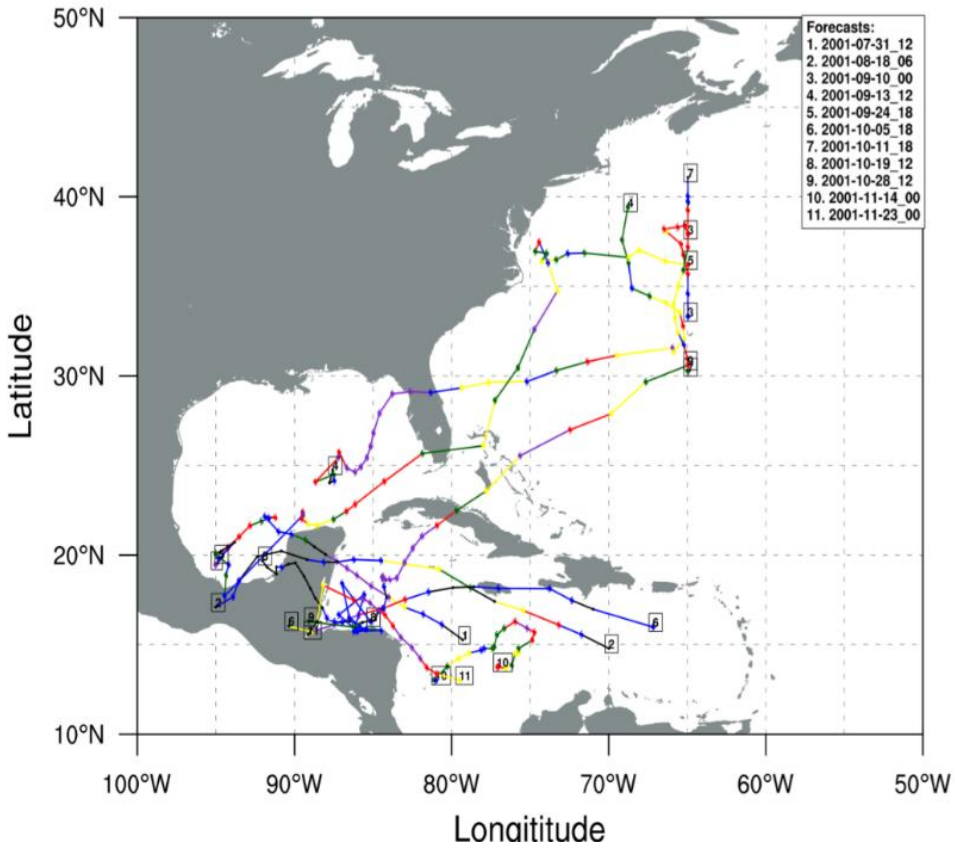

Figure 3.4.4 SSDA track map 2001

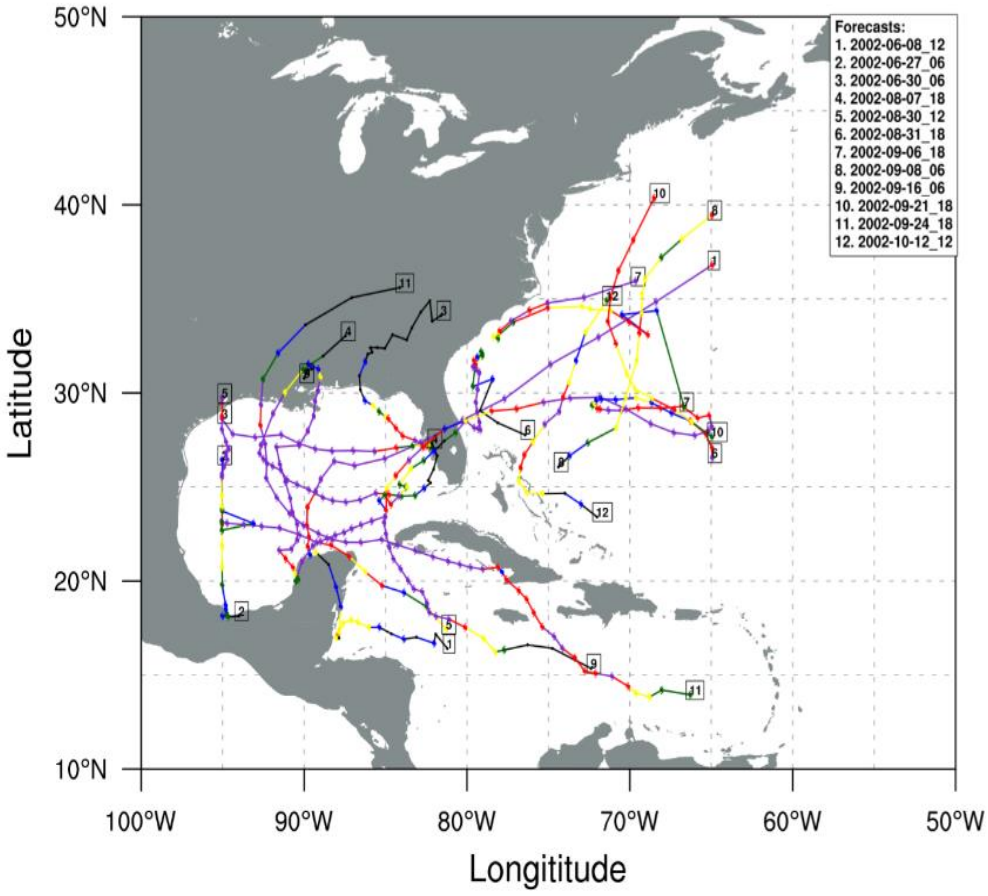

Figure 3.4.5 SSDA track map 2002

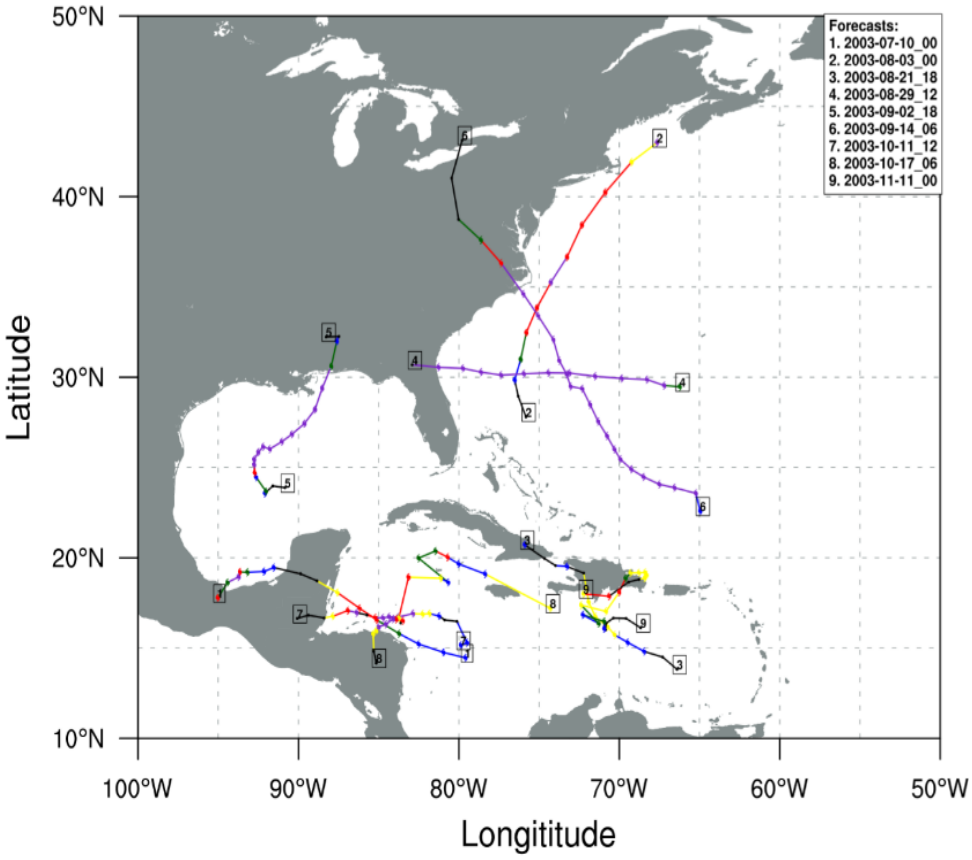

Figure 3.4.6 SSDA track map 2003

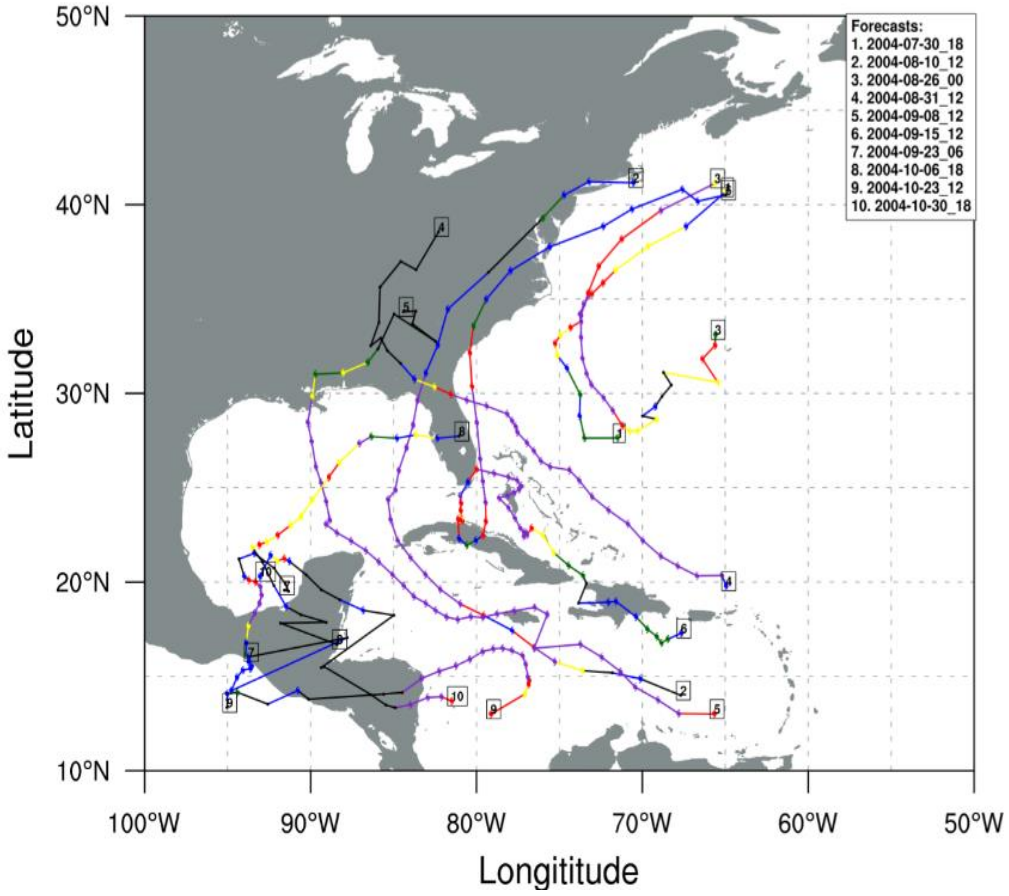

Figure 3.4.7 SSDA track map 2004

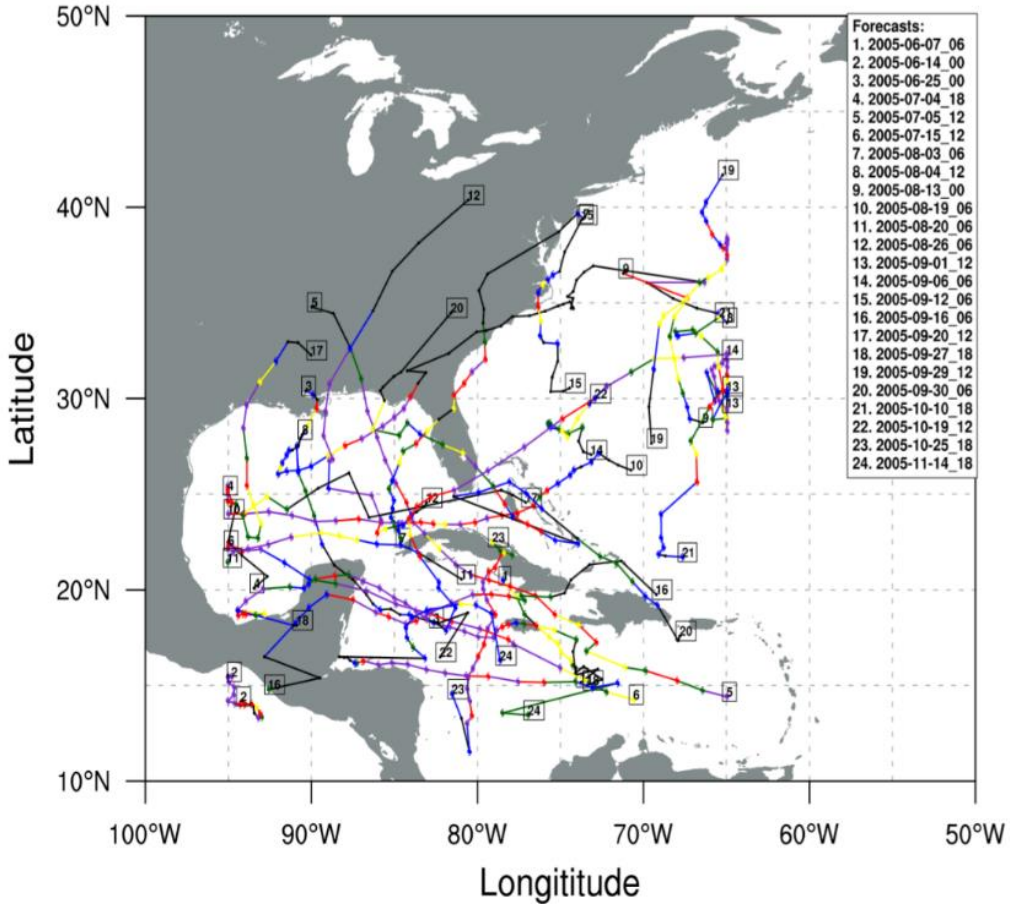

Figure 3.4.8 SSDA track map 2005

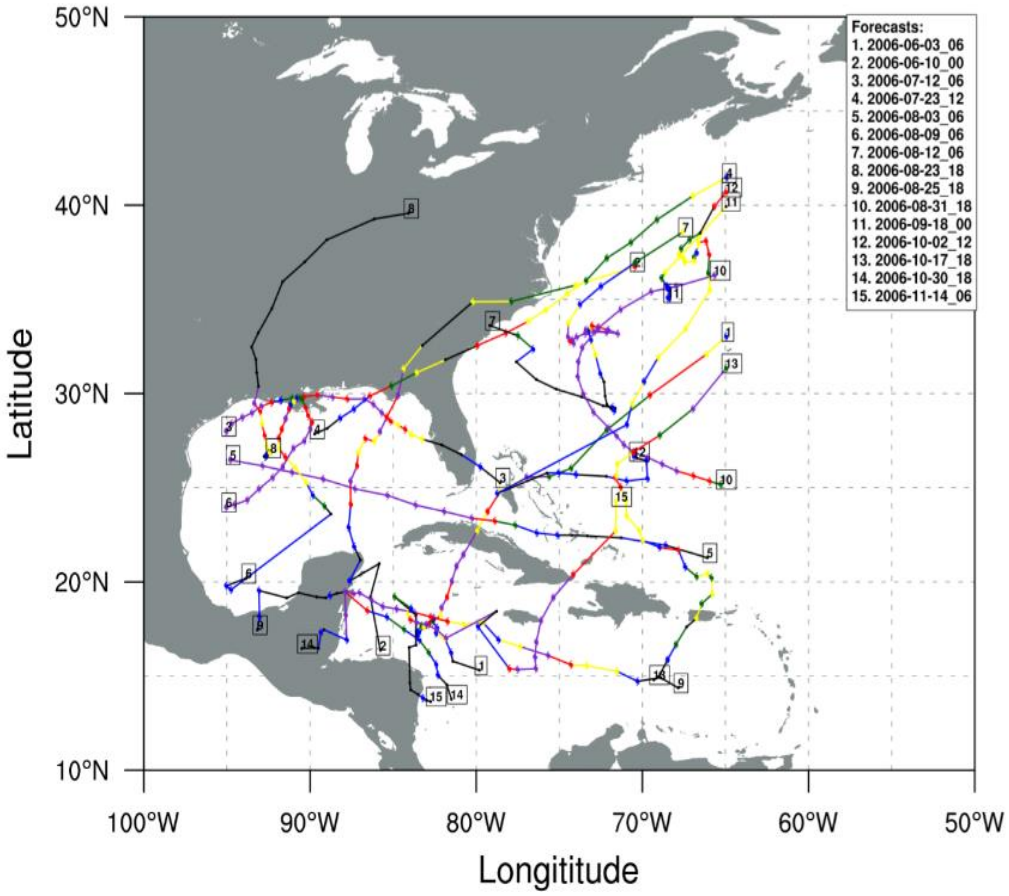

Figure 3.4.9 SSDA track map 2006

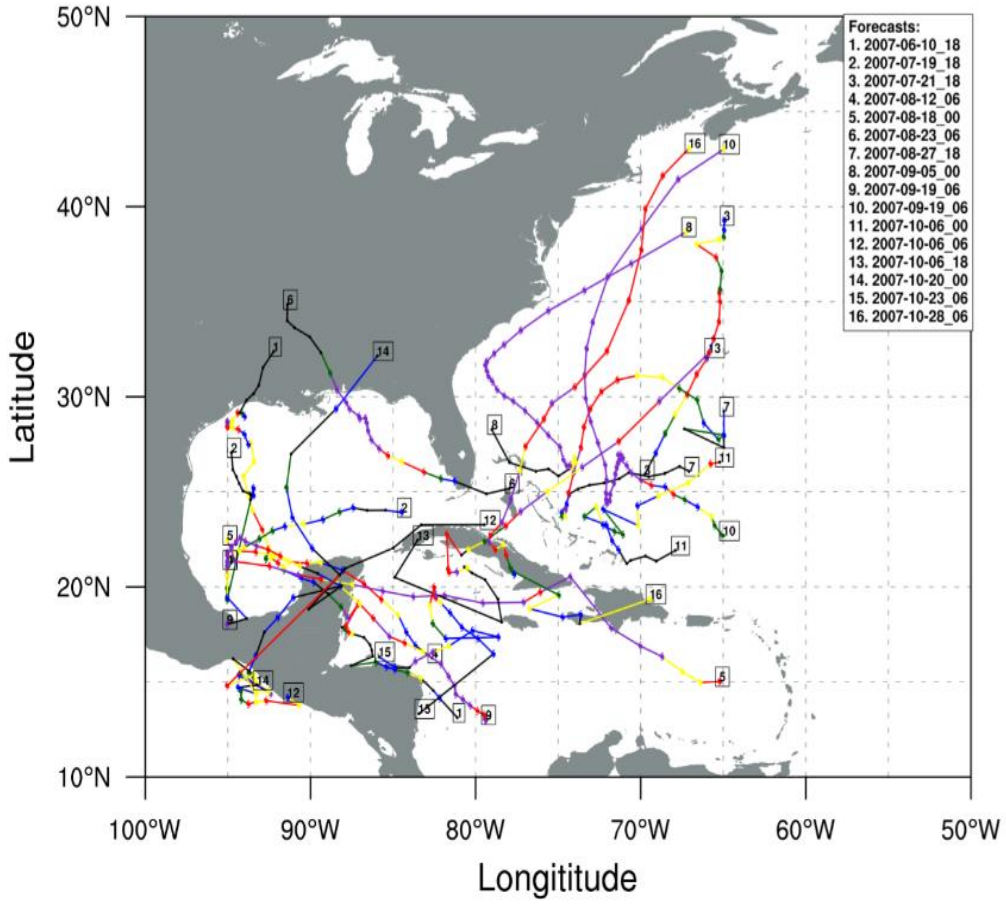

Figure 3.4.10 SSDA track map 2007

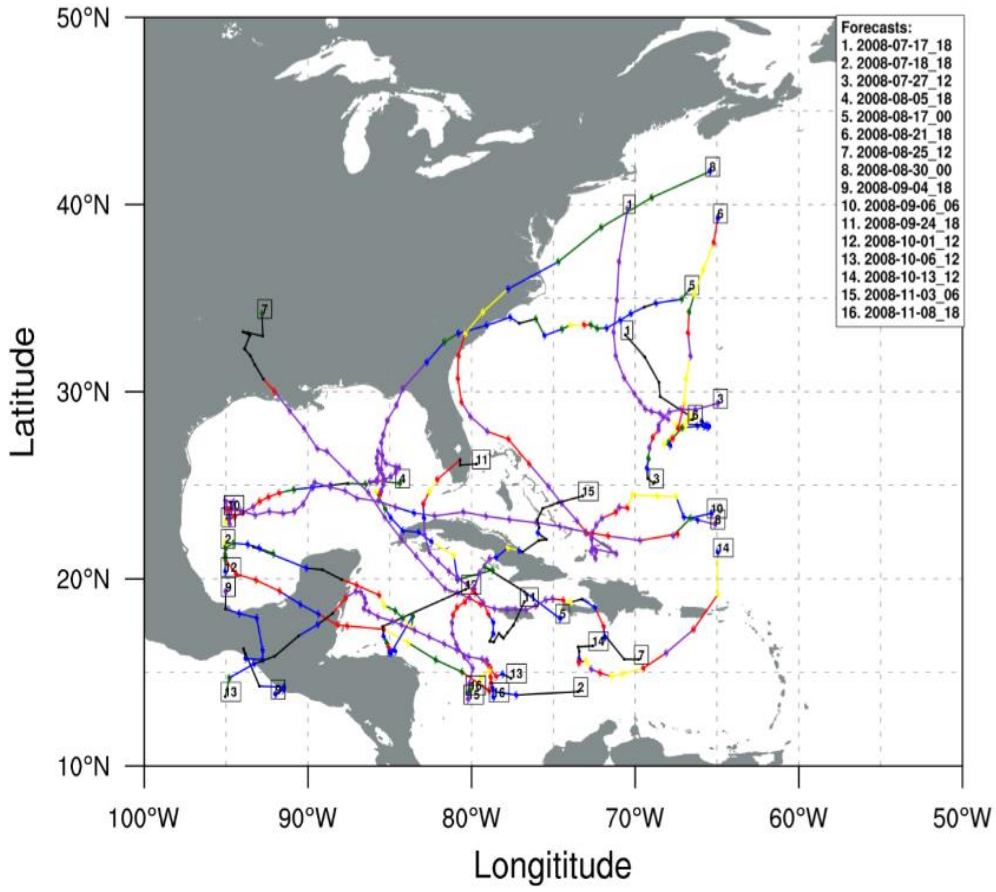

Figure 3.4.11 SSDA track map 2008

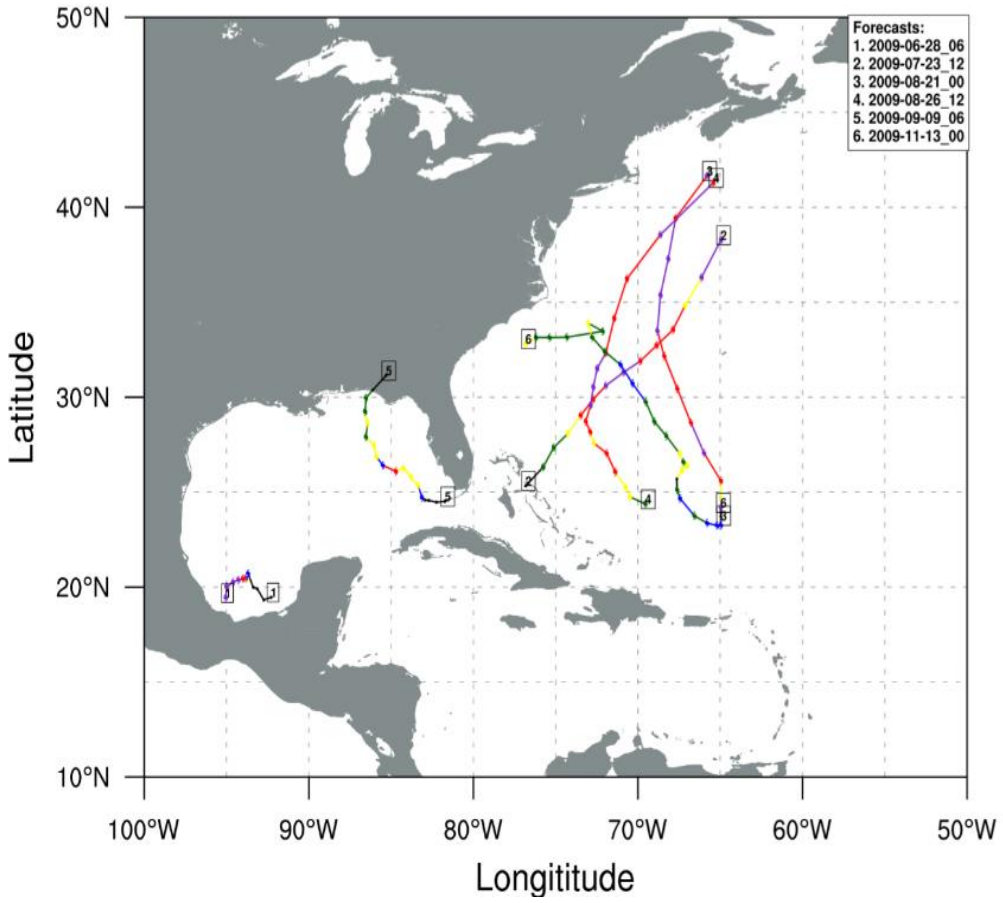

Figure 3.4.12 SSDA track map 2009

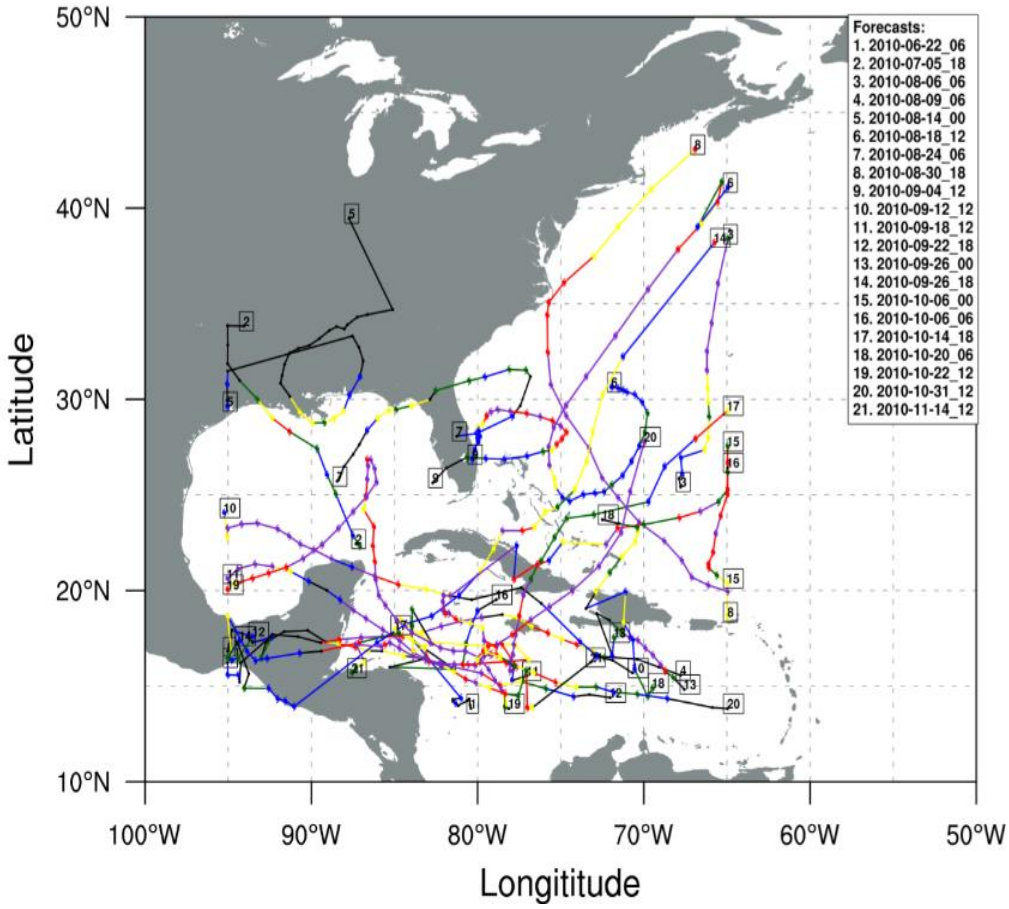

Figure 3.4.13 SSDA track map 2010

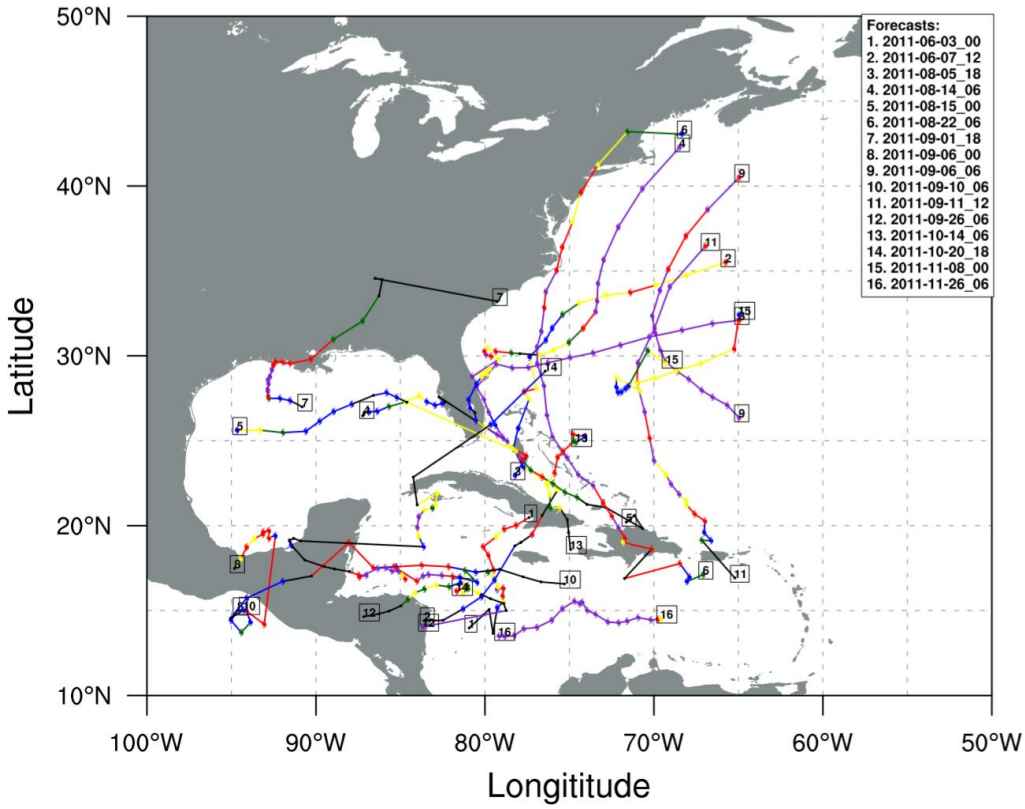

Figure 3.4.14 SSDA track map 2011

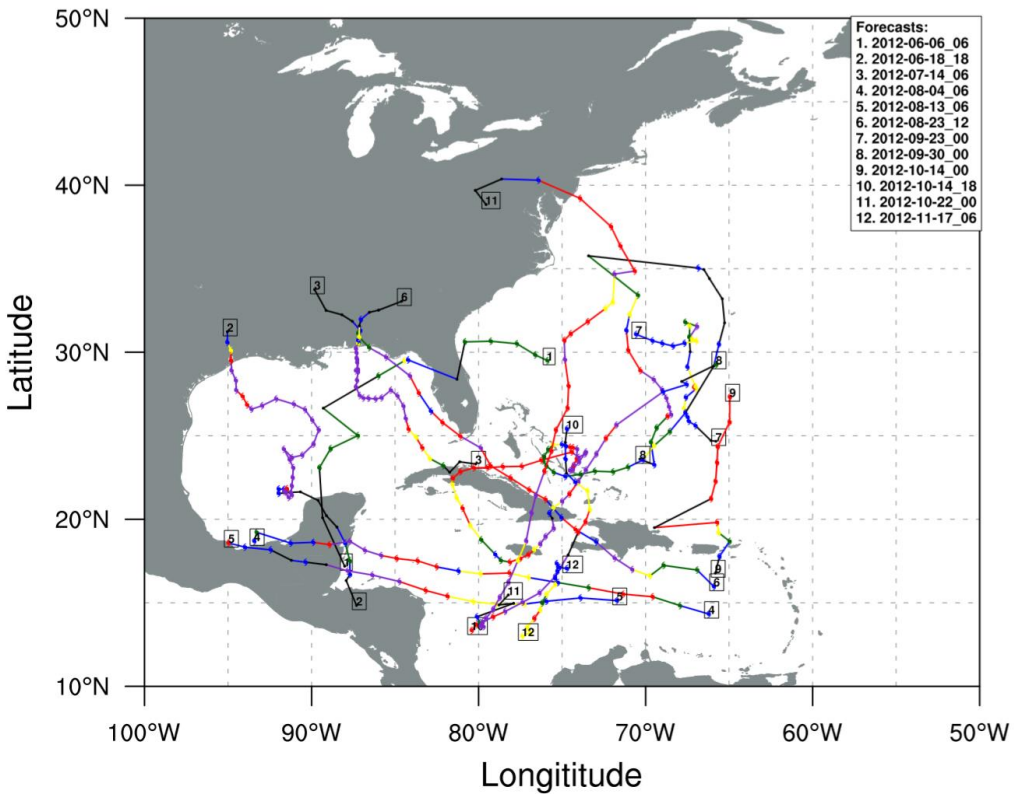

Figure 3.4.15 SSDA track map 2012

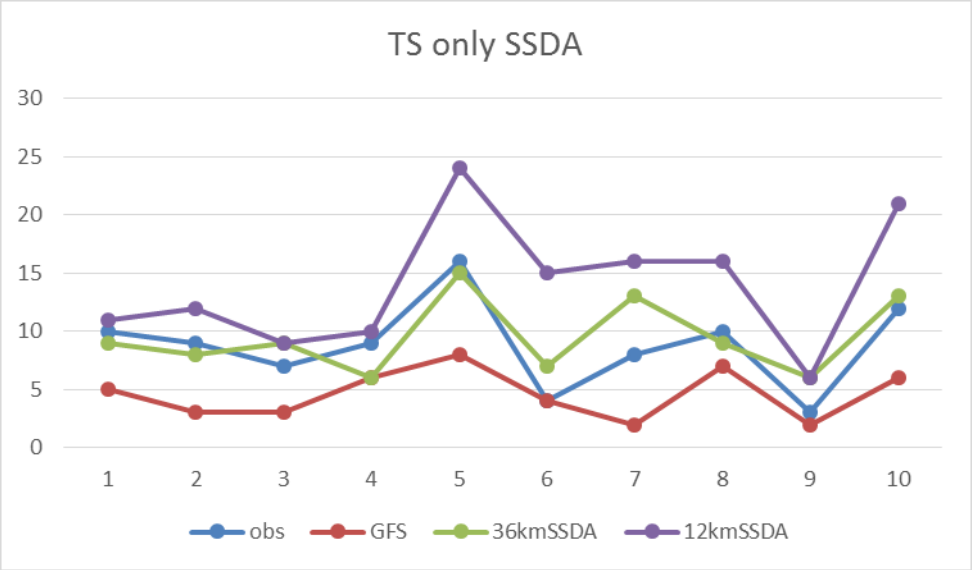

Figure 3.5.1 Sensitivity of detection to resolution, global, 36 km and 12 km detected storms

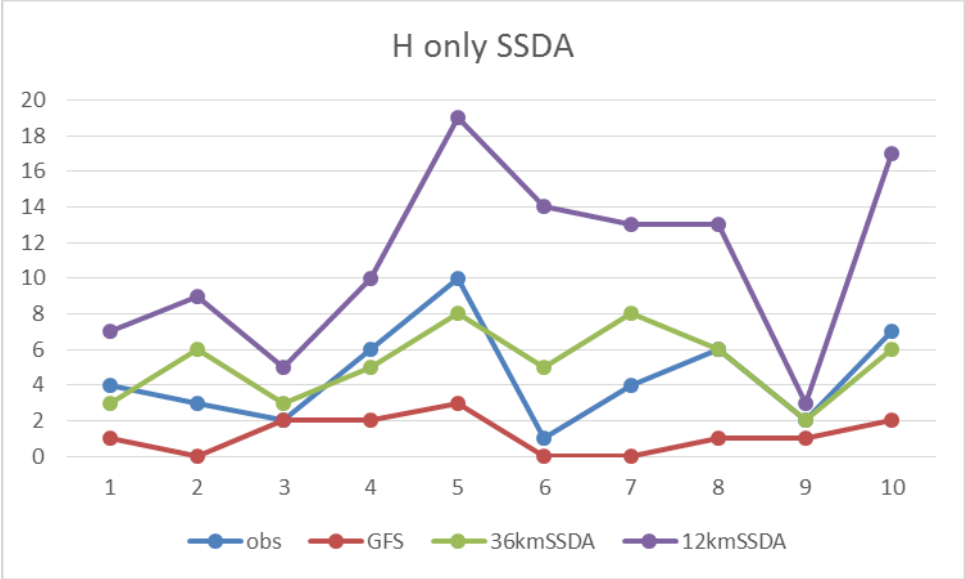

Figure 3.5.2 Sensitivity of detection to resolution, global, 36 km and 12 km detected hurricanes

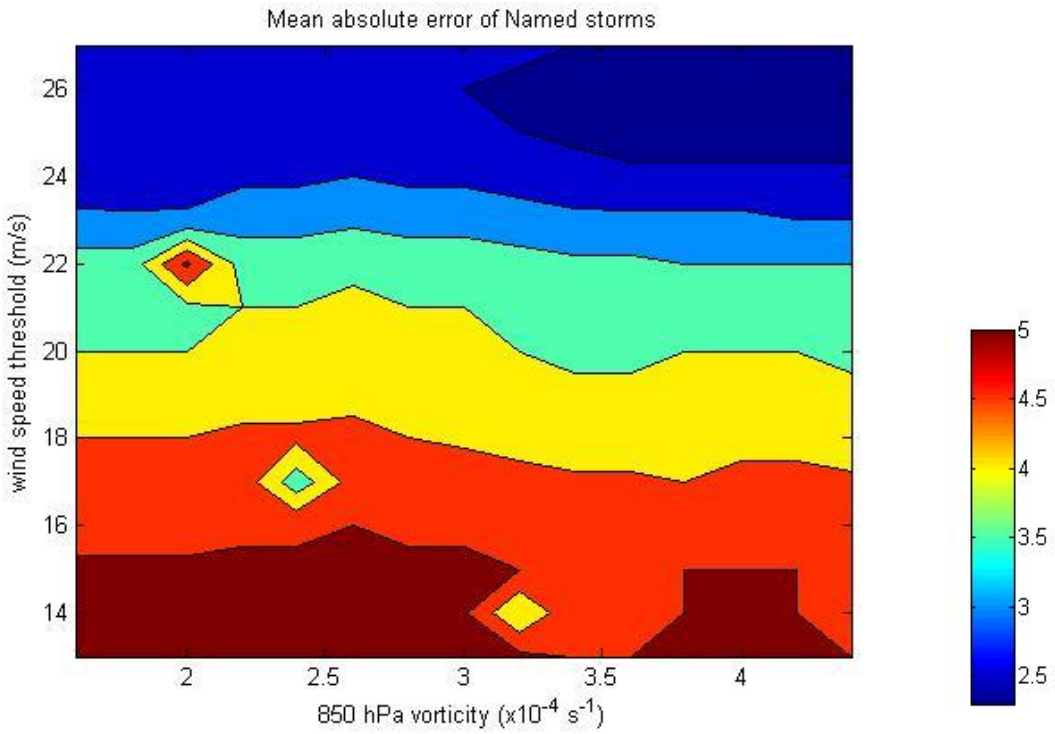

Figure 3.6.1 Mean absolute error contour plot to changes in detection algorithm criteria, 13-27 m/s wind speed and 1.6 to 4.4 x 10-4 s^{-1} vorticity

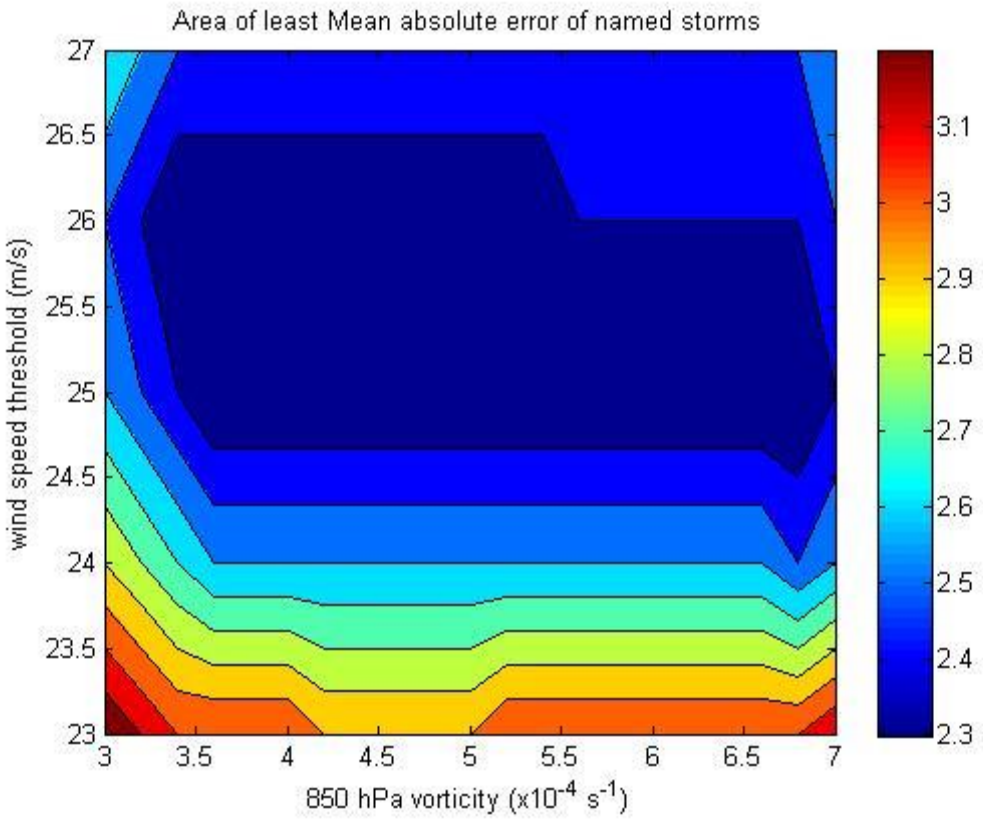

Figure 3.6.2 Mean absolute error contour plot extended cases, 23-27 m/s wind speed and 3.0-7.0 x 10-4 s^{-1} vorticity. Area with the lowest error

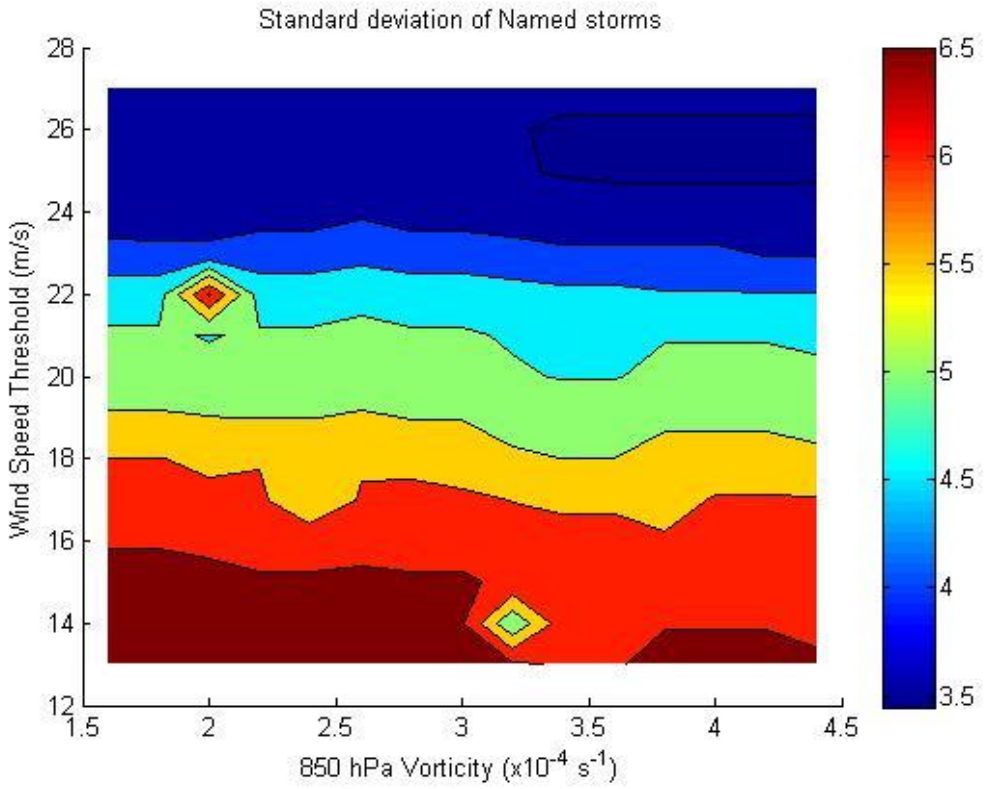

Figure 3.7.1 Standard Deviation contour map 13-27 m/s wind speed and 1.6 to 4.4 x 10-4 s^{-1} vorticity

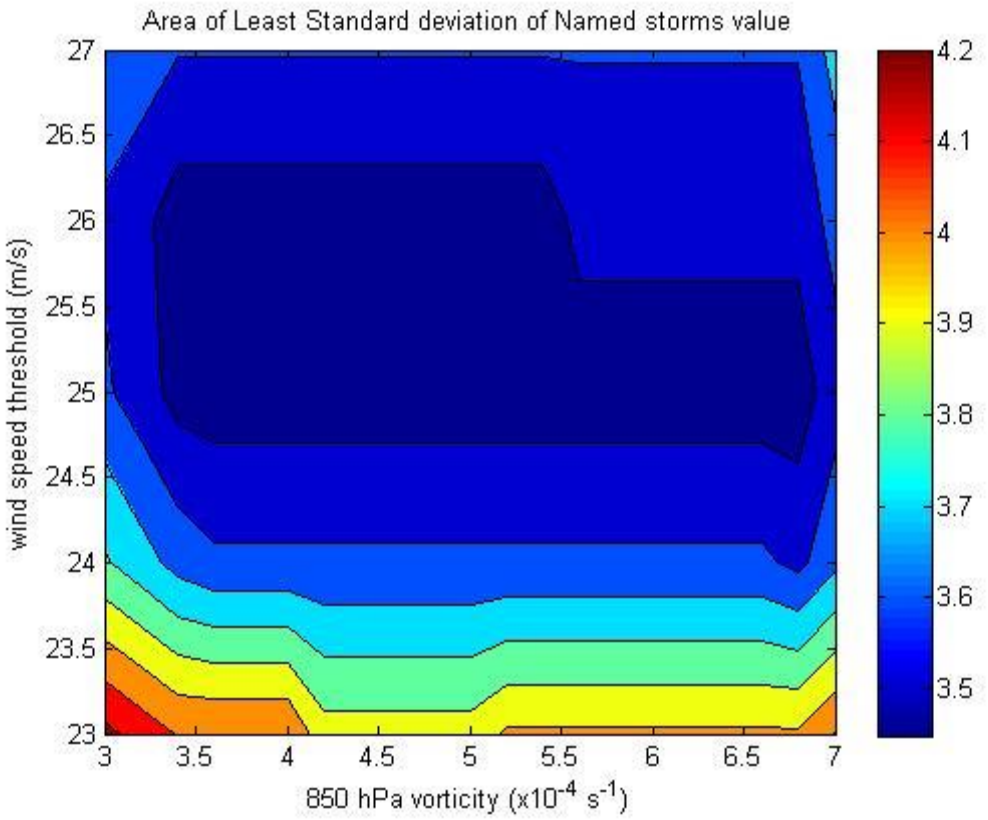

Figure 3.7.2 Standard Deviation contour map 23-27 m/s wind speed and 3.0-7.0 x 10^{-4} s^{-1} vorticity, area with the lowest error

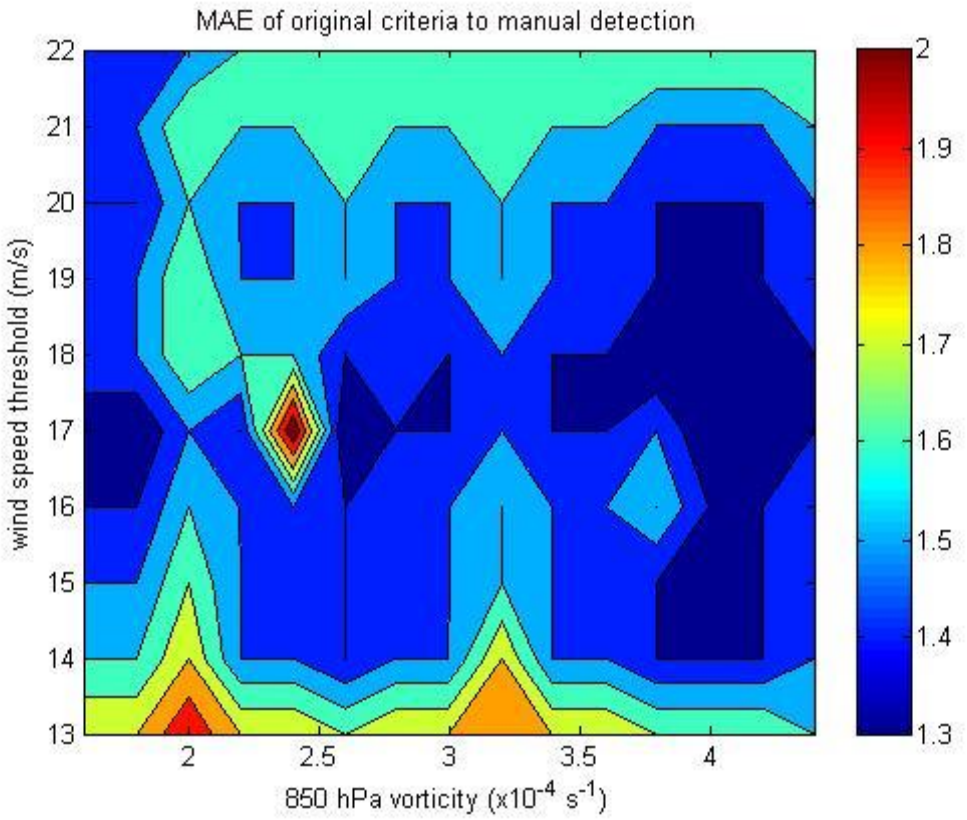

Figure 3.8.1 Mean Absolute Error contour map to manual detection. 13-22 m/s wind speed and 1.6 - 4.4 x 10-4 s^{-1} vorticity

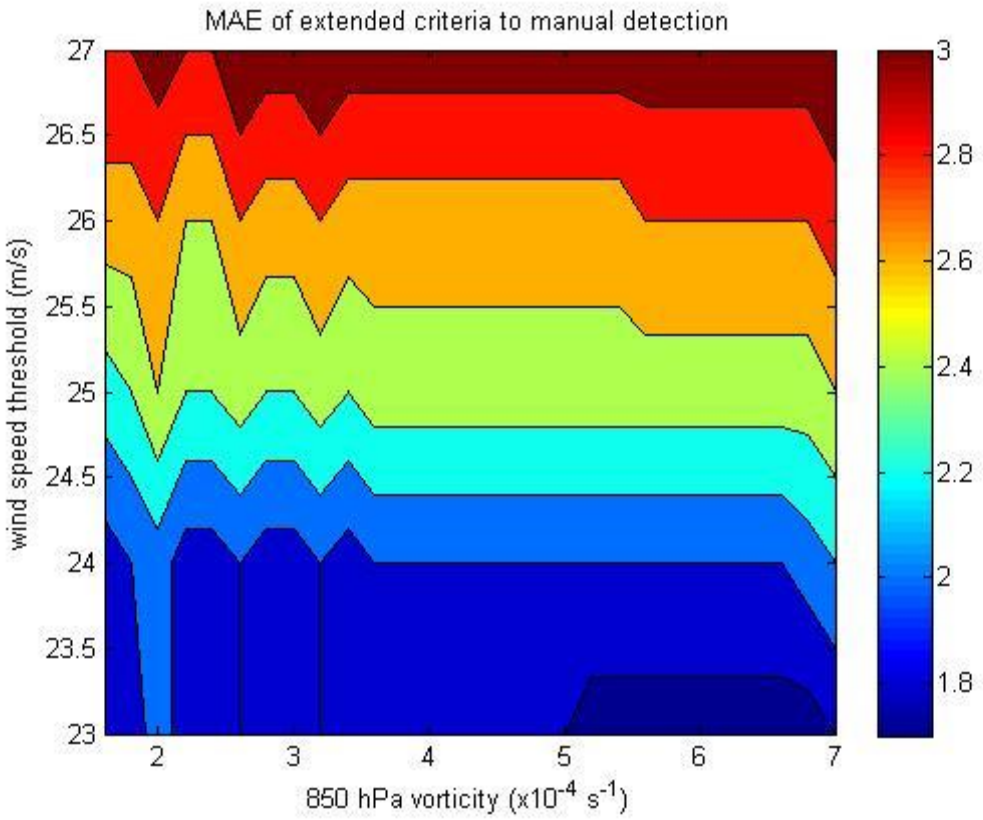

Figure 3.8.2 Mean Absolute Error contour map to manual detection. 23-27 m/s wind speed and 1.6-7.0 x 10-4 s^{-1} vorticity

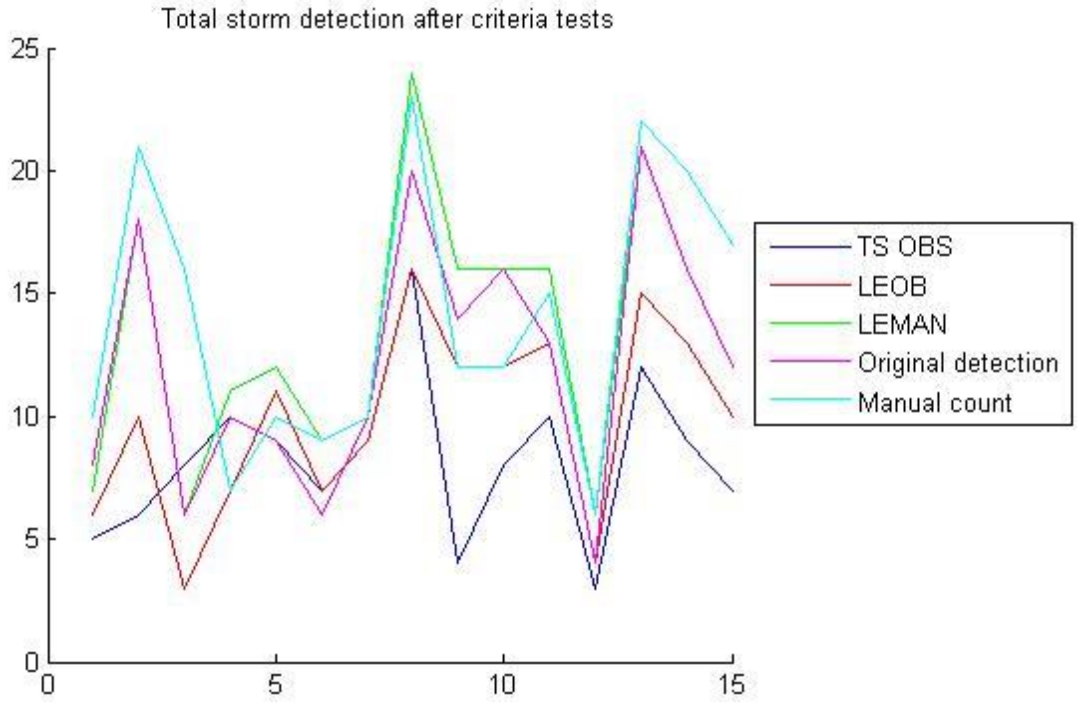

Figure 3.9.1 Criteria correction total storm numbers: Observations, SSDA LEOB, SSDA LEMAN, Original SSDA detection, and manual count

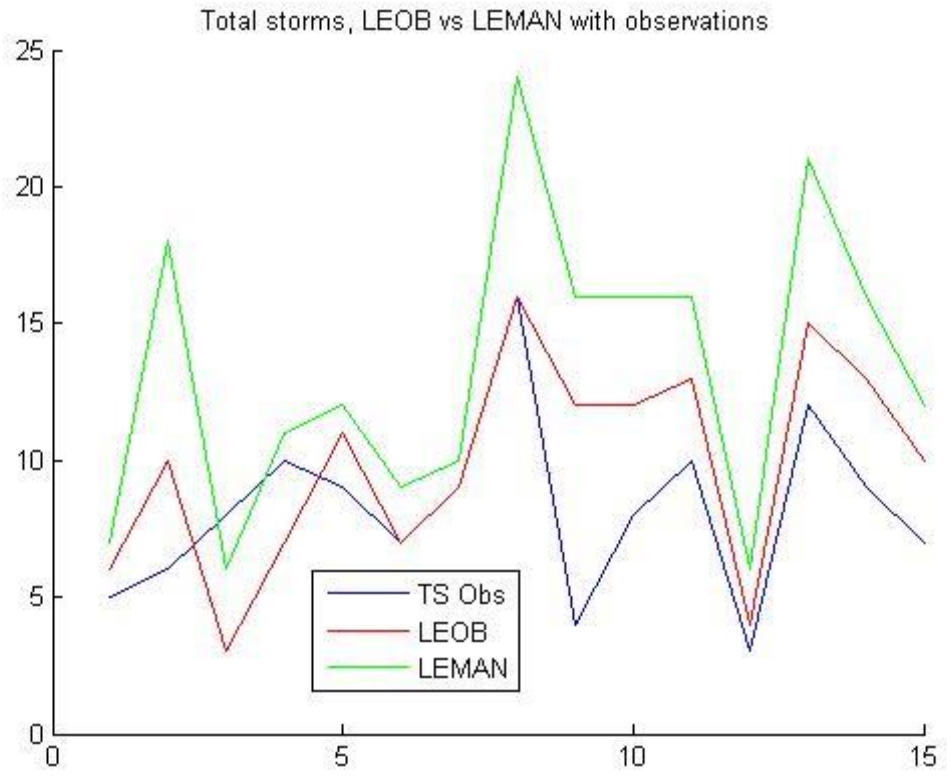

Figure 3.9.2 Criteria corrected total storm numbers: observations, SSDA LEOB, and SSDA LEMAN

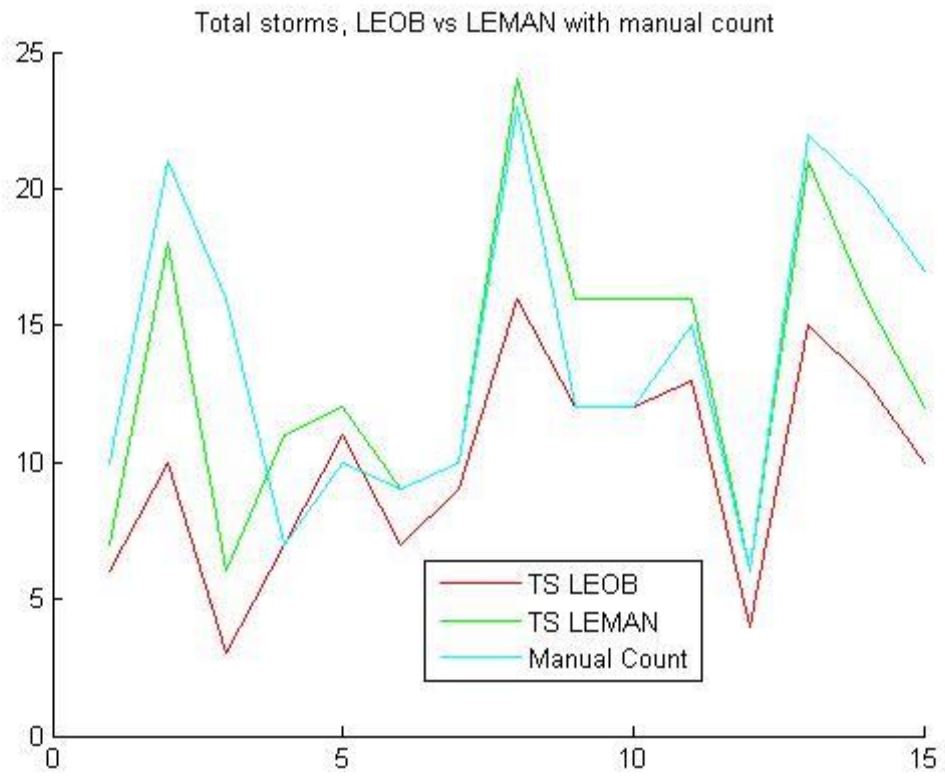

Figure 3.9.3 Criteria corrected total storm numbers: SSDA LEOB, SSDA LEMAN, and Manual count

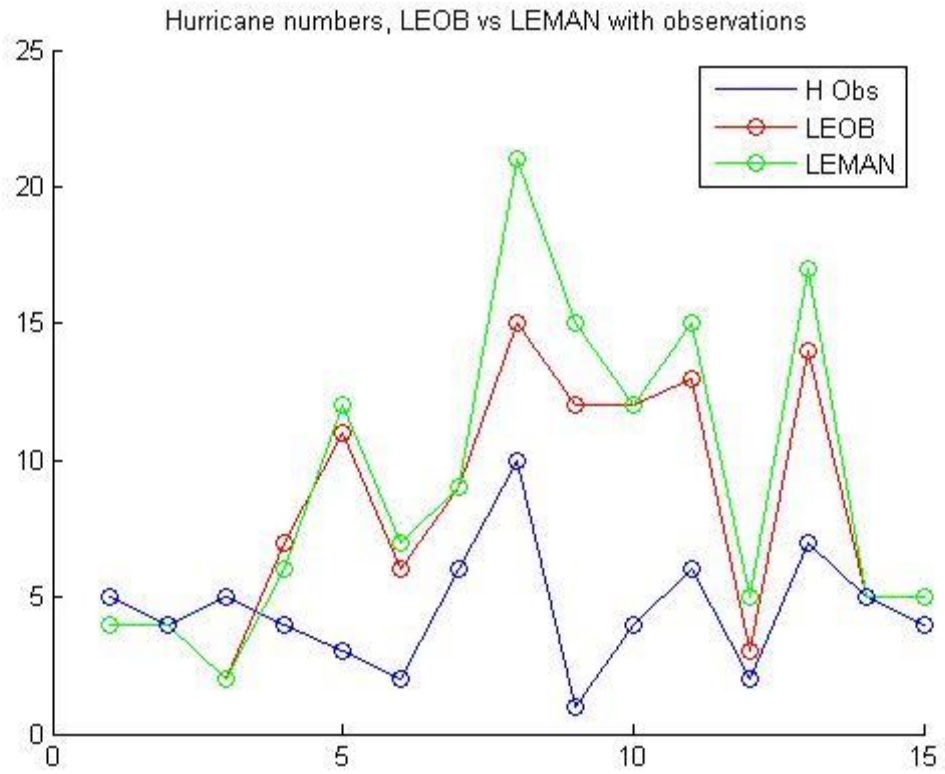

Figure 3.10 Criteria corrected hurricane numbers: Observations, SSDA LEOB, and SSDA LEMAN

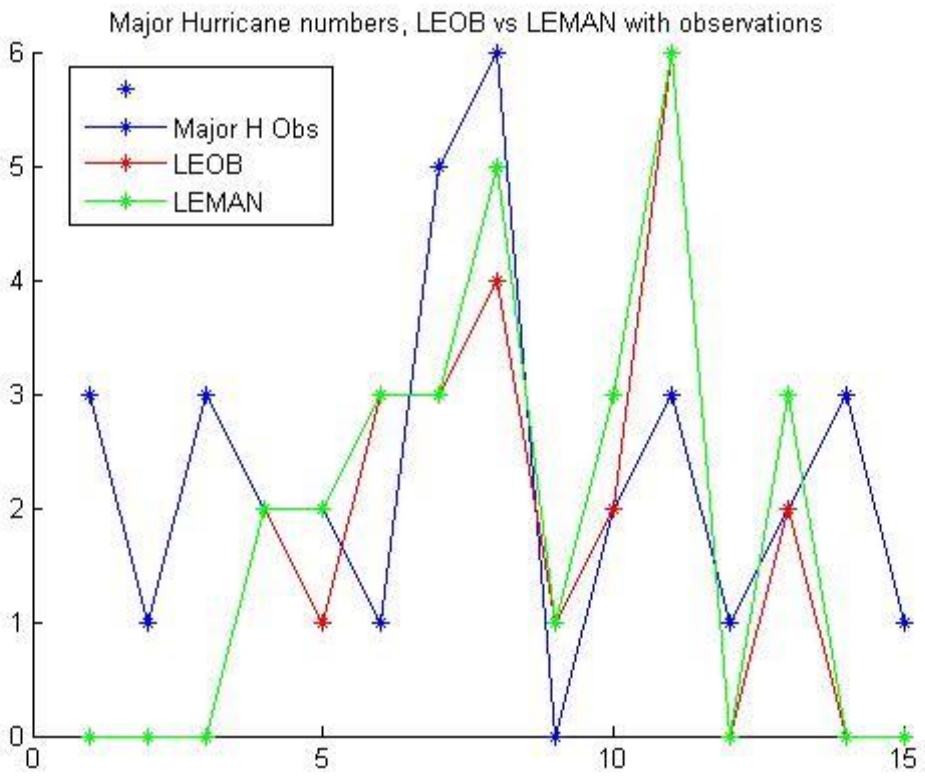

Figure 3.11 Criteria corrected major hurricane numbers: Observations, SSDA LEOB, and SSDA LEMAN

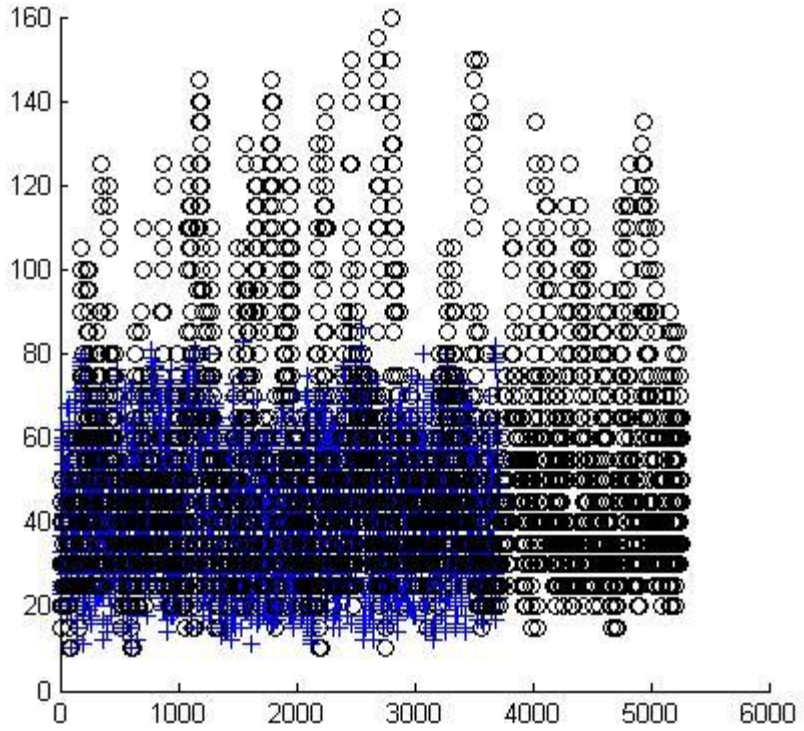

Figure 3.12 Intensity correction Step 1: Scatter detected values with observed values

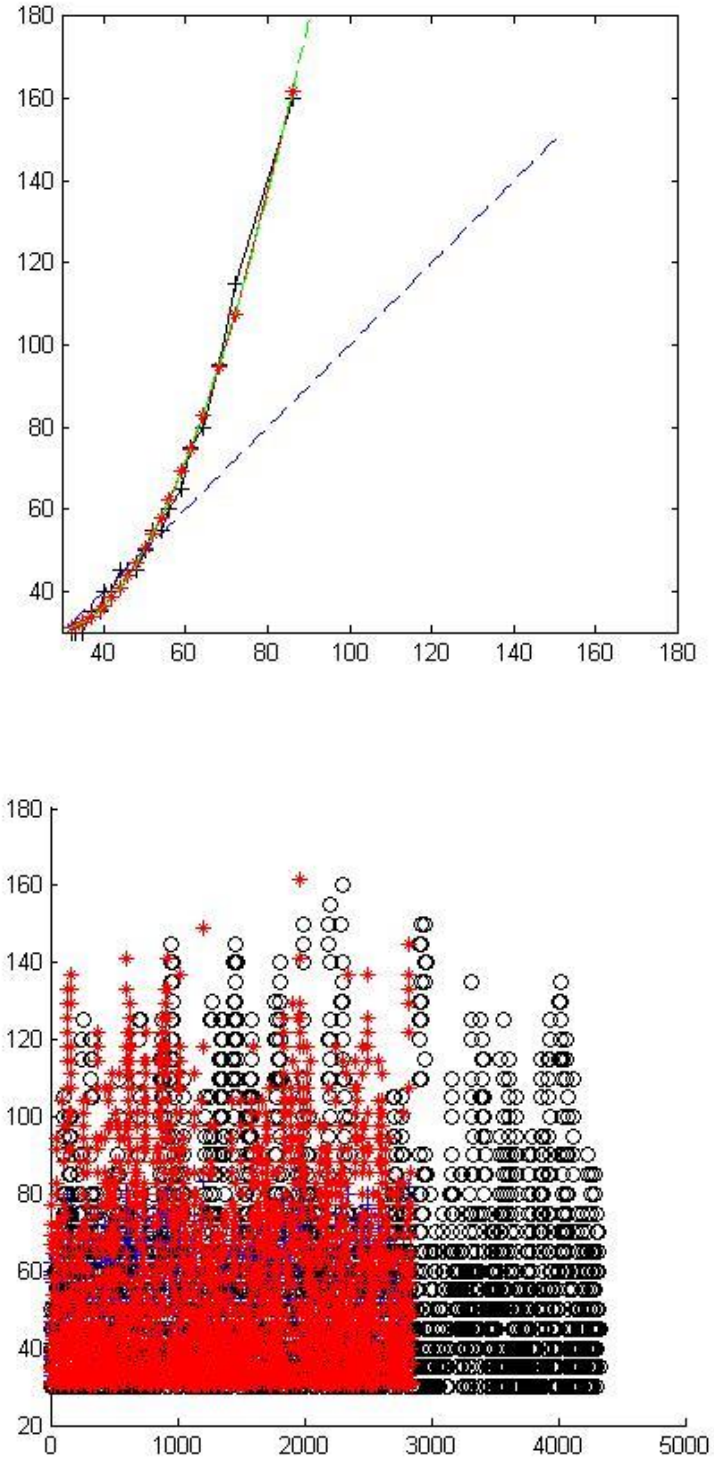

Figure 3.13.1-2 Intensity correction method 1

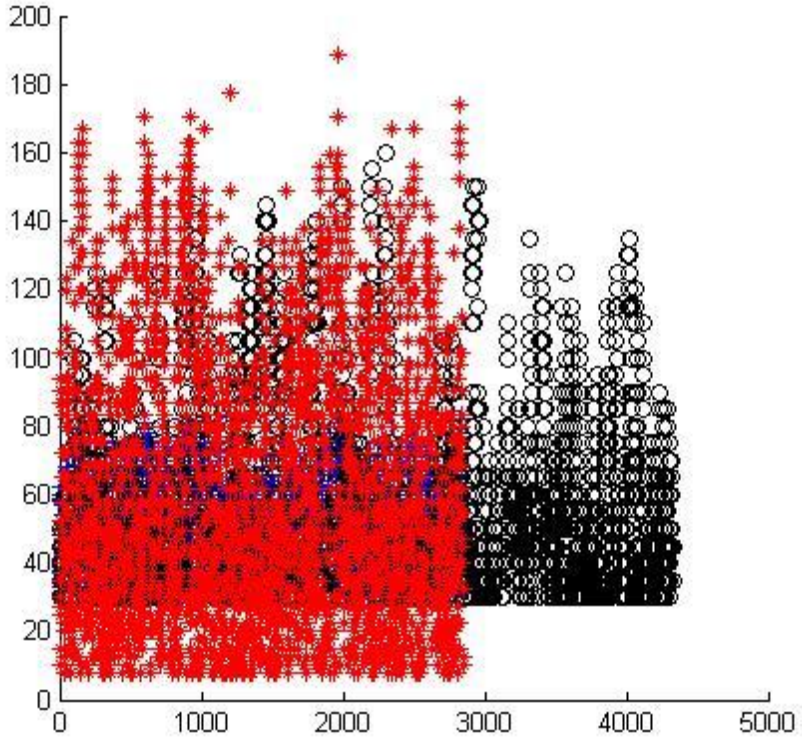

Figure 3.14 Intensity correction method 2

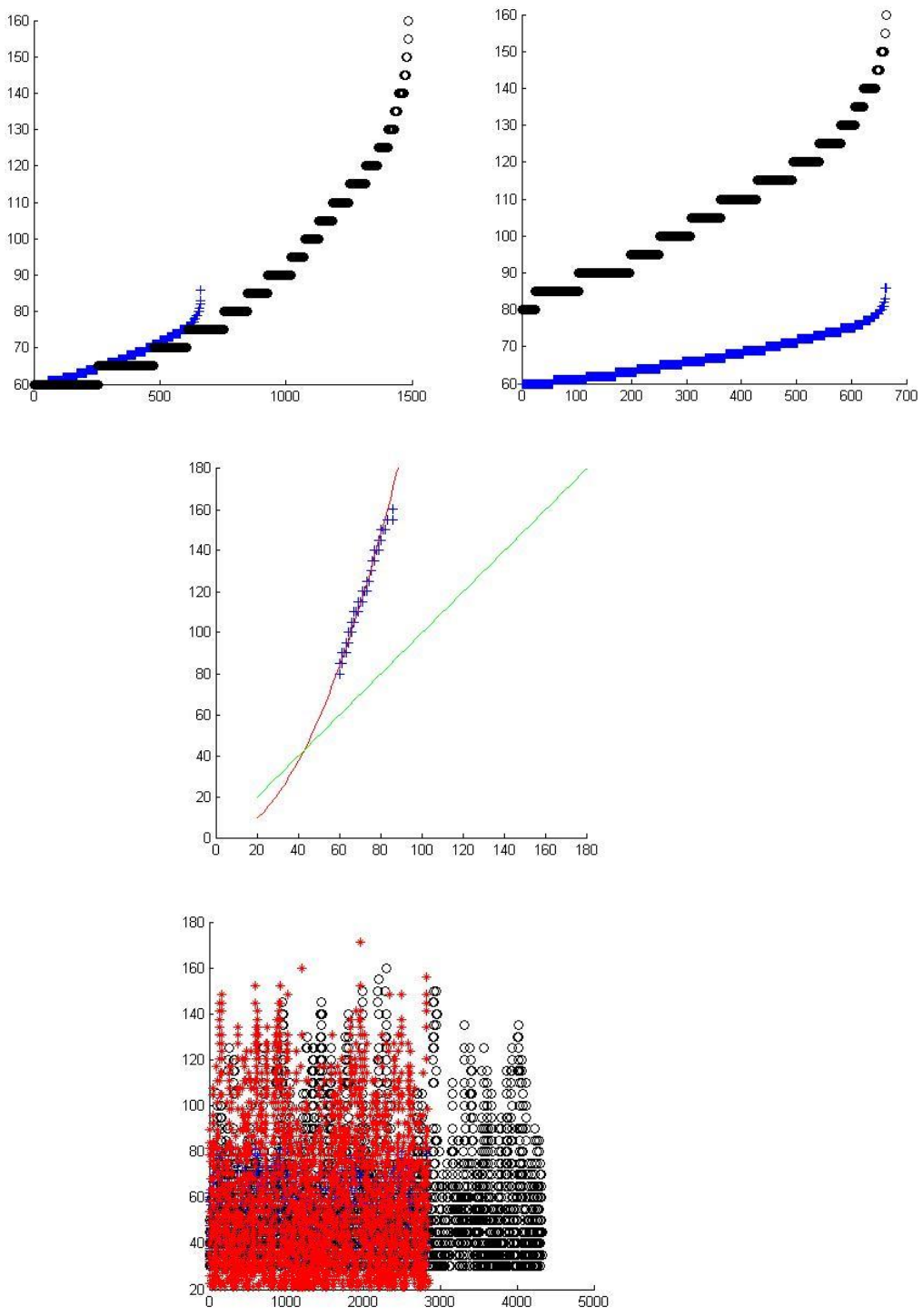

Figure 3.15.1-4 Intensity correction method 3

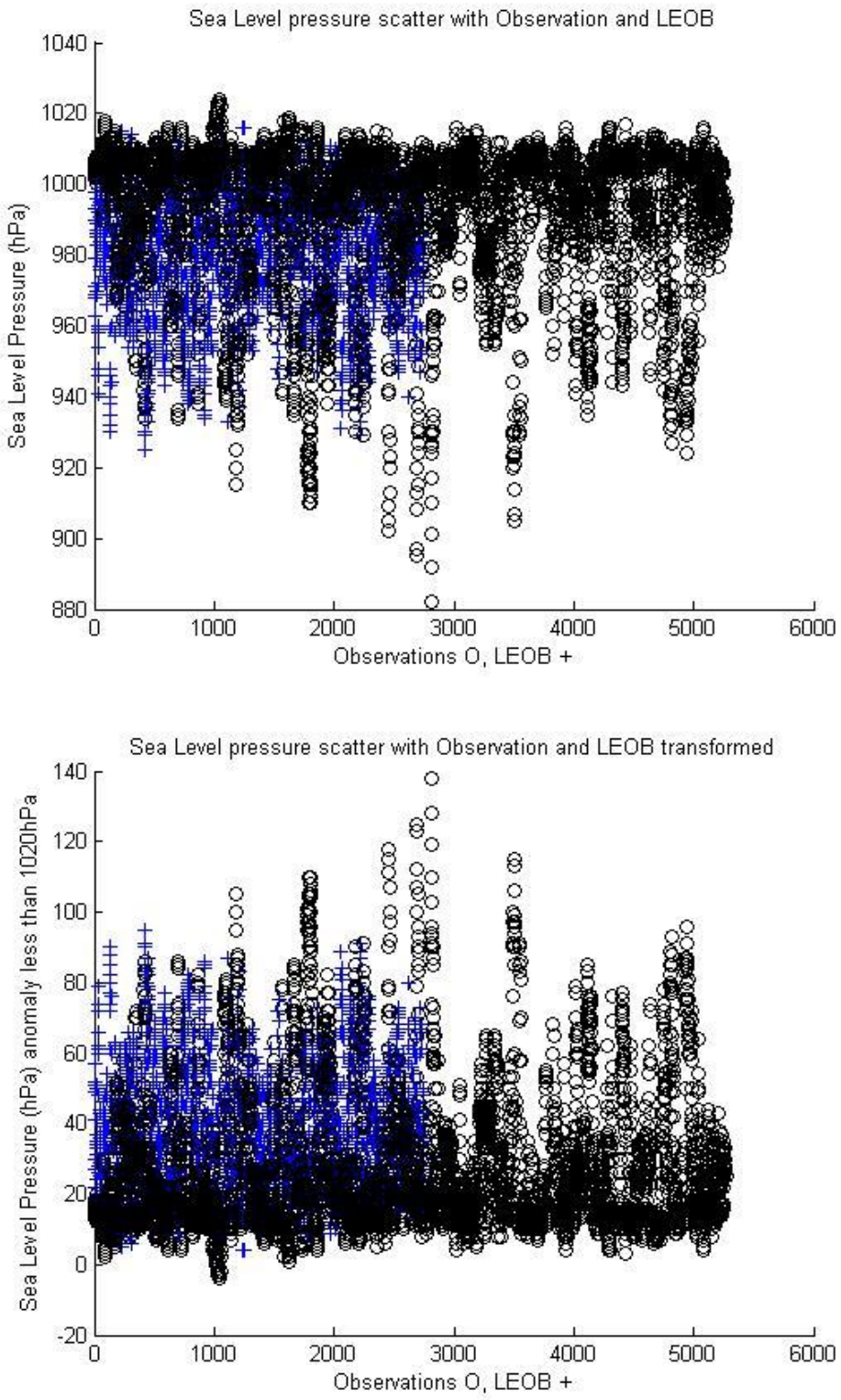

Figure 3.16.1-2 Pressure data scatter intensity correction step 1 and transform

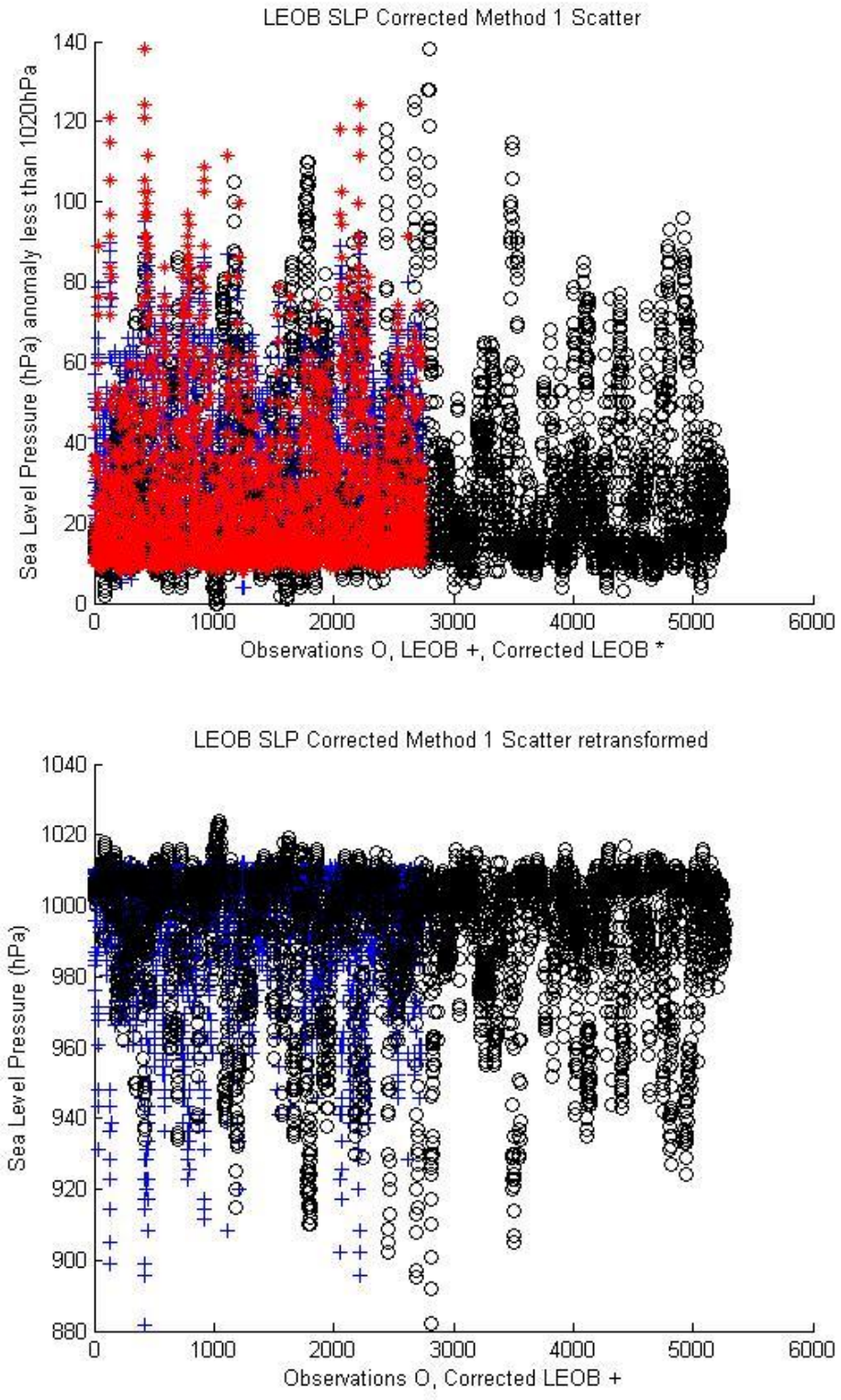

Figure 3.17.1-2 Pressure data intensity correction method 1 and retransform

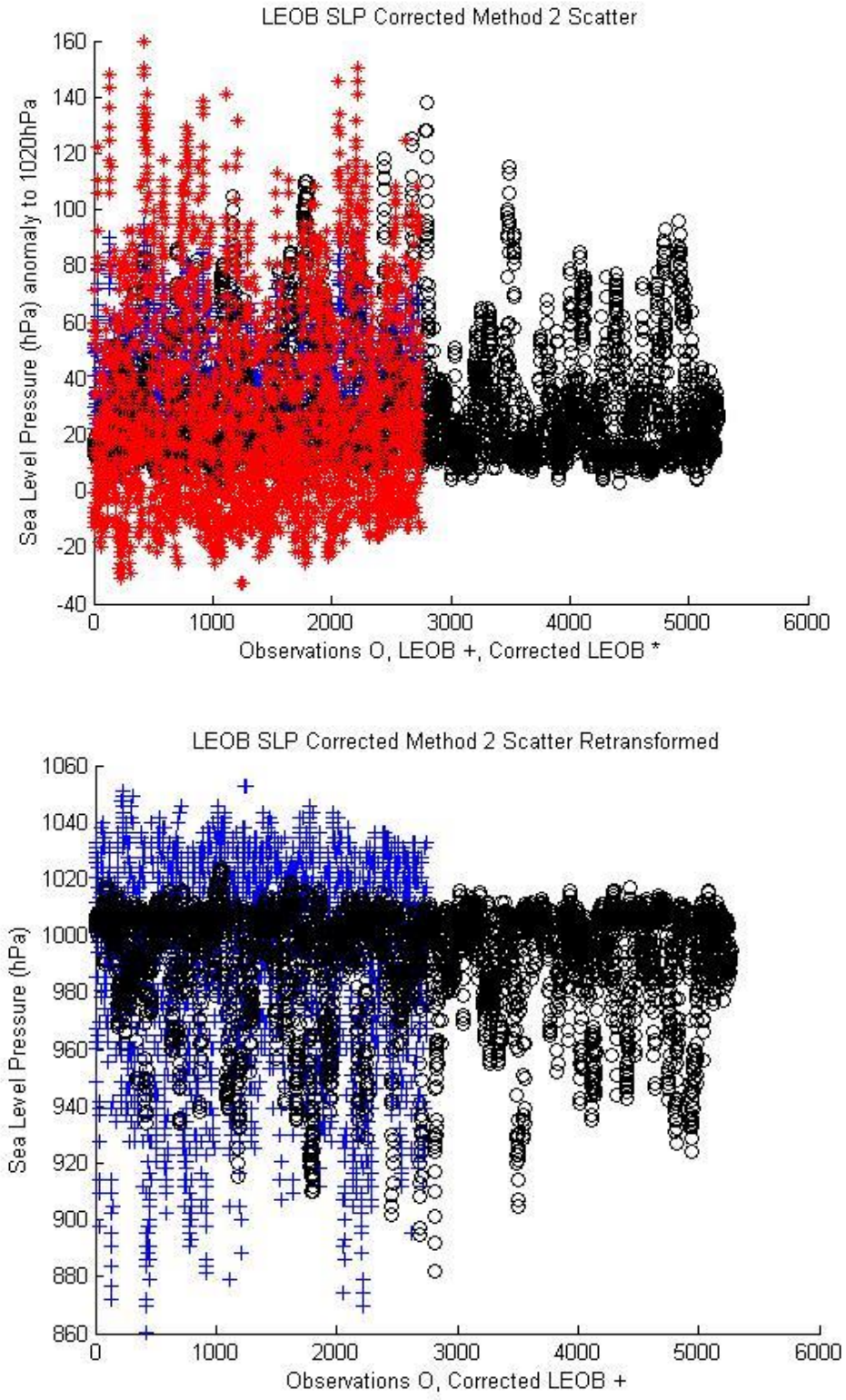

Figure 3.18.1-2 Pressure data intensity correction method 2 and retransform

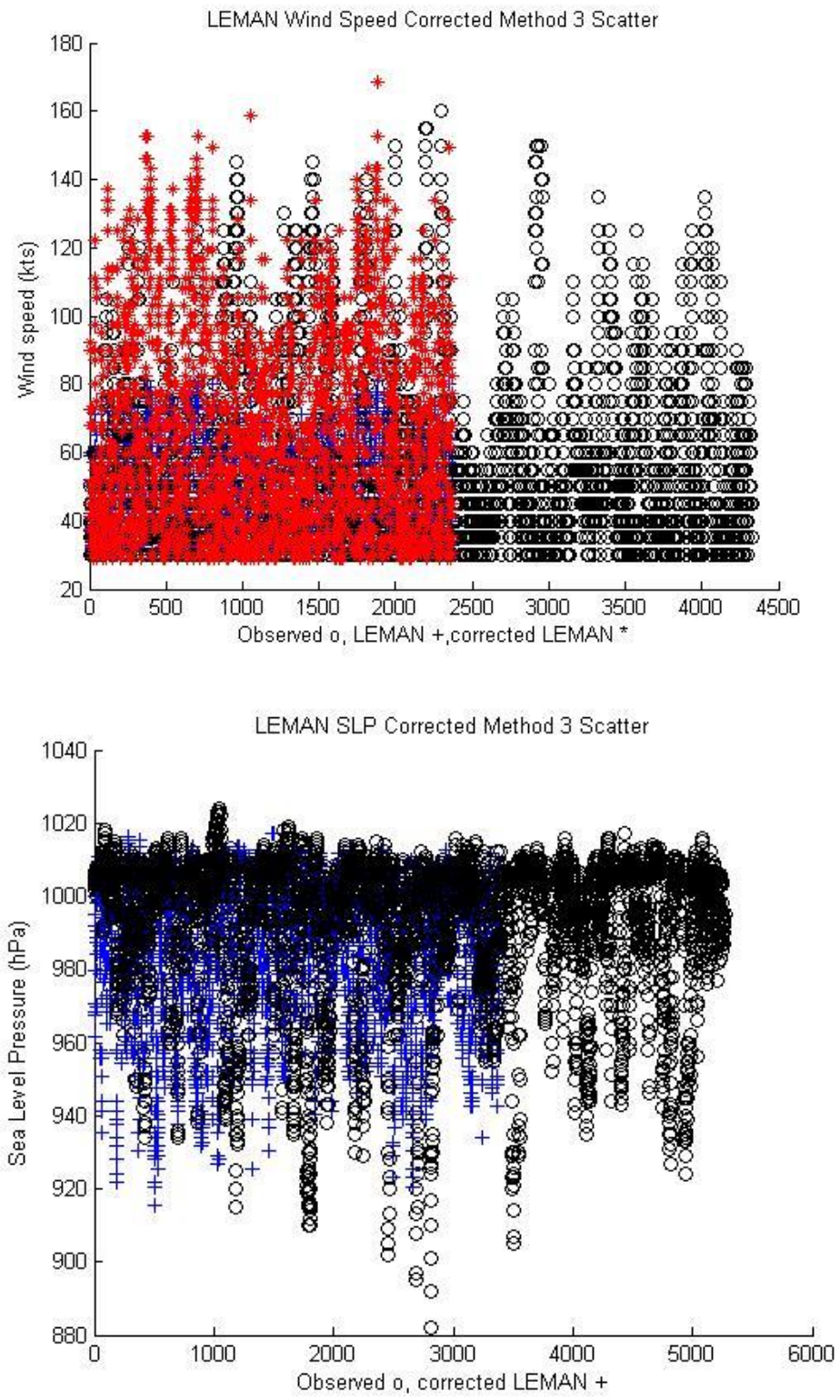

Figure 3.19.1-5 Pressure data intensity correction method 3 and retransform

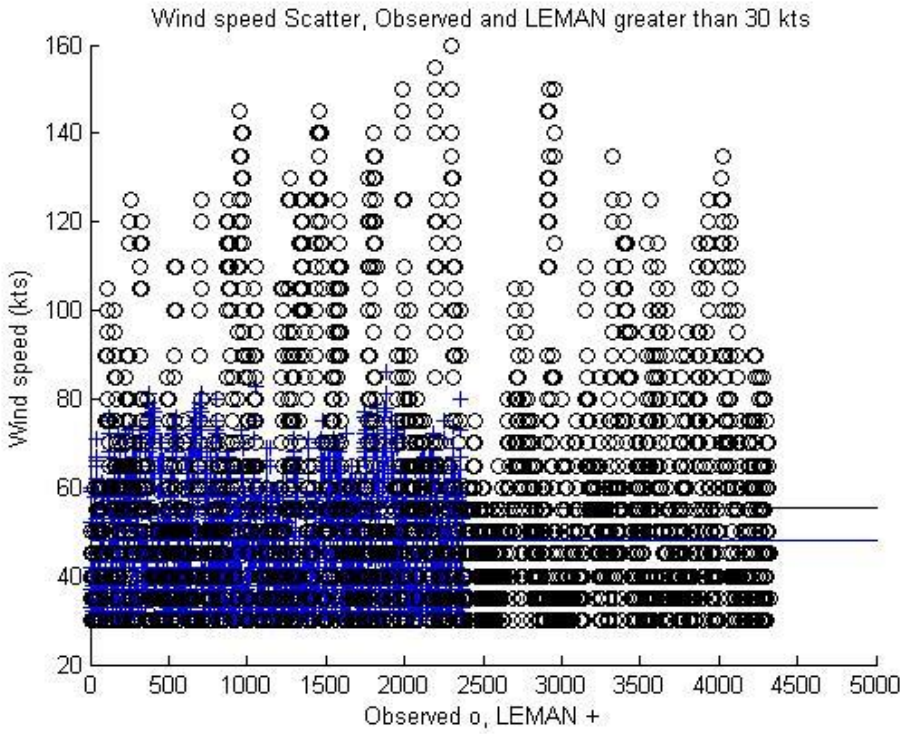

Figure 3.20.1 LEMAN data intensity correction wind data: step 1

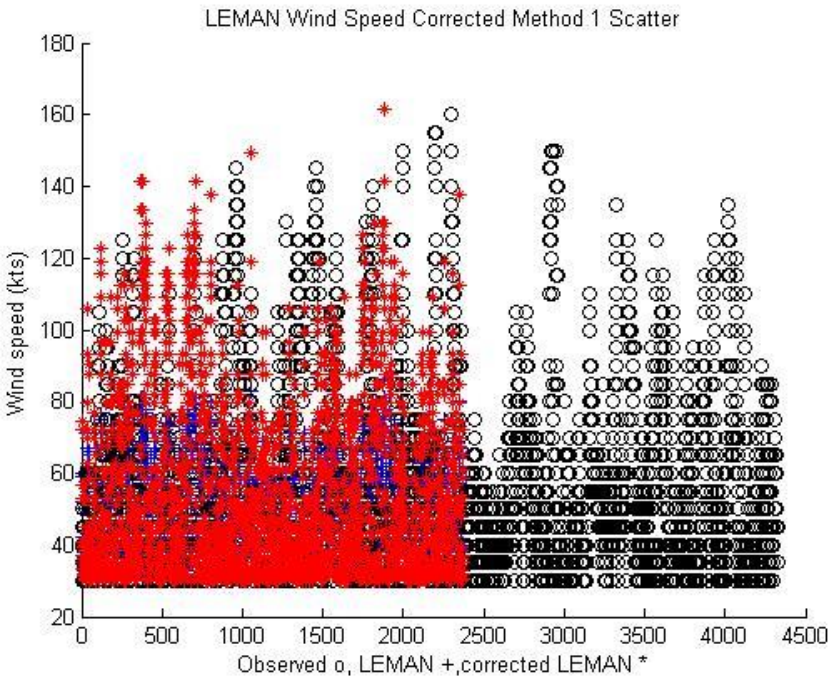

Figure 3.20.2 LEMAN data intensity correction wind data: method 1

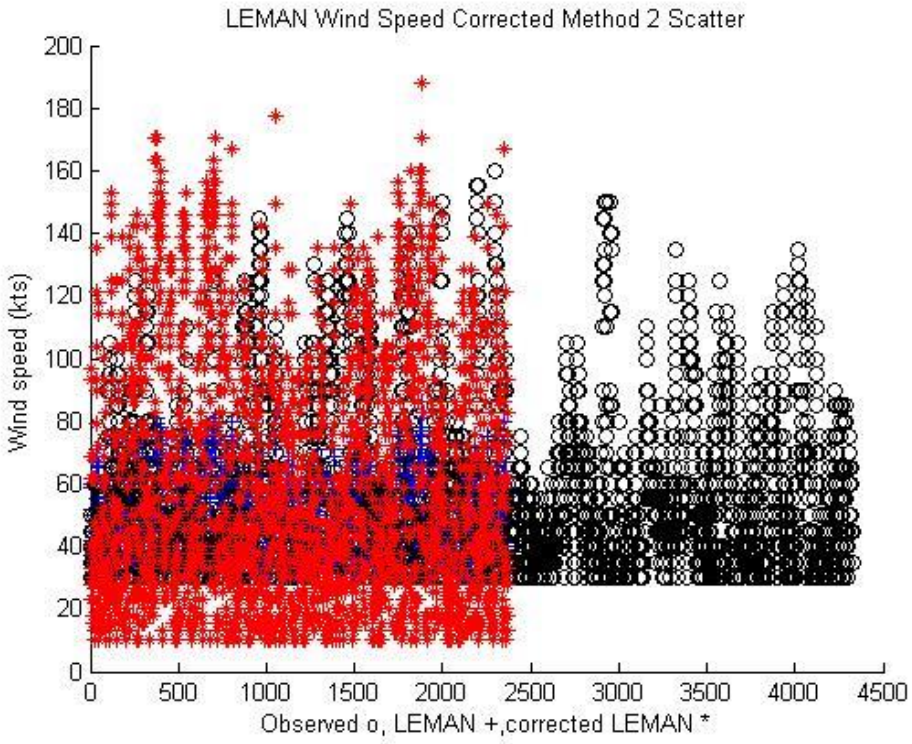

Figure 3.20.3 LEMAN data intensity correction wind data: method 2

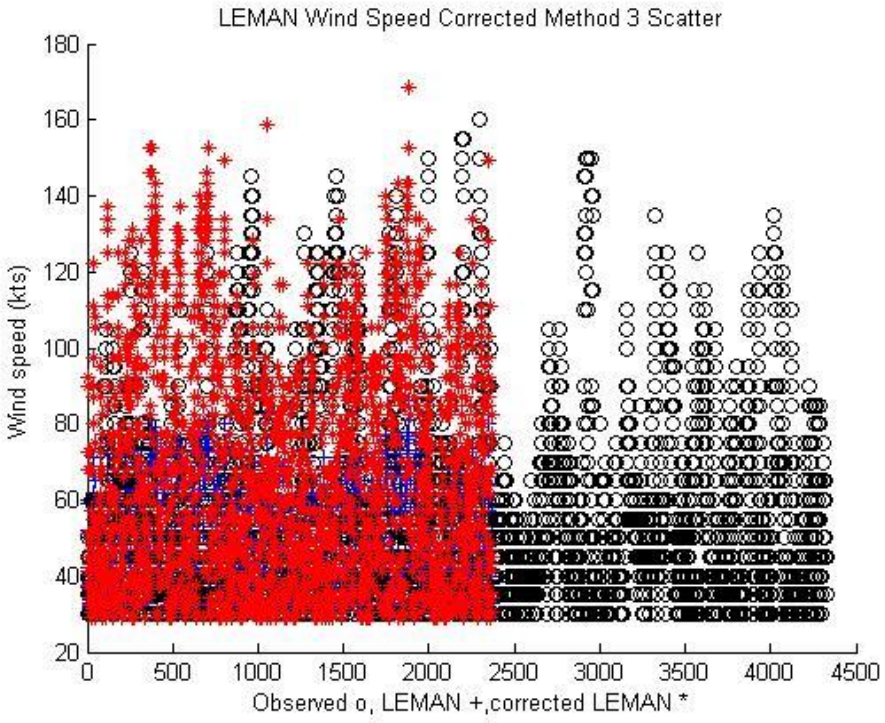

Figure 3.20.4 LEMAN data intensity correction wind data: method 3

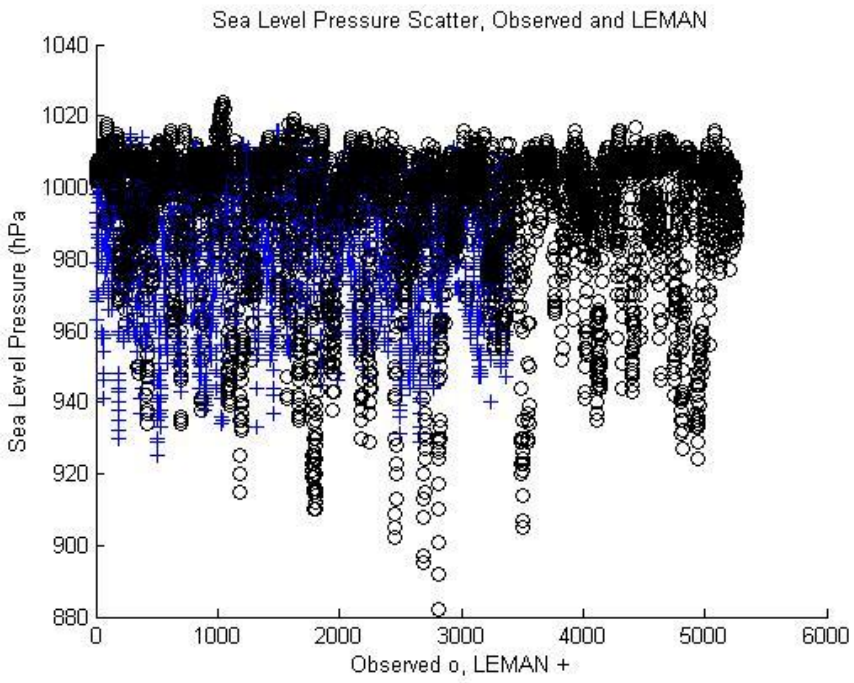

Figure 3.20.5 LEMAN data intensity correction pressure data: step 1

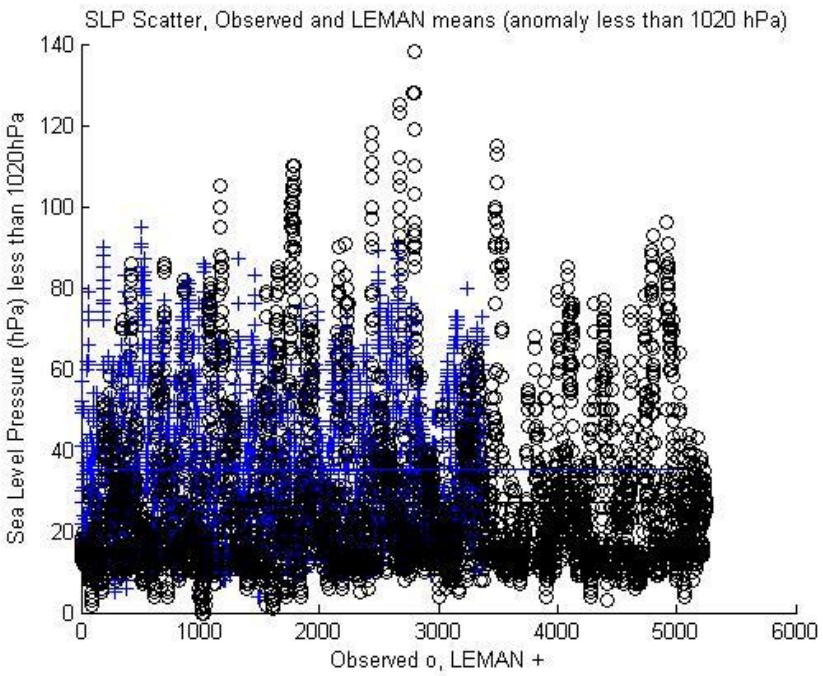

Figure 3.20.6 LEMAN data intensity correction pressure data: step 1 transformed with mean

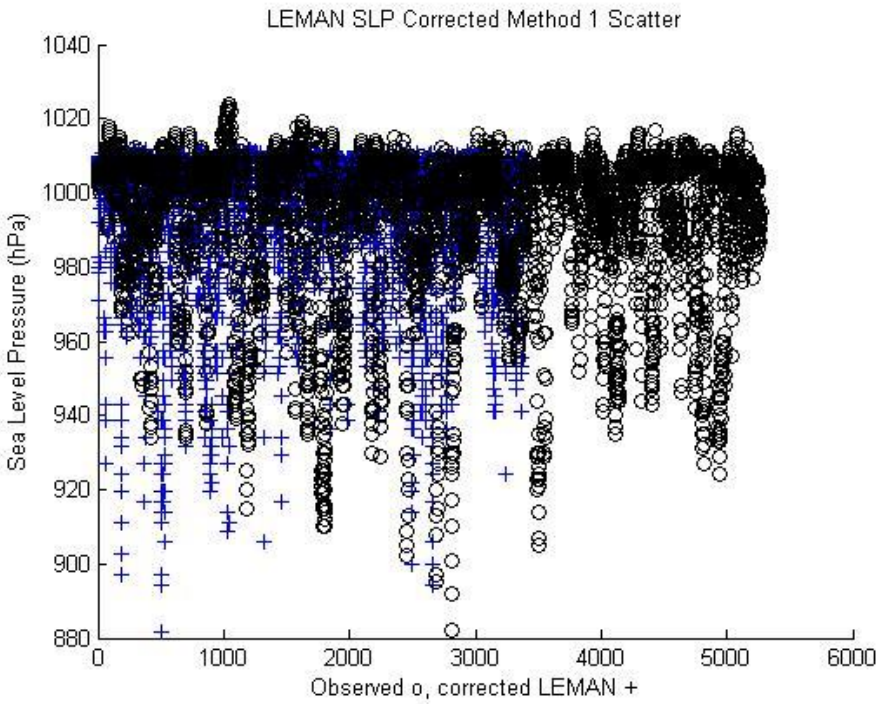

Figure 3.20.7 LEMAN data intensity correction pressure data: method 1

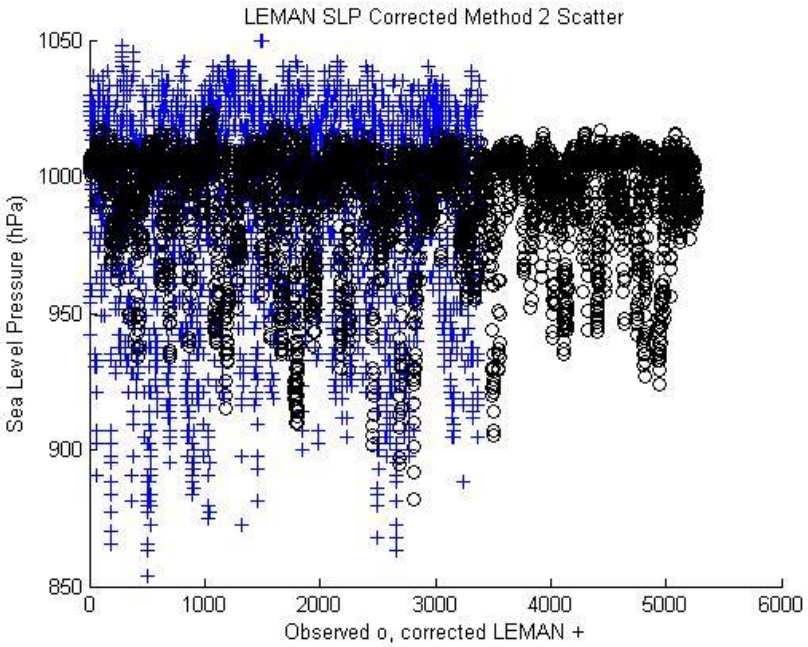

Figure 3.20.8 LEMAN data intensity correction pressure data: method 2

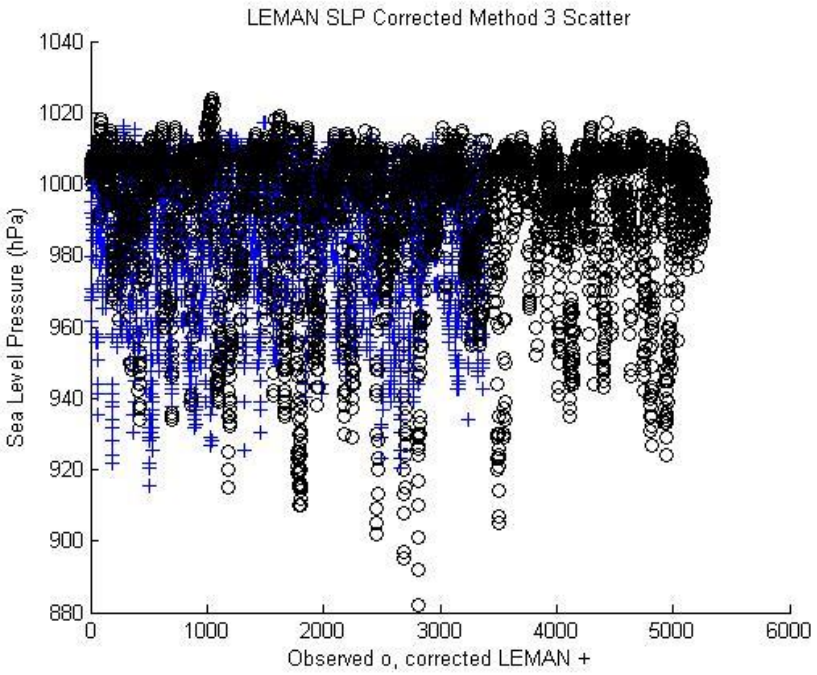

Figure 3.20.9 LEMAN data intensity correction pressure data: method 3

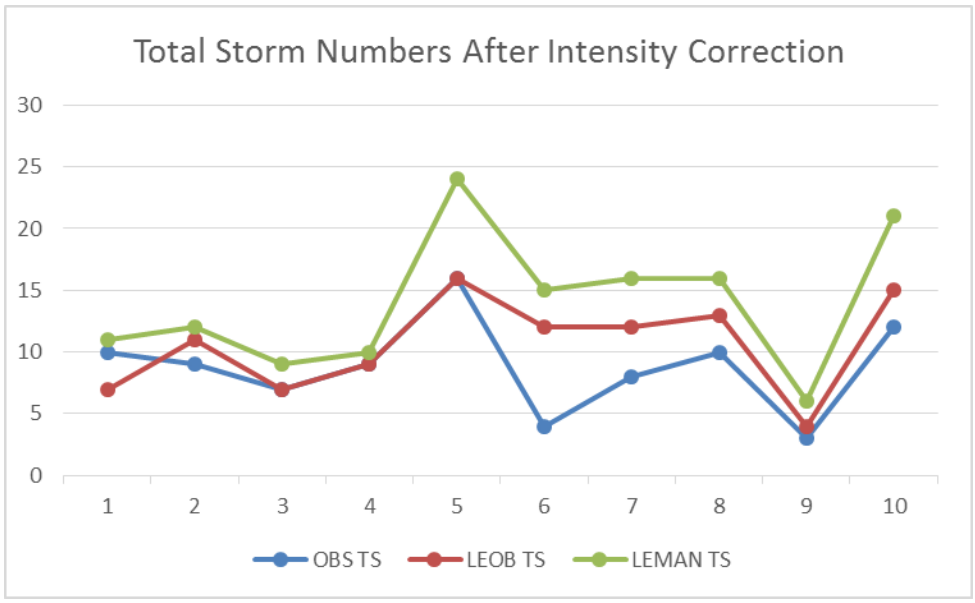

Figure 3.21.1 LEOB versus LEMAN intensity corrected total storm numbers

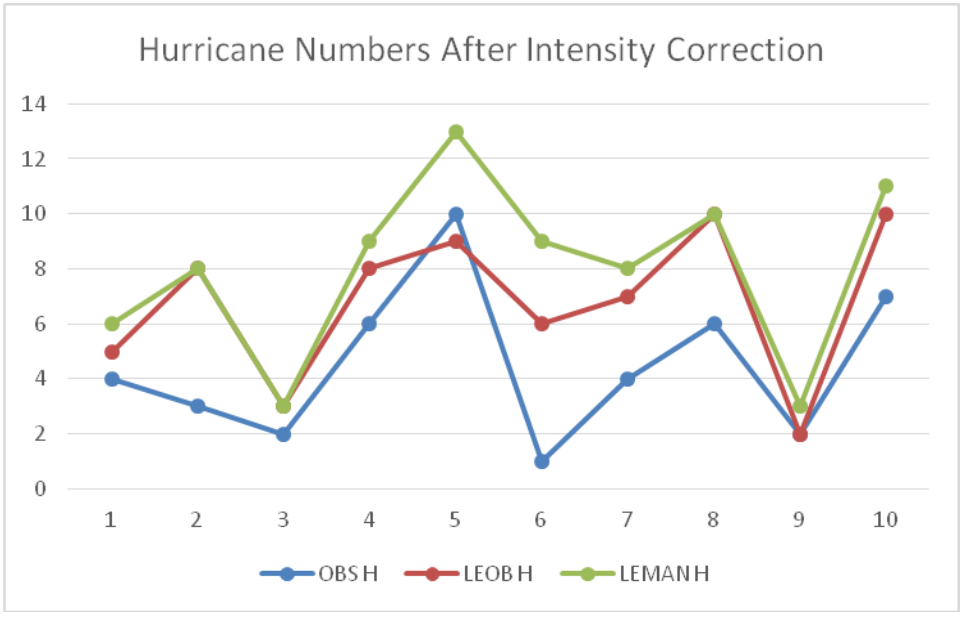

Figure 3.21.2 LEOB versus LEMAN intensity correction hurricane numbers

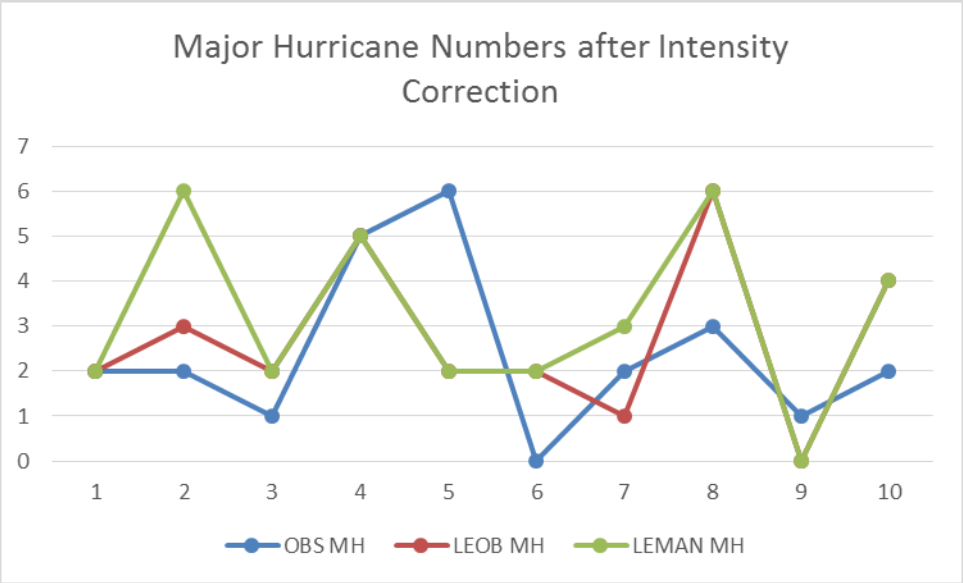

Figure 3.21.3 LEOB versus LEMAN intensity correction major hurricane numbers

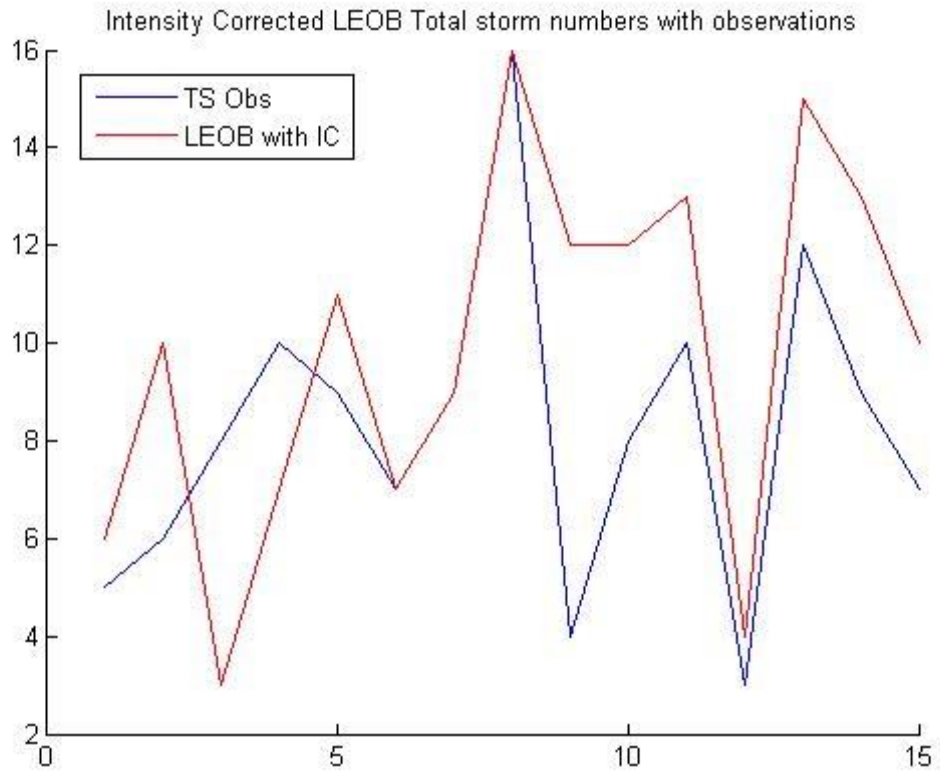

Figure 3.22.1 LEOB intensity corrected total storm numbers for all 15 years

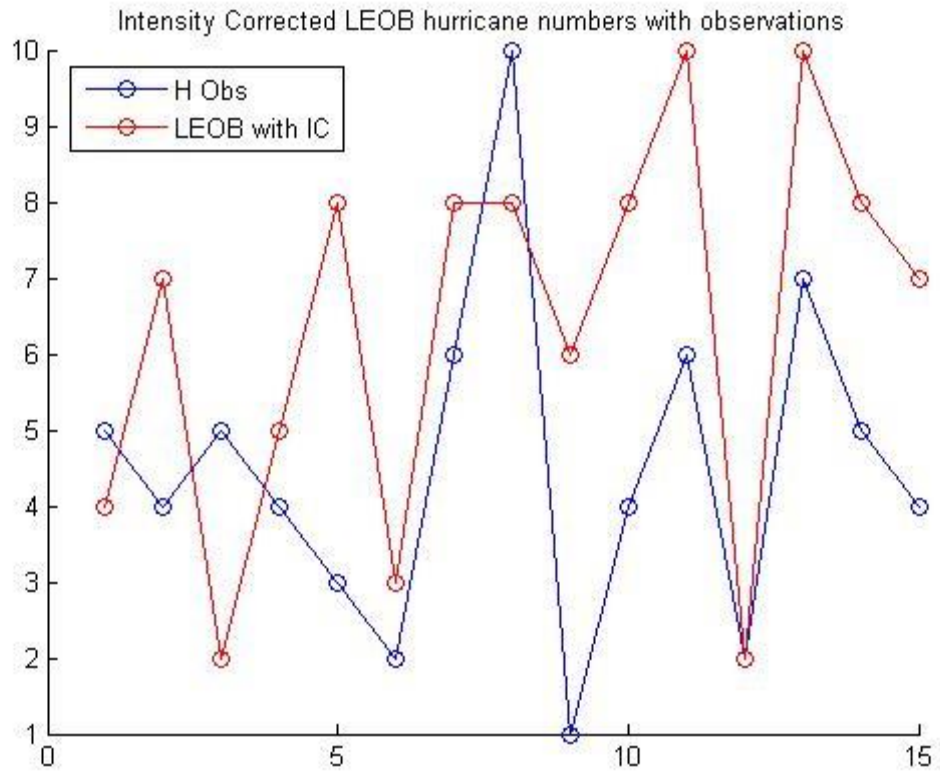

Figure 3.22.2 LEOB intensity correction hurricane numbers for all 15 years

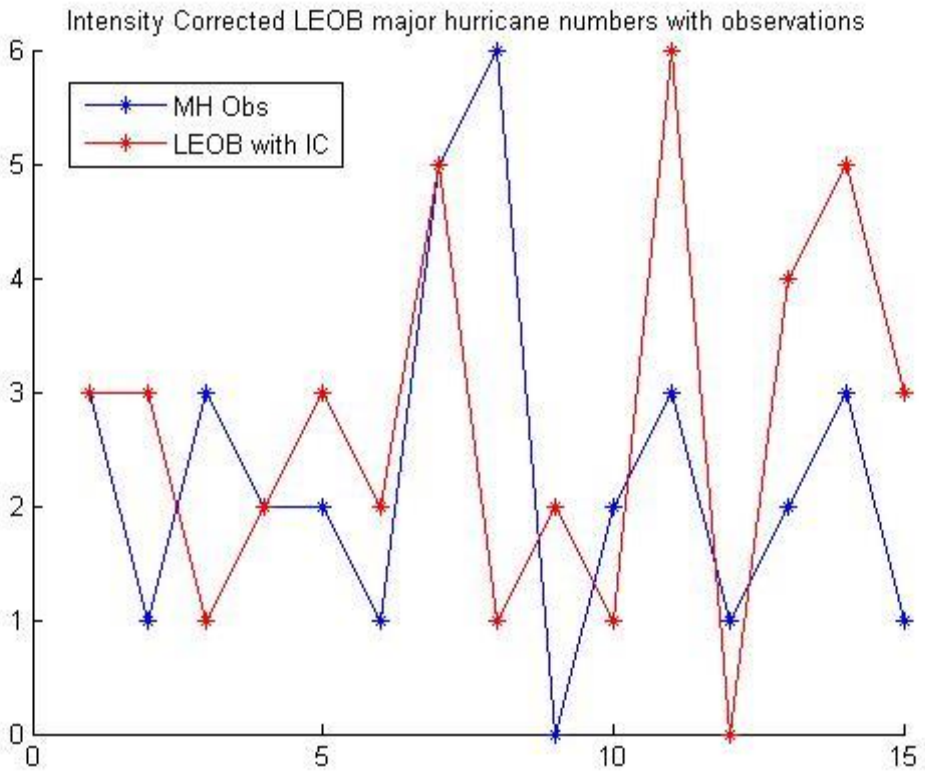

Figure 3.22.3 LEOB intensity correction major hurricane numbers for all 15 years

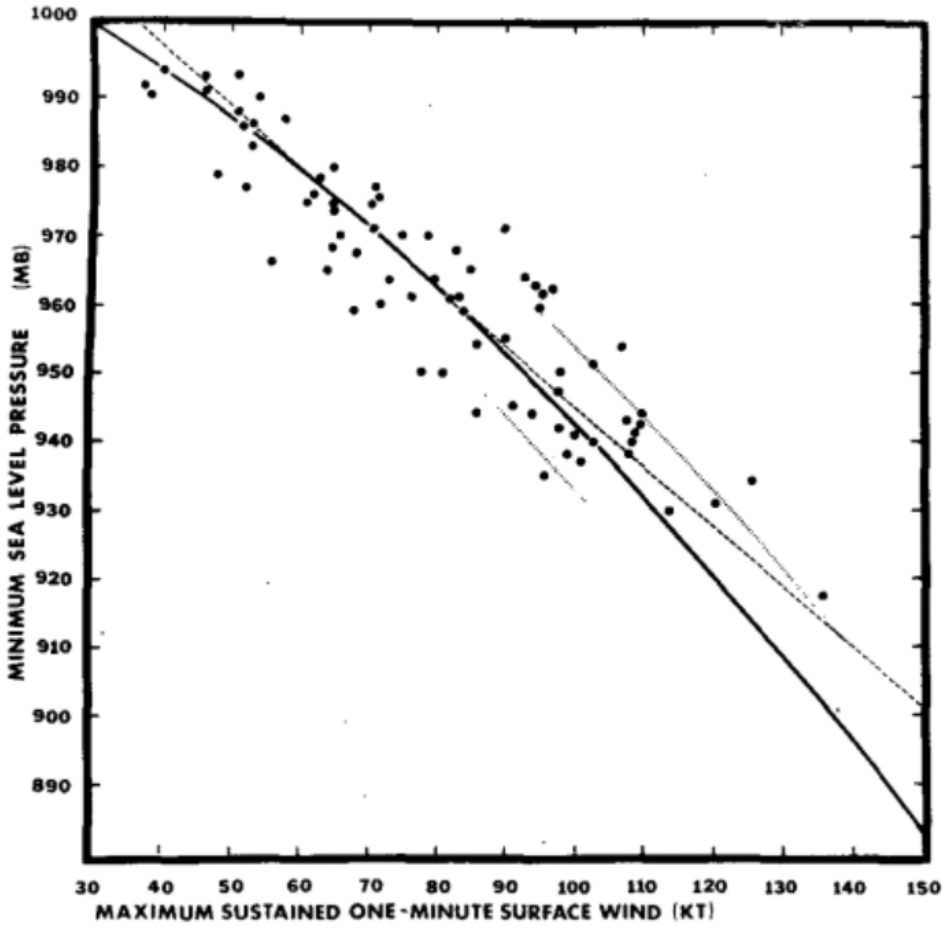

FIG. 5. Plotted data of derived sustained surface wind speeds in tropical cyclones versus minimum sea level pressures with nonlinear (solid) and linear (dashed) regression lines of best fit. Hatched lines show deviations of ±10 kt from the nonlinear regression line.

Figure 3.23 Wind-Pressure relationship result from Atkinson and Holliday (1977)

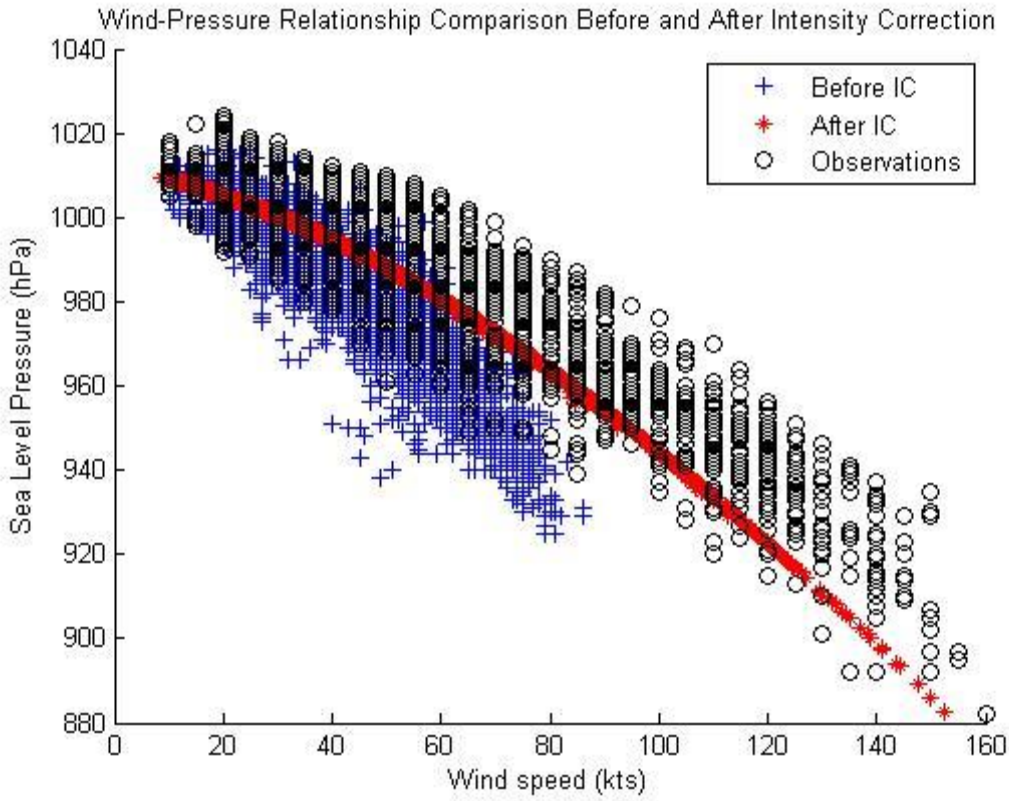

Figure 3.24 Wind-Pressure relationship, LEOB data before intensity correction, LEOB data after intensity correction, and Observed data

Chapter 4: Statistical and Dynamical downscaling

4.1 Methods

4.1.1 Statistical regression

The goal of this chapter is to further improve the dynamical results to replicate the observed frequencies of total storms, hurricanes and major hurricanes in each season. The results from the previous chapter are not very skillful at replicating the observations, especially for the general trend of major hurricanes. SSDA dynamical downscaling still needs improvement; statistical regression will be applied to this end. Regression directly uses the observations as a response variable to create coefficients and a constant for the model equation. The coefficients are applied to predictor elements of the model as weights. This equation is then used to predict or downscale the number of storms and hurricanes per year in the coastal region. Two response variables are tested with the regression, the observed coastal number and the ratio of the observed coastal number to the North Atlantic total.

4.1.2 Matlab Stepwise

The predictor analysis and regression is conducted using Matlab from MathWorks. Matlab has a statistical toolbox to conduct statistical analysis. Stepwise linear regression procedure is used to pick the best predictors for each model to correct each intensity count. The stepwise regression applies the predictors to the regression one at a time (forward) or includes all predictors in the equation and removes the predictors one at a time with highest

p-value/lowest correlation (backwards), until only the predictors with the low p-value and high correlation are left. The backwards stepwise regression is used here. The Matlab input statement is

[b , se , pval , inmodel , stats , nextstep , history] = stepwisefit(predictor_matrix, response_vector, number_of_predictors_to_include).

The stepwisefit is automated, and allows for many output statistics. It lists the coefficient (b), standard error (se), and p-value (pval) for each predictor tested, the predictors included and excluded from the model (inmodel), stats and history the last two of which collect many variables. Stats contains the models degrees of freedom for error, degrees of freedom for the regression, total sum of squares of the response, sum of squares of the residuals, F-statistic, p-value of the F-statistic, the root mean square error, the residuals for predictors not included in the model, residuals for the predictors included, beta coefficients for all even if predictor is not included, standard errors for coefficient estimates, t statistic for coefficient estimates, p-value for coefficient estimates, y intercept, and, finally, any NaN values in the model. The history collects the matrix of beta regression coefficients, root mean square errors, the degrees of freedom of the regression, and the predictors included in the model, all for every step when a predictor is removed from the model. This tool gives the best model for the given response/predictand, with the predictors to include in the model, the coefficient values to apply to the predictors, and the constant value to add. The model equation will look like this:

$$y(1:15) = \exp(Ao + \beta 1 * X(1:15,1) + \beta 2 * X(1:15,2) + \beta 3 * X(1:15,3) + \cdots + \beta N * X(1:15,N))$$

with y as the predictand vector, Ao as the constant y intercept, β the regression coefficient for each predictor, X the matrix of predictors with each predictor in separate columns.

The regression equation above has an exponent being applied to the right-hand side to allow for log-linear regression. As stated above, log-linear regression is necessary when the response variable is the count of storm or hurricanes for each year (Elsner and Villarini 2011). The stepwise procedure is done with the natural log of the response variable. To get the resulting response count values, the exponential value of the predictors with their regression coefficients are summed with the y-intercept.

4.1.3 Climate indices

General statistical hurricane predictions only use indices that represent the different climate factors that affect the hurricane numbers as the predictors. There are 32 climate indices available from NOAA Earth System Research Laboratory. The climate index data is available monthly for the entire year, and seasonal averages are commonly used in statistical modeling. Each climate predictor is narrowed down by correlating the observed number of total storms, the hurricane numbers, and the major hurricane numbers for the coastal zone. Hence, the correlation analysis rules out the months and seasons with low correlation to get one value to represent one year. The seasonal averages tested are January February March (JFM), April May June (AMJ), July August September (JAS), and October November December (OND). All three observation types are used since there needs to be 3 models for each hurricane intensity count prediction.

Stepwise procedure is used to test 768 combinations of climate predictors, for each

observation set. Many of these indices are related. The combinations do not include more than one SST, ENSO, Pacific oscillation, Atlantic oscillation, or solar index at once. The predictors used the most often of each predictor type are then tested one last time together for the best final climate predictor combination. The SST predictors that are tested are Main development region sea surface temperature (MDRSST), Dipole mode (DM), Atlantic multidecadal oscillation (AMON), Atlantic meridional mode (AMMSST), North Atlantic temperature (TNA), South Atlantic temperature (TSA), Western hemisphere warm pool (WHWP), Global GIS surface temperature anomaly (GGST), North hemisphere GIS surface temperature anomaly (NGST), South hemisphere GIS surface temperature anomaly (SGST), limited area Caribbean SSTs (LIMCAR), limited area East Atlantic SSTs (LIMEA), limited area Hawaiian SSTs (LIMHAW), limited area Indian Ocean SSTs (LIMIND), limited area Northern tropical Atlantic SSTs (LIMNTA), and limited area Southern tropical Atlantic SSTs (LIMSTA). The ENSO predictors tested are the Southern oscillation index (SOI), El Niño/Southern oscillation area 3 and 4 values (NINO34a), ENSO area 1 and 2 values (NINO12a), ENSO area 3 values (NINO3a), ENSO area 4 values (NINO4a), and Multivariate ENSO index (MEI). The other predictors that alternate in the different tests are Solar Radiation Index (SRI) and Solar Flux Index (SFI), North Atlantic Oscillation (NAO) and Arctic Oscillation (AO), and East Pacific Oscillation (EPO) and Pacific-North America index (PNA). The rest are tested in every model, Quasi-Biennial Oscillation (QBO), Main development region outgoing longwave radiation (MDROLR), MDR sea level pressure (MDRSLP), and MDR vertical wind shear (MDRVWS).

4.1.4 Dynamical predictors

The combination of climate predictors and dynamical variables will create a new form of climate modeling. This will use certain variables that affect storm and hurricane numbers in the regional model. The dynamical predictors are calculated using GrADS. The temperature difference (DTKD) between the upper atmosphere (200 hPa) and the middle levels (850 hPa level) is averaged over the section of the Main Development Region (MDR) in the regional domain, 10N to 20N and 85W to 65W. Vertical wind shear (DVWS) is the difference between the 200hPa winds and the 850 hPa winds and is averaged over the same location. The third dynamical predictor is the mean sea level pressure (DMSLP) over the same location. All three variables are averaged for each of the six months and also for 3 two month periods, 2 three month periods and other combinations for the peak of hurricane season (June, July, A, S, O, N, JJ, AS, ON, JJA, SON, JA, AS, ASO).

Once all the averages are complete, another correlation analysis is conducted to decide which month or combinations of months to use. The correlation limit value is 0.4 for storm and major hurricane numbers and 0.3 for hurricane numbers. For DTKD, the storm and hurricane numbers are well correlated with the May average, and major hurricane numbers with the March average. The December average of DVWS is correlated with the storm and hurricane numbers, and the May average with major hurricane numbers. All three models use the June average for DMSLP. The last dynamical predictor is the corrected dynamical model prediction for storm numbers, hurricane numbers, and major hurricane numbers, the LEOB data after intensity correction.

Assuming it can be known what the total North Atlantic basin storm and hurricane numbers will be for that season, it can be used as a predictor in the model to find the coastal storms. The predictor would come from the global model data that is downscaled by the regional model. Here, it is the observed total (TTS, TH, TMaH). This predictor is tested in separate models.

4.2 Climate indices tests

To choose the climate predictors and test a purely statistical regression, 768 combinations of climate predictors are tested for total storm number, hurricane numbers, and major hurricane number models. The process is automated using the stepwisefit tool. The models created are widely varied using from 1 to 7 predictors. The models using the most predictors have the least root mean square error (RMSE). To reduce this issue, a 769th stepwise test is conducted. The last test is a combination of the predictors that are used the most in all of the 768 tests. One predictor of each alternating type is chosen based on how many times it is included over its counterpart. The final test for total storm numbers begins with MDRSLP, SOI, AO, PNA, and NGST as the predictors. For hurricane numbers, the predictors starts out as AO, LIMHAW, MDRVWS, SFI, SOI, and EPO, and the final test for major hurricane numbers uses SFI, AO, EPO, SOI, QBO, and MDROLR.

The purely statistical regression for total storms in the coastal zone go through one last stepwise procedure. The 5 predictors above reduce to 4, as AO has a p-value nearer to 1. The final purely statistical log-linear regression model includes NGST, MDRSLP, SOI, and

PNA, all with p-values less than 0.02. This model:

$$y(1:15) = \exp(-289.99 + \beta 1 * NGST + \beta 2 * MDRSLP + \beta 3 * SOI + \beta 5 * PNA)$$

creates storm numbers with MAE of 0.9441. The model has a RMSE of 0.1930 (Table 4.1), which is better than most of the 768 tests, but not the lowest RMSE. Figure 4.1 shows the statistical model frequency against the observed numbers. This model performs fairly well when compared with the observations.

This total storm model suggests that the Northern Hemisphere land- and sea- surface temperature anomaly, sea level pressure in the Main Development Region, Southern Oscillation Index, and Pacific/North American index have the most influence on the North Atlantic coastal zone storm frequency. NGST is the northern hemispheric surface temperature monthly anomaly from a 30 year mean. When NGST is positive, the total storm numbers in the North Atlantic might be above average. MDRSLP has a more direct connection with tropical cyclone numbers. When MDRSLP is low/below average, tropical cyclones have above average intensities and are more frequent. SOI indicates ENSO patterns through sea level pressure anomalies. Negative phase SOI corresponds with positive phase ENSO, which prevents Atlantic storm formation. PNA represents the alternating 500hPa geopotential heights over N Pacific and NW North America. Positive PNA brings high heights over SE US and NW Atlantic, preventing recurvature, which aids in longer lived tropical cyclones.

The purely statistical regression model for hurricanes in the coastal zone last stepwise procedure produces a model with 3 predictors, AO, SFI, and EPO. These predictors have p-

values below 0.05, the lowest belonging to EPO with 0.0014. This model:

$$yh(1:15) = \exp(0.7866 + \beta 1 * AO + \beta 4 * SFI + \beta 6 * EPO)$$

follows the observed trend very well (Figure 4.2). The MAE is less than that of the total storm numbers above. The regression coefficients β and model error statistics are listed in table 4.2. This model performs well with these three predictors relating to hurricane counts. The AO represents the oscillations of the coupled atmospheric pressures over the pole and the subtropics. In the positive phase, the atmospheric pressure over the North Pole is lower than normal and the subtropical high pressure is higher than normal, allowing stronger trade winds and preventing recurvature of hurricanes. SFI affects the hurricane intensity and temperature. EPO represents the oscillation of the coupled pressures over the NE Pacific, similar to the NAO, with a similar effect as the PNA in positive phase. These predictors generally affect the lifetime of the storm, with positive phase allowing storms to develop into hurricanes in the coastal zone.

The final retest of statistical predictors is for major hurricane numbers. The pure statistical major hurricane regression model ends up containing 4 predictors, MDROLR, SOI, EPO, and SFI. The p-values of these predictors remain below 0.02. SOI and EPO have the lowest p-values, lower than 0.001. The model:

$$ymh(1:15) = \exp(-42.299 + \beta 1 * MDROLR + \beta 3 * SOI + \beta 4 * EPO + \beta 6 * SFI)$$

creates major hurricane numbers that generally follow the trend of the observations. An exception to this is that for the first 5 years the trend in the observations appears opposite to that of the models (Fig. 4.3). The biggest error is for 1997, where the modeled number of

major hurricanes is much greater than the observed number. The overall error is still very low. The regression coefficients and model error statistics are in Table 4.3. The one different predictor here than the two before is the MDROLR. This can be a measure of cloud top height. Lower MDROLR values mean higher cloud tops. Higher cloud tops represent stronger storms, and cloud areas that can form into strong major hurricanes. The next section combines these models with dynamical variables.

4.3 Statistical and Dynamical Model Tests

4.3.1 Coastal Zone Total Storm Hybrid Model Tests

Taking the statistical model for total storm numbers above, the hybrid model is created by adding the dynamical variables, DTKD, DMSLP, DVWS, and the intensity corrected LEOB total storm number. As above, a simple log-linear regression model is created using backwards stepwise technique. The procedure removes the dynamically predicted number of total storms, DMSLP, and DVWS. These predictors had p-values greater than 0.05. The only aspect that makes this model a hybrid statistical-dynamical model is the DTKD:

$$y(1:15) = \exp(-344.83 + \beta 2 * DTKD + \beta 5 * NGST + \beta 6 * MDRSLP + \beta 7 * SOI + \beta 8 * PNA)$$

This model, when all values are applied for regression coefficient (Table 4.4), results in values for each year that match with the observations (Fig. 4.4) with a MAE of 0.5428 and RMSE of 0.1101. This model simulates the number of storms for the coastal zone better than

the values produced by pure dynamical model SSDA LEOB, which the stepwise procedure found to be unskillful.

A second total storm model test includes the entire North Atlantic storm numbers. These values are applied as a ninth predictor to be tested in the stepwise procedure. This predictor is removed, in addition to the same predictors in the first test, producing the same model as the first:

$$y(1:15) = \exp(-344.83 + \beta 2 * DTKD + \beta 5 * NGST + \beta 6 * MDRSLP + \beta 7 * SOI + \beta 8 * PNA)$$

The number of storms created by this second test are the same as the first (Fig. 4.5).

The third and final test for total storm number linear regression model uses the ratio of the coastal zone observed number of storms to the full North Atlantic number of storms as the response variable. The stepwise procedure again produces a model with the same predictors as the first two tests above:

$$y(1:15) = TTS * (-94.45 + \beta 2 * DTKD + \beta 5 * NGST + \beta 6 * MDRSLP + \beta 7 * SOI + \beta 8 * PNA)$$

However, this model has higher error than the first two. The MAE is 2.9806 and is noticeable in Figure 4.6 for all years except 2005. The regression coefficients and the model error statistics for the three regression tests are listed in Table 4.4.

4.3.2 Coastal Zone Hurricane Hybrid Model Tests

The predictors chosen for the purely statistical model for hurricane numbers are combined here with the dynamical predictors to create a hybrid model for hurricane numbers.

The stepwise procedure removed four predictors and included the DMSLP and EPO for the hurricane log-linear model:

$$yh(1:15) = \exp(-447.35 + \beta 1 * DMSLP + \beta 7 * EPO)$$

This model is a simple form of statistical-dynamical model, with one dynamical predictor and one climate predictor. The MAE here is 0.7707. This model regression's results do not reach many of the peaks seen in the observations (Fig. 4.7). The regression coefficients and other error statistics for all hurricane regression tests are in table 4.5.

The second hurricane regression test adds a predictor of the hurricane numbers for the entire North Atlantic. The stepwise procedure creates a model that includes DMSLP, EPO and TH:

$$yh(1:15) = \exp(-368.26 + \beta 1 * DMSLP + \beta 7 * EPO + \beta 8 * TH)$$

This model has MAE of 0.5495, and follows the trend of the observations very well (Fig. 4.8).

The third hurricane regression test uses the basin total storm numbers as the 8th predictor. This relates the number of hurricanes in the coastal zone to the number of total storms that form in the North Atlantic. The stepwise regression includes the same predictors as before, DMSLP, EPO, and TTS:

$$yh(1:15) = \exp(-377.22 + \beta 1 * DMSLP + \beta 7 * EPO + \beta 8 * TTS)$$

This model performs very closely with the second test, as can be seen in figure 4.9 and the MAE, 0.5524. The hurricane regression tests handle the basin total predictors much better than the tests for total storm number regression models.

This second to last hurricane regression test uses the ratio of coastal hurricane numbers to basin total hurricane numbers as the response variable. The stepwise procedure included DMSLP, AO and EPO as the predictors for the model:

$$yh(1:15) = \mathrm{TH} * (-54.23 + \beta 1 * DMSLP + \beta 5 * AO + \beta 7 * EPO)$$

The MAE for this model is greater than for the previous hurricane regression tests, 1.8188. The resulting hurricane numbers follow the trend in the observations very well (Fig. 4.10). However, the values are lower for every year.

The final hurricane regression test uses the ratio response, but from coastal hurricane numbers to basin total storm numbers. Like the third hurricane regression test, this acknowledges the relationship that hurricane numbers in the coastal zone rely on the total storm numbers in the basin. The stepwise procedure includes the same predictors as the fourth hurricane regression test, DMSLP, AO, and EPO:

$$yh(1:15) = \mathrm{TTS} * (-31.28 + \beta 1 * DMSLP + \beta 5 * AO + \beta 7 * EPO)$$

This model has lower MAE than the fourth test, with MAE of 1.6725. They perform very similarly though (Fig. 4.11).

4.3.3 Coastal Zone Major Hurricane Hybrid Model Tests

As previously, the predictors chosen in the purely statistical regression from major hurricanes are combined with dynamical variables and the dynamically detected number of major hurricanes. This statistical regression is necessary to fix any remaining issues in major hurricane detection after the intensity correction. The statistical errors and regression coefficients for these tests are displayed in table 4.6. The first major hurricane regression test

only includes the climate predictors, MDROLR, SOI, EPO and SFI. The stepwise procedure found all the dynamical predictors to be unskillful in predicting major hurricanes. The model appears the same as the pure statistical model,

$$ymh(1:15) = \exp(-42.299 + \beta5 * MDROLR + \beta6 * SOI + \beta7 * EPO + \beta8 * SFI)$$

and the MAE is the same, 0.8845. The results in figure 4.12 are the same as figure 4.3. Also, the second, third and fourth major hurricane regression tests remove all the dynamical variables and keep the purely statistical model. These tests included the basin wide numbers for major hurricanes, hurricanes and total storms as a 9th predictor respectively.

The fifth major hurricane regression test uses a ratio response of coastal major hurricanes to total major hurricanes. The stepwise procedure includes two dynamical variables and one climate index, DTKD, DVWS, and EPO. The model appears as:

$$ymh(1:15) = \text{TMH} * (-20.225 + \beta2 * DTKD + \beta3 * DVWS + \beta7 * EPO)$$

This model follows the general trend in the observations (Fig. 4.13), but the values are still lower than observations for many of the years. The MAE for this model is 0.9530.

The sixth major hurricane regression test uses the ratio response of major hurricanes in the coastal zone to hurricanes in the entire basin. The stepwise procedure includes the same predictors as the fifth test. The model is the same as before, but multiplied by the total number of hurricanes rather than major hurricanes:

$$ymh(1:15) = \text{TH} * (-9.438 + \beta2 * DTKD + \beta3 * DVWS + \beta7 * EPO)$$

The MAE for this model is slightly less at 0.9524.

Following along with this trend of tests, this last regression test uses the ratio

response of major hurricanes to basin-wide storm numbers, and creates a model that includes the same predictors as the fifth and sixth tests. The model appears similar, with multiplication by total number of storms for the entire basin:

$$ymh(1:15) = \mathrm{TTS} * (-5.445 + \beta 2 * DTKD + \beta 3 * DVWS + \beta 7 * EPO)$$

The MAE for this model is 0.9524, also. Even though these last three models had similar errors, and similar predictors, the results do differ, as can be seen in figures 4.13-15 and in the value of the y-intercept. The intercept shows the largest negative value for the first ratio major hurricane regression test, and the least negative value for the last ratio major hurricane regression test.

4.3.4 Best Statistical and Dynamical Model

The best model of each type of statistical-dynamical model must first include a dynamical variable, and secondly have the lowest MAE of the tests. For total storm numbers, the best model is created by both the first and second tests. The predictors included are DTKD, NGST, MDRSLP, SOI, and PNA. This adds to the purely statistical model by one dynamical variable. This variable represents the upper atmospheric warm temperatures necessary for tropical storm development. The best model for hurricane numbers is created by the second test. This model includes DMSLP, EPO and the basin wide number of hurricanes as predictors. The first predictor represents the average sea level pressure for the MDR in the coastal zone. When these values are low, the number of hurricanes is expected to be high. This model also assumes there is a prior knowledge of the basin wide hurricane numbers, which is not a problem in downscaling. The best model for major hurricane

numbers does not have the lowest MAE. It can either be the 6th or 7th tested model. Both assume a prior knowledge of basin wide numbers, hurricanes and total storms respectively. These models both use EPO and two dynamical predictors. DVWS represents the average vertical wind shear over the MDR in the coastal zone, which would need to be low if the numbers of major hurricanes are to be above average.

4.4 Statistical vs. Dynamical vs. Statistical and Dynamical model

The results of each type of model used in this thesis, SSDA LEOB after intensity correction, pure statistical model, and combined statistical and dynamical model, are plotted in figures 4.16-18 for total storm numbers, hurricane numbers and major hurricane numbers respectively. The hybrid statistical-dynamical model performs best for tropical cyclone number and hurricane numbers. For major hurricane numbers, the pure statistical model performs the best, but the error is only greater in the statistical-dynamical models by 0.1 storms.

Table 4.1 Purely Statistical Total storms regression coefficients, p-value, standard error, model root mean square error, and model mean absolute error

Predictor	**NGST**	**MDRSLP**	**SOI**	**AO**	**PNA**	**Full Model**
Beta	0.007768	0.2873388	0.17163401	0	0.164838	
P-value	0.009378	0.0043831	0.00132338	0.12543	0.018594	
SE	0.002422	0.0784902	0.03895777	0.09082	0.058739	
RMSE						0.193
MAE						0.9441

Table 4.2 Purely Statistical Hurricanes regression coefficients, pval, SE, model RMSE, and model MAE

Predictor	**AO**	**LIMHAW**	**MDRVWS**	**SFI**	**SOI**	**EPO**	**Full model**
Beta	-0.39215	0	0	0.000478	0	-0.37166906	
P-value	0.01249	0.8063883	0.90885318	0.042809	0.234102	0.00142244	
SE	0.13154	0.4461808	0.09998381	0.000209	0.103298	0.08795248	
RMSE							0.318636813
MAE							0.8801

Table 4.3 Purely Statistical Major Hurricanes regression coefficients, pval, SE, model RMSE, and model MAE

Predictor	**SFI**	**AO**	**EPO**	**SOI**	**QBO**	**MDROLR**	**Full model**
Beta	0.15619	0	0.79546565	-1.47572	0	0.00125058	
P-value	0.00737	0.6631819	0.000141	0.000217	0.271274	0.01139162	
SE	0.046629	0.0174036	0.13366326	0.261956	0.728989	0.00040437	
RMSE							0.664163575
MAE							0.8845

Table 4.4 Statistical-Dynamical Total storms regression coefficients, pval, SE, model RMSE, and model MAE

Predictor	**DMSLP**	**DTKD**	**DVWS**	**DTS**	**NGST**	**MDRSLP**	**SOI**	**PNA**	**TTS**	**Full Model**
Beta1	0	0.405989	0	0	0.007063	0.370830	0.153421	0.135632		
Pvalue1	0.83956	0.001183	0.350943	0.215254	0.000662	3.03E-05	7.91E-05	0.003212		
SE1	0.06640	0.087098	0.085261	0.012746	0.00139	0.048226	0.022565	0.03409		
RMSE1										0.1101
MAE1										0.5428
Beta2	0	0.405989	0	0	0.007063	0.370830	0.153421	0.135632	0	
Pvalue2	0.83956	0.001183	0.350943	0.215254	0.000662	3.03E-05	7.91E-05	0.003212	0.7217	
SE2	0.06640	0.087098	0.085261	0.012746	0.00139	0.048226	0.022565	0.03409	0.0217	
RMSE2										0.1101
MAE2										0.5428
Beta3	0	0.147881	0	0	0.001831	0.104001	0.034607	0.050726		
Pvalue3	0.28386	0.000492	0.291175	0.522467	0.002626	8.52E-05	0.000988	0.001208		
SE3	0.01975	0.027892	0.026865	0.004399	0.000445	0.015444	0.007226	0.010917		
RMSE3										0.0353
MAE3										2.9806

Table 4.5 Statistical-Dynamical Hurricanes regression coefficients, pval, SE, model RMSE, and model MAE

Predictor	**DMSLP**	**DTKD**	**DVWS**	**DH**	**AO**	**SFI**	**EPO**	**TTS,TH**	**Full model**
Beta	0.443858	0	0	0	0	0	-0.32173978		
Pvalue	0.000286	0.1577542	0.35713486	0.918011	0.221554	0.95417087	0.000268019		
SE	0.087933	0.15897	0.10817348	0.031186	0.101988	0.00017346	0.063261406		
RMSE									0.244441
MAE									0.7707
Beta2	0.365194	0	0	0	0	0	-0.24459429	0.055588	
Pvalue2	0.001047	0.5777897	0.81889309	0.873902	0.646022	0.97447373	0.002772323	0.041852	
SE2	0.08282	0.1718432	0.10507387	0.026851	0.10432	0.00014948	0.063786306	0.024143	
RMSE2									0.209727
MAE2									0.5495
Beta3	0.373934	0	0	0	0	0	-0.26423865	0.03676	
Pvalue3	0.000778	0.8878907	0.94692853	0.582762	0.606475	0.8620083	0.001038966	0.042611	
SE3	0.08148	0.23749	0.11343813	0.027016	0.102796	0.00015039	0.059865119	0.016037	
RMSE3									0.21003
MAE3									0.5524
Beta4	0.053948	0	0	0	-0.08369	0	-0.07247149		
Pvalue4	0.099165	0.5374407	0.92744047	0.107155	0.027076	0.82915244	0.004742573		
SE4	0.029956	0.0738212	0.05674982	0.012926	0.03284	6.43E-05	0.020549593		
RMSE4									0.076571
MAE4									1.8188
Beta5	0.031124	0	0	0	-0.04828	0	-0.04181048		
Pvalue5	0.099165	0.5374407	0.92744047	0.107155	0.027076	0.82915244	0.004742573		
SE5	0.017282	0.0425892	0.03274028	0.007457	0.018946	3.71E-05	0.011855534		

Table 4.5 continued

RMSE5									0.044176
MAE5									1.6725

Table 4.6 Statistical-Dynamical Major hurricanes regression coefficients, pval, SE, model RMSE, and model MAE

Predictor	**DMSLP**	**DTKD**	**DVWS**	**DMH**	**MDROLR**	**SOI**	**EPO**	**SFI**	**Basin**	**Full model**
Beta	0	0	0	0	0.15619	0.795465	-1.475721	0.001251		
Pvalue	0.6102	0.666843	0.433681	0.710585	0.00737	0.000141	0.000217	0.011392		
SE	0.33624	0.637253	0.256683	0.116139	0.046629	0.133663	0.261955	0.000404		
RMSE										0.6645
MAE										0.8845
Beta5	0	-0.280009	-0.129487	0	0	0	-0.189192	0		
Pvalue5	0.53327	0.011511	0.008285	0.149472	0.353917	0.159910	0.000889	0.533025		
SE5	0.05229	0.092504	0.040321	0.018446	0.007922	0.023665	0.041971	8.82E-05		
RMSE5										0.1210
MAE5										0.953
Beta6	0	-0.130671	-0.060427	0	0	0	-0.088289	0		
Pvalue6	0.53327	0.011511	0.008285	0.149472	0.353917	0.159910	0.000889	0.533025		
SE6	0.02440	0.043168	0.018816	0.008608	0.003697	0.011043	0.019586	4.11E-05		
RMSE6										0.0565
MAE6										0.9524
Beta7	0	-0.075387	-0.034862	0	0	0	-0.050936	0		
Pvalue7	0.53327	0.011511	0.008285	0.149472	0.353917	0.159910	0.000889	0.533025		
SE7	0.01408	0.024905	0.010855	0.004966	0.002133	0.006371	0.011299	2.37E-05		
RMSE7										0.0326
MAE7										0.9524

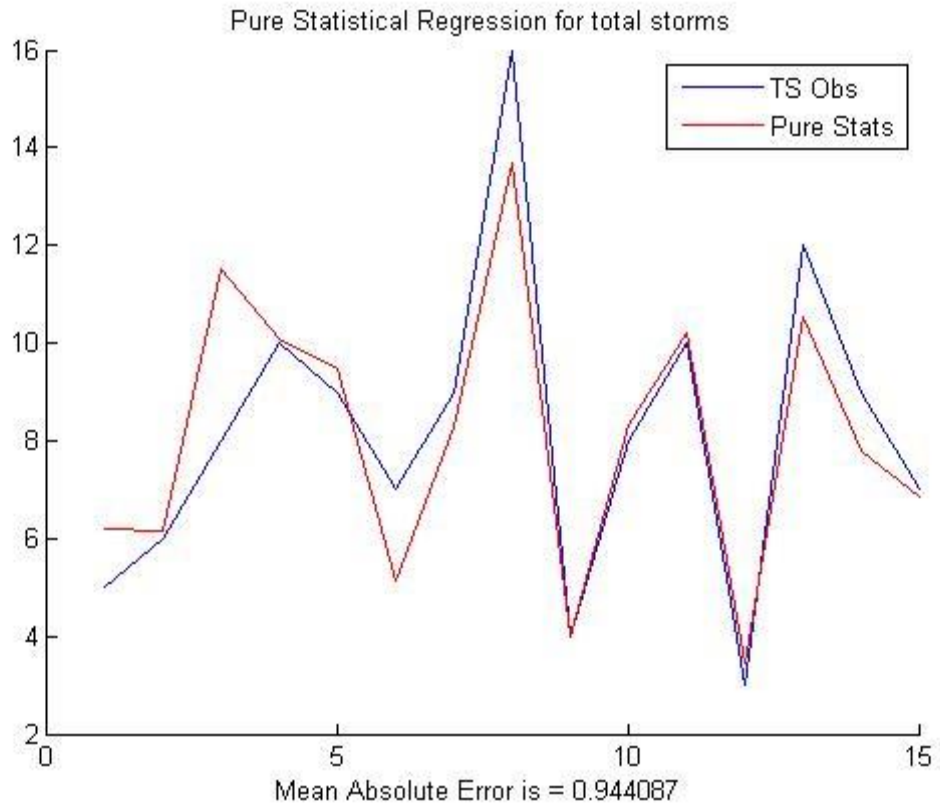

Figure 4.1 Pure statistical model total storm numbers and MAE

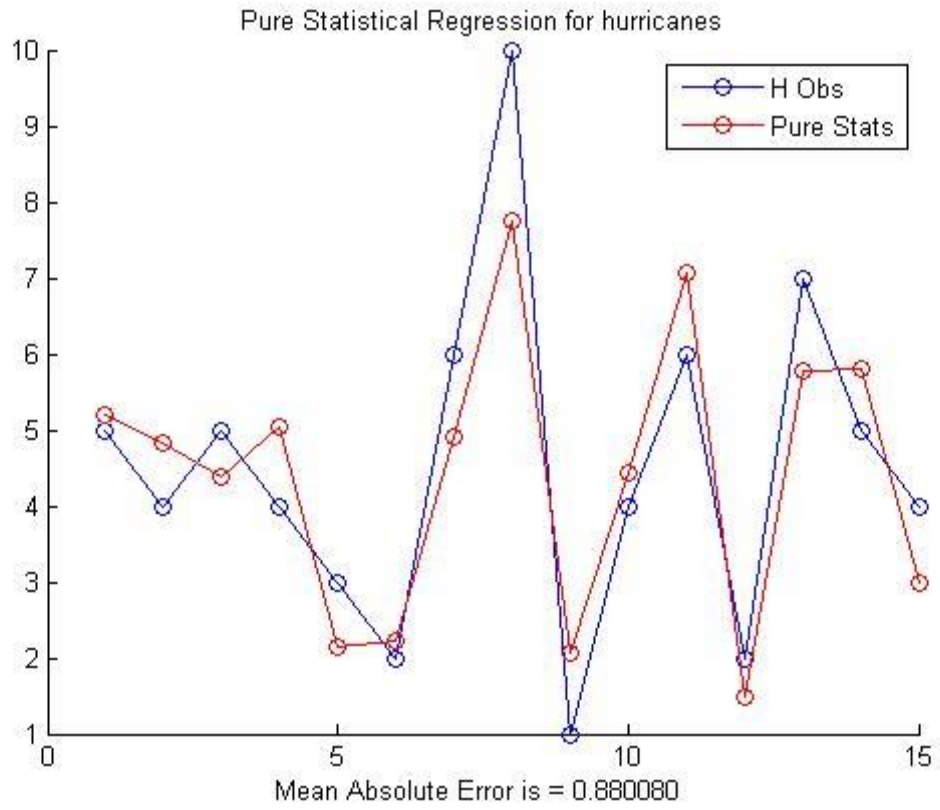

Figure 4.2 Pure statistical model hurricane numbers and MAE

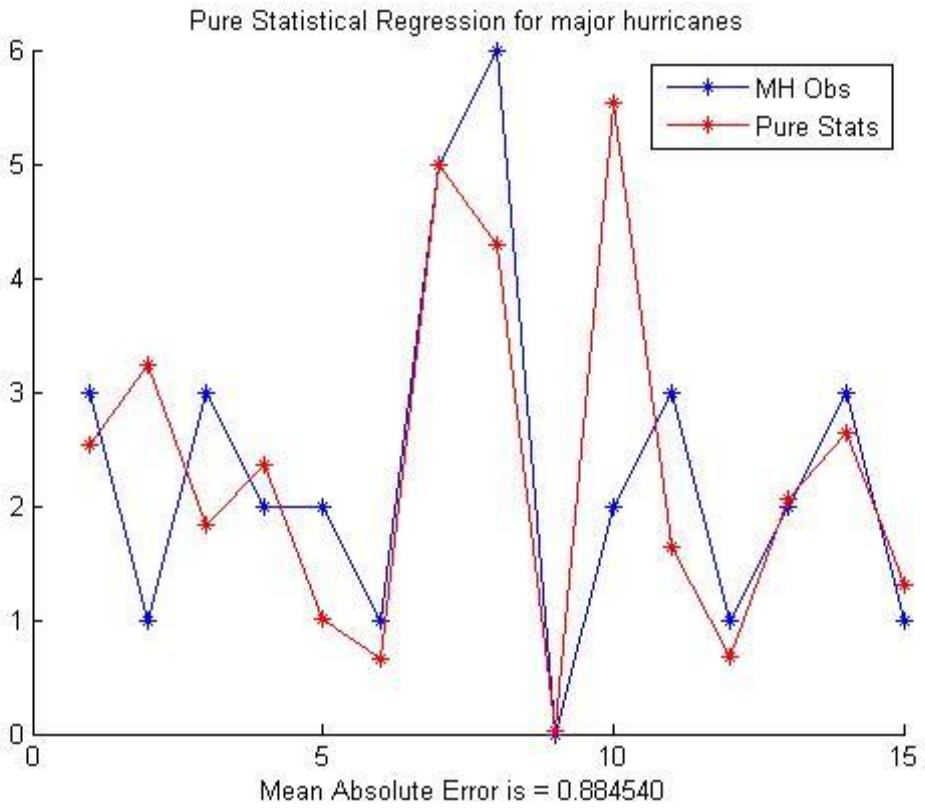

Figure 4.3 Pure Statistical model major hurricane numbers and MAE

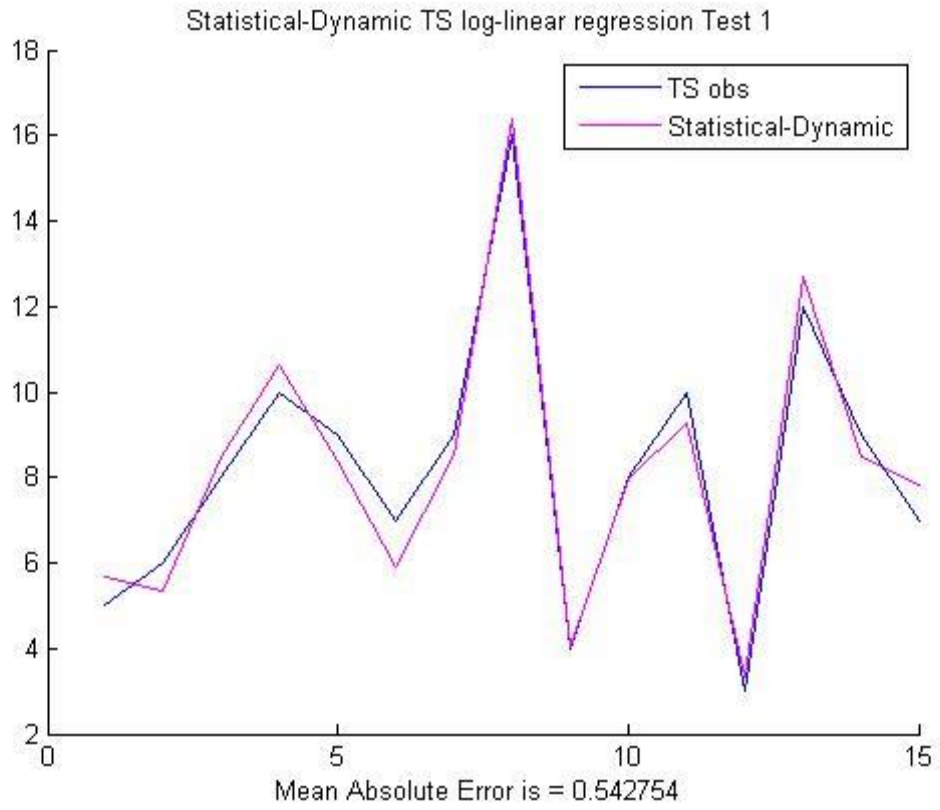

Figure 4.4 Statistical and Dynamical total storm regression test 1 and MAE

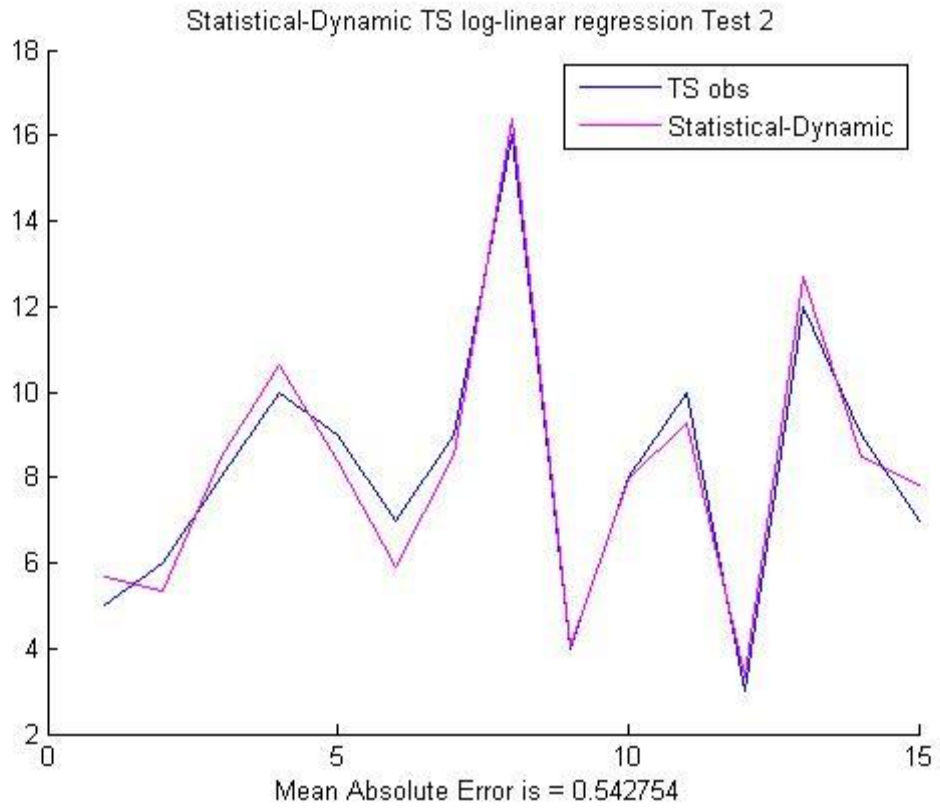

Figure 4.5 Statistical and Dynamical total storm regression test 2 and MAE

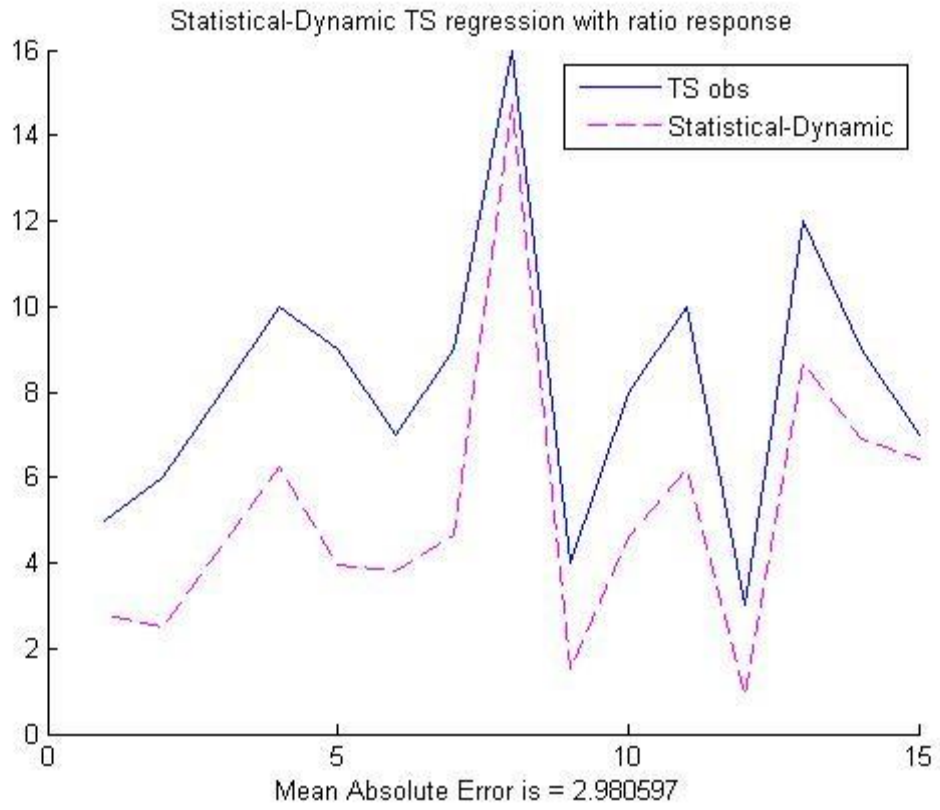

Figure 4.6 Statistical and Dynamical total storm regression ratio response and MAE

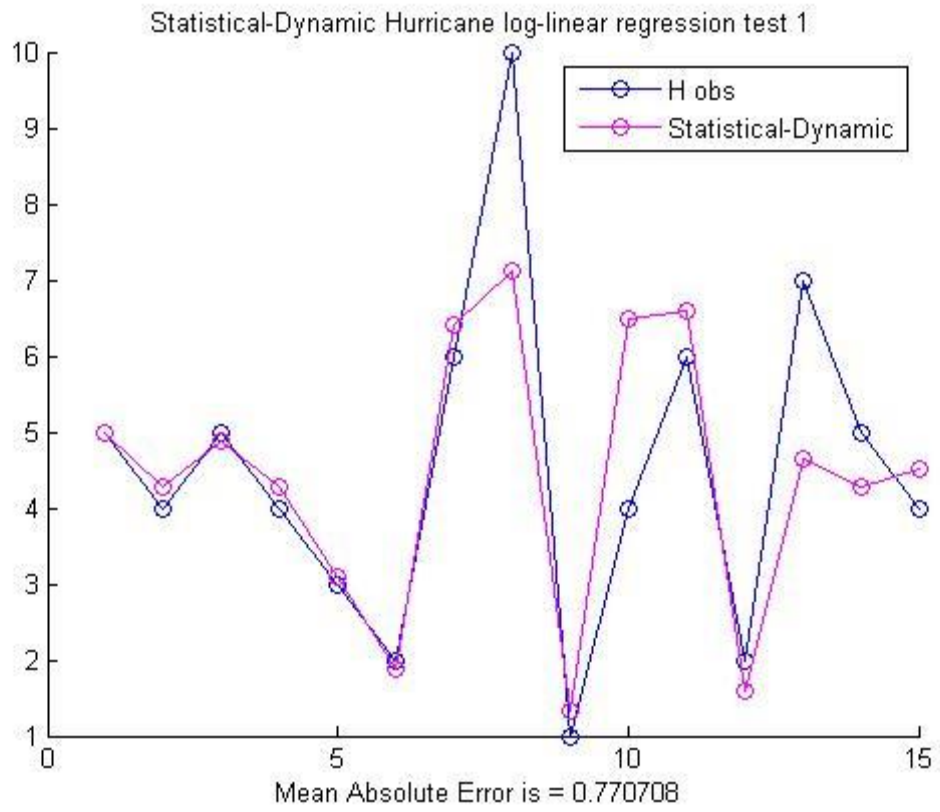

Figure 4.7 Statistical and Dynamical hurricane regression test 1 and MAE

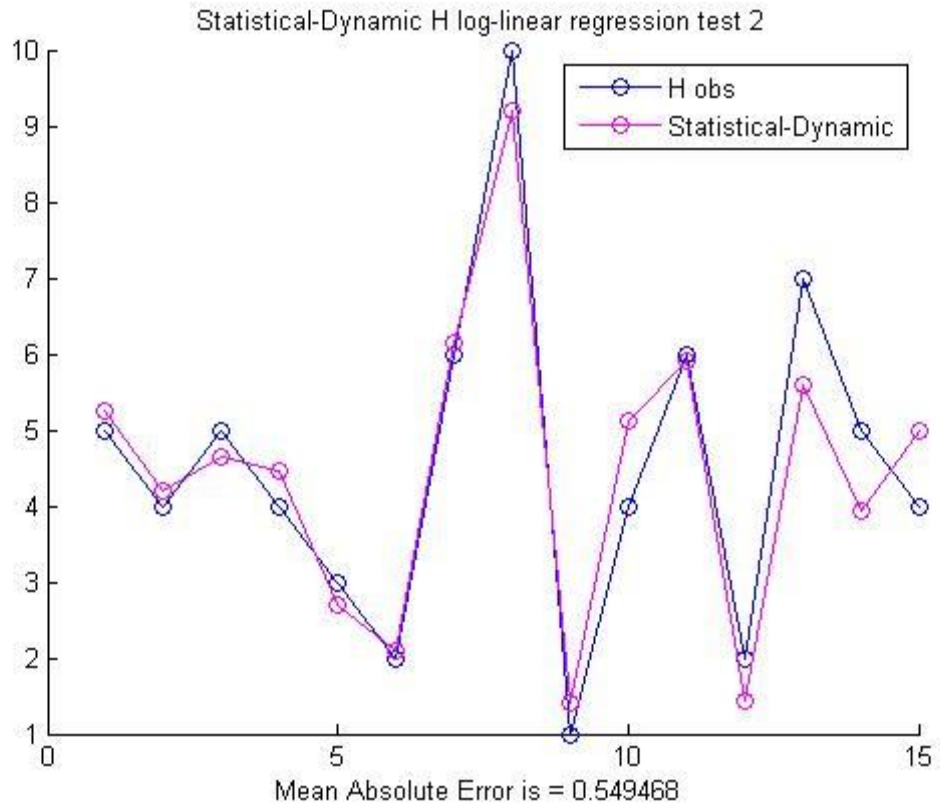

Figure 4.8 Statistical and Dynamical hurricane regression test 2 and MAE

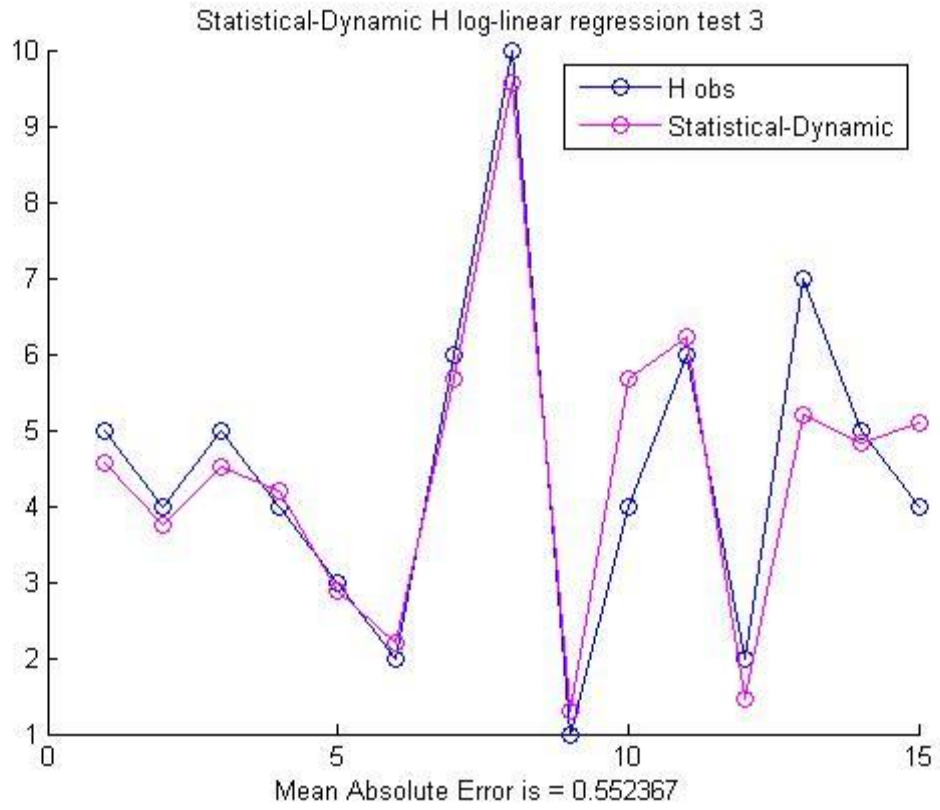

Figure 4.9 Statistical and Dynamical hurricane regression test 3 and MAE

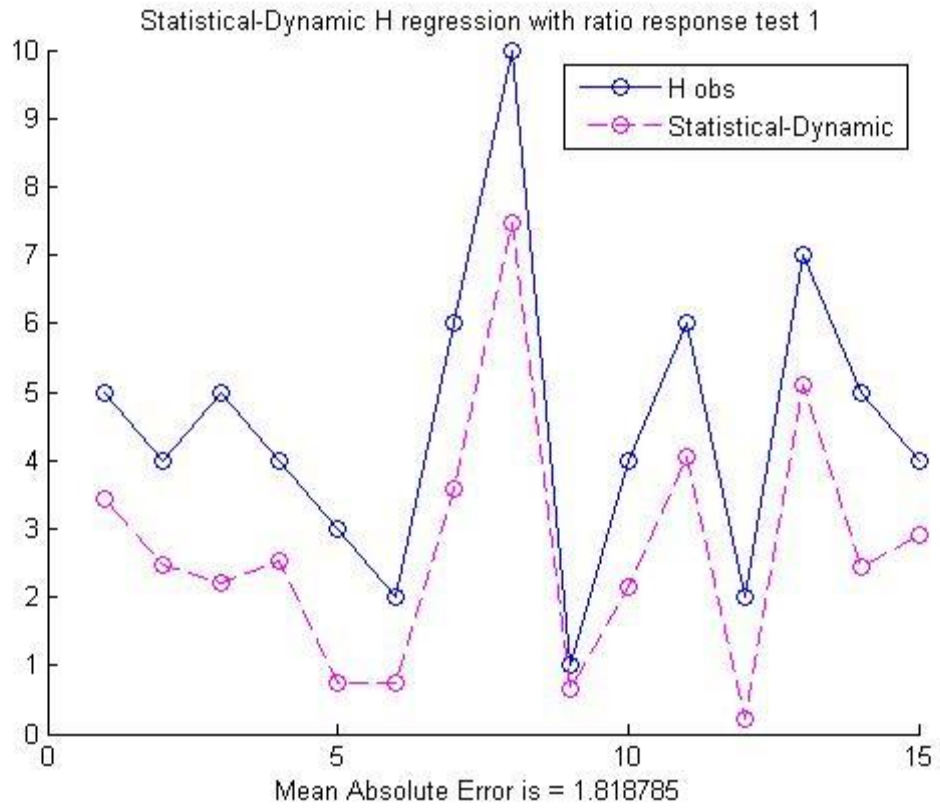

Figure 4.10 Statistical and Dynamical hurricane regression ratio response test 1 and MAE

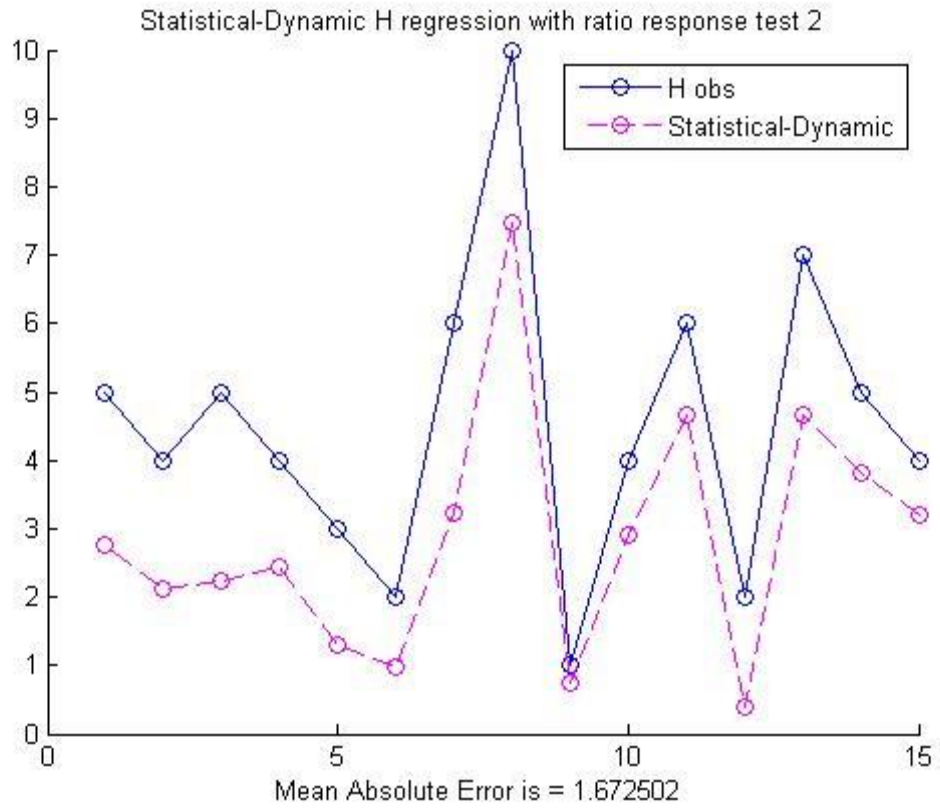

Figure 4.11 Statistical and Dynamical hurricane regression ratio response test 2 and MAE

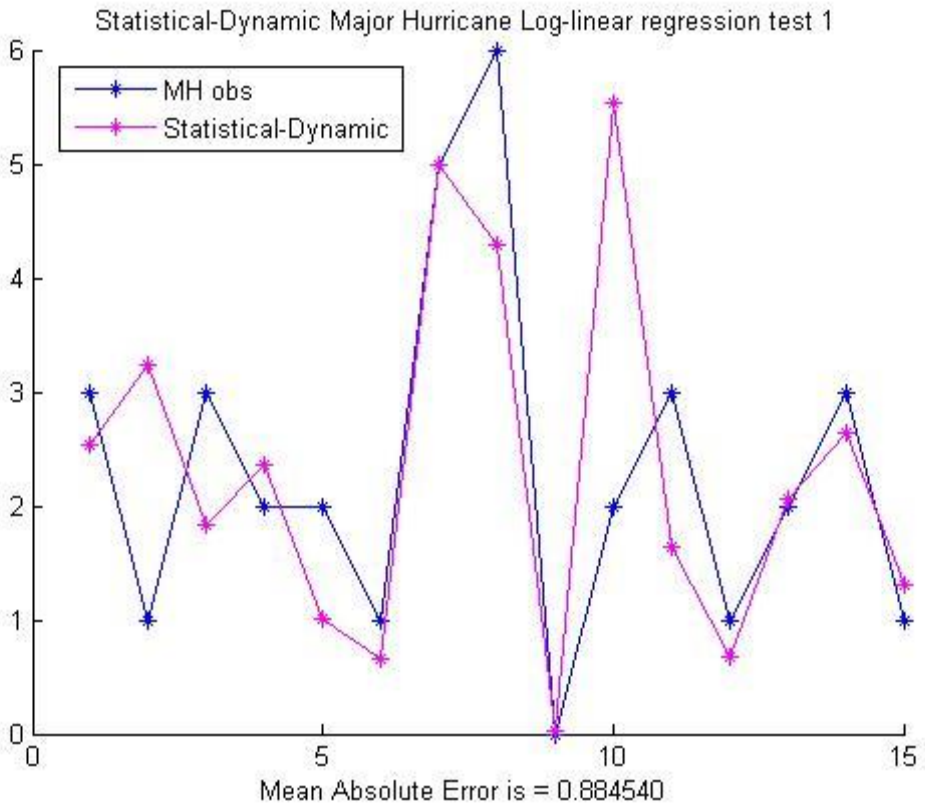

Figure 4.12 Statistical and Dynamical major hurricane regression test 1 and MAE

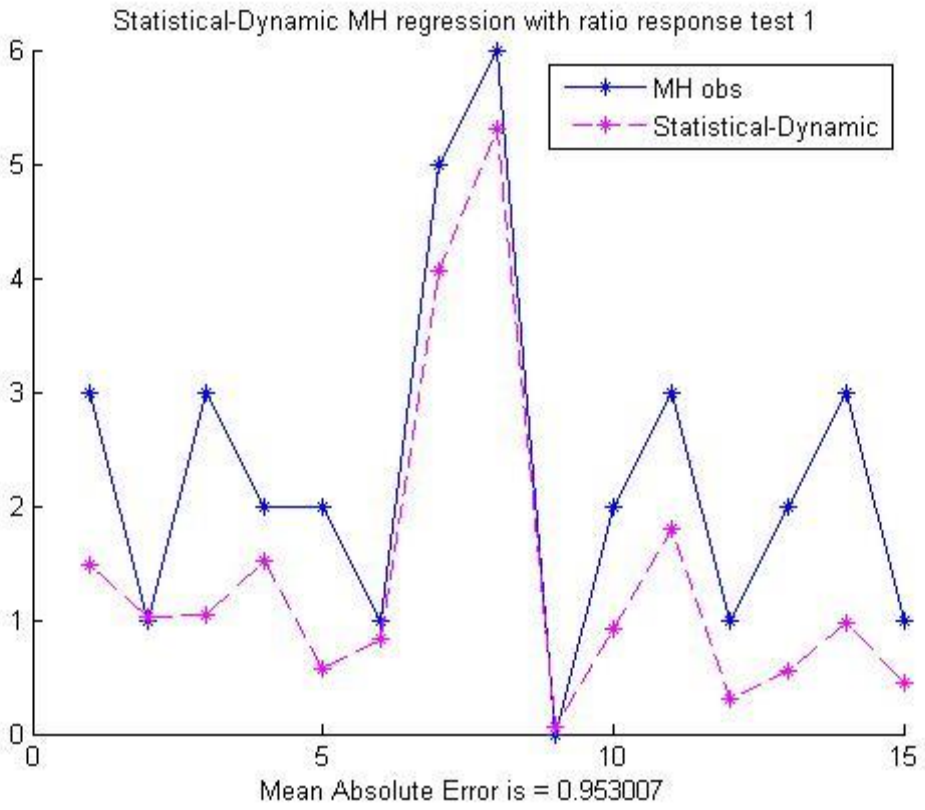

Figure 4.13 Statistical and Dynamical major hurricane regression ratio response test 1 and MAE

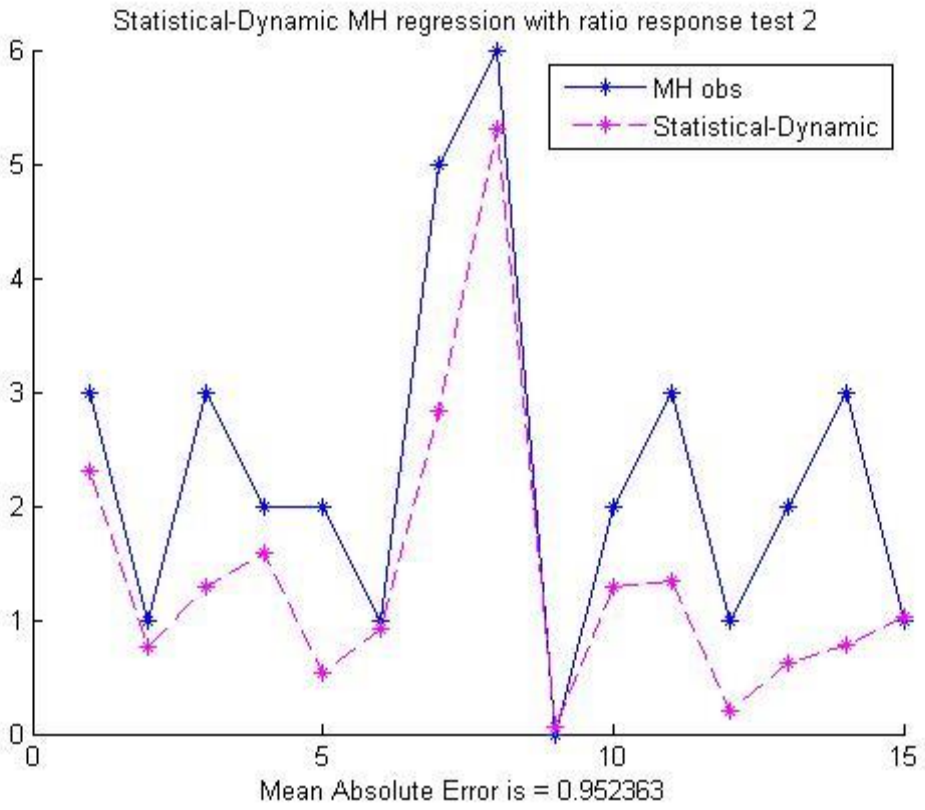

Figure 4.14 Statistical and Dynamical major hurricane regression ratio response test 2 and MAE

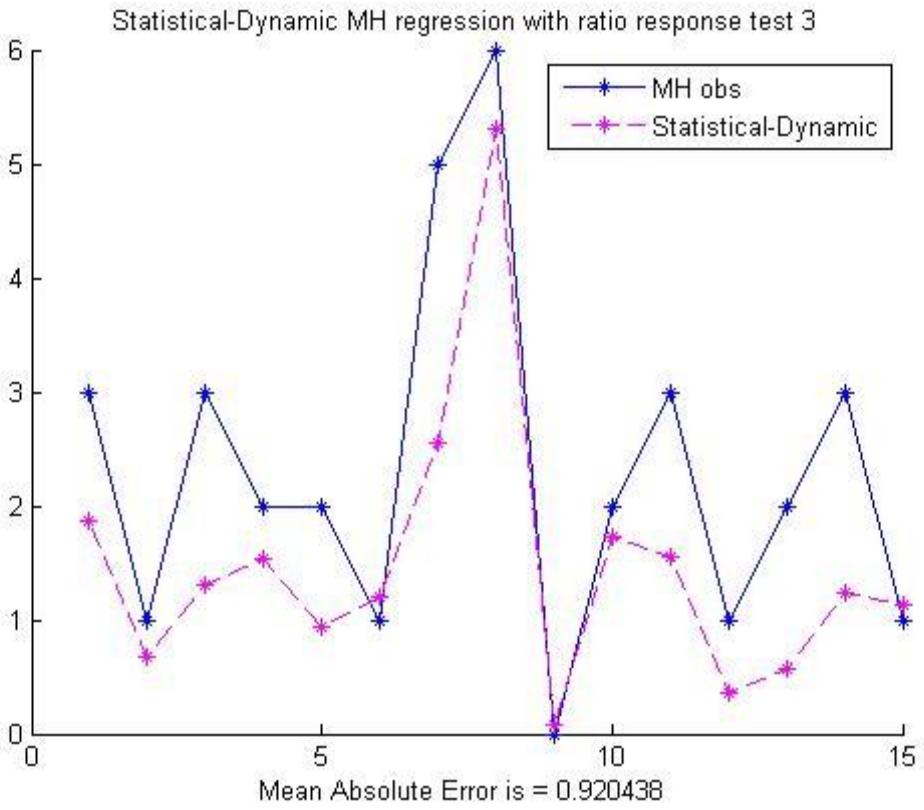

Figure 4.15 Statistical and Dynamical major hurricane regression ratio response test 3 and MAE

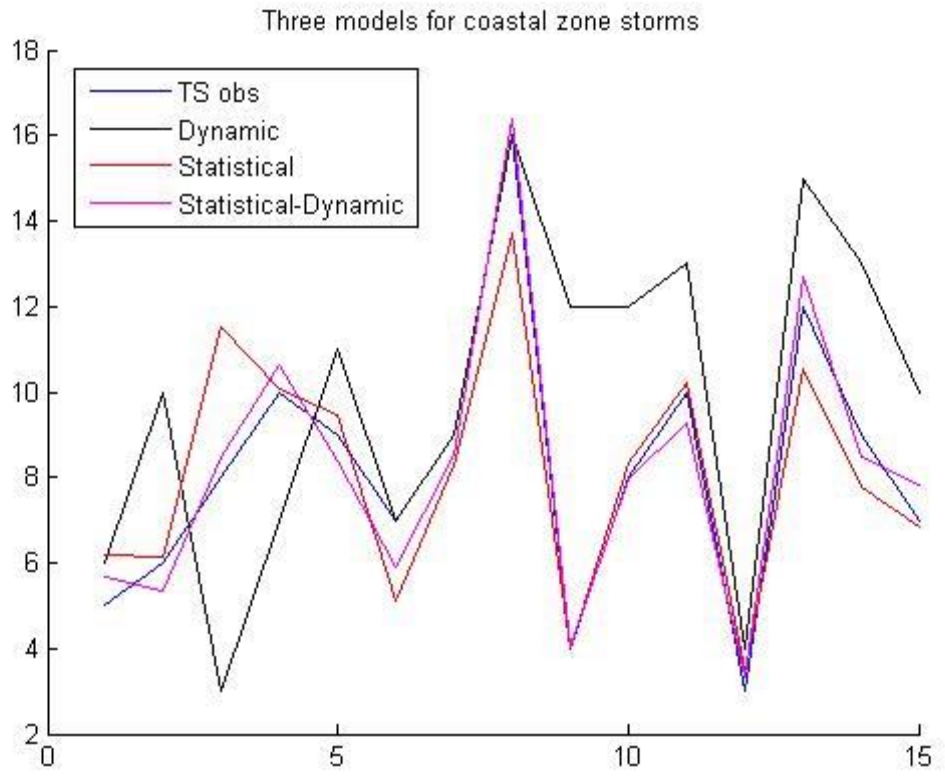

Figure 4.16 Model output comparison for total storm counts, between SSDA LEOB (dynamical model), purely statistical model, and statistical-dynamical model

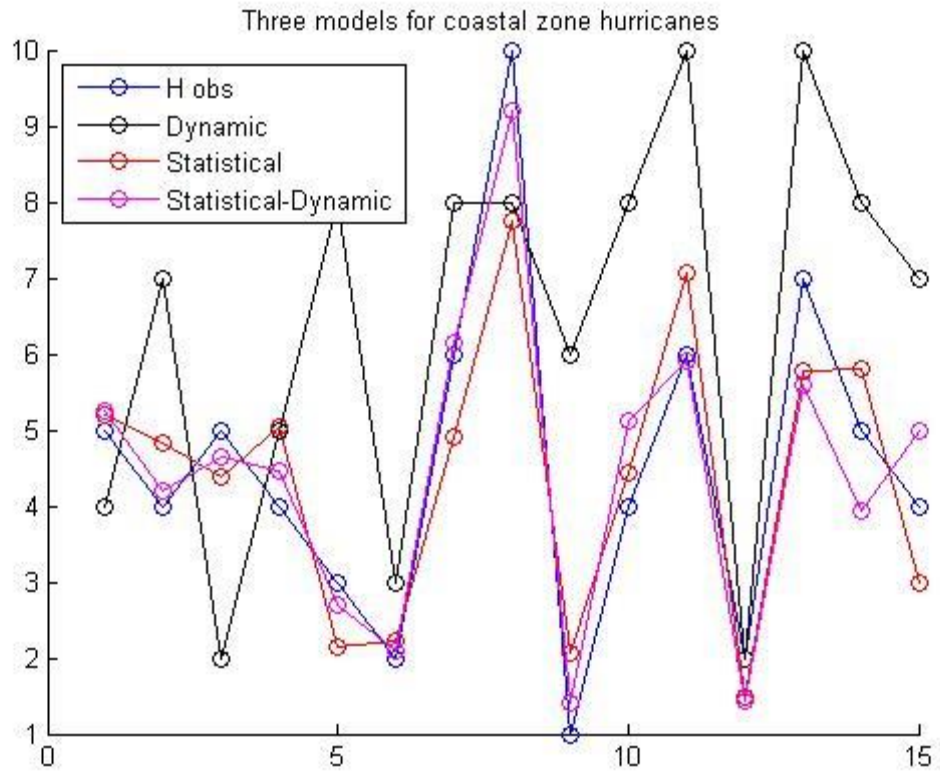

Figure 4.17 Model output comparison for hurricane counts, between SSDA LEOB (dynamical model), purely statistical model, and statistical-dynamical model

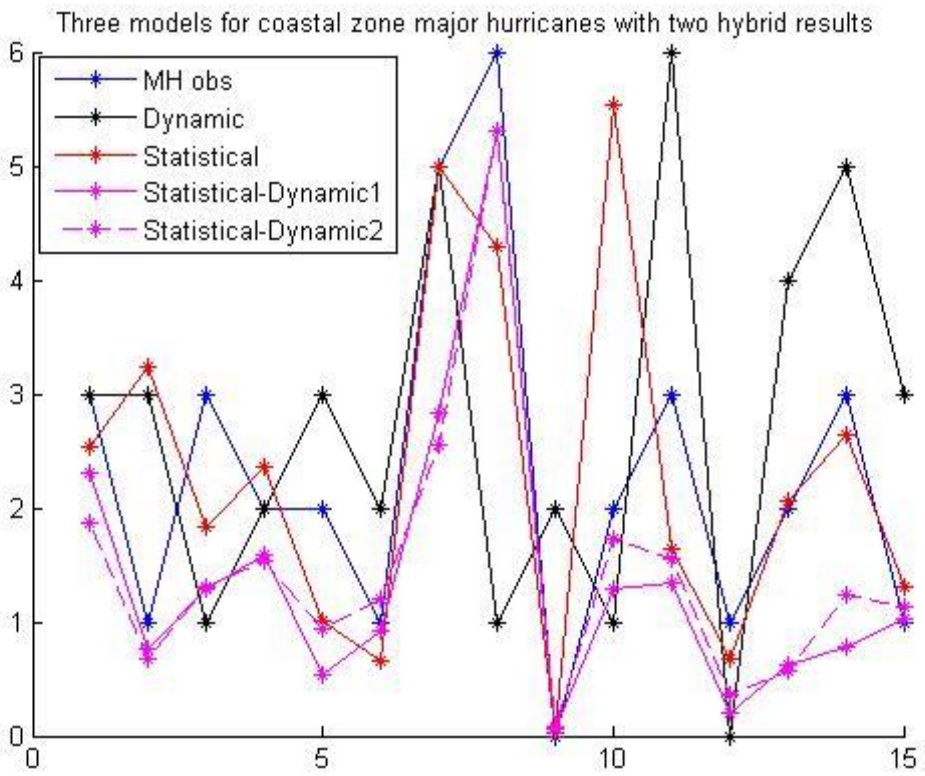

Figure 4.18 Model output comparison for major hurricane counts, between SSDA LEOB (dynamical model), purely statistical model, and statistical-dynamical model (ratio response) test2, and statistical-dynamical model (ratio response) test3

Chapter 5: Conclusions

5.1 Overview

Hurricanes affect the Southeast coastal region of the United States more than any other part of the US, and coastal populations are set to increase. Improving the downscaling of hurricanes through hindcasting is consequently vital to improve hurricane forecasting. Dynamical downscaling of hurricanes allows more realistic intensities to develop. The statistical forecasting of hurricanes is limited to using climatic factors for the entire basin. Combining these two methods will improve the accuracy of both to model hurricanes. The statistical regression improves the dynamical downscaled intensity, and the dynamical data adds new knowledge to the statistical model that directly relates to hurricane activity. Statistical-dynamical downscaling of tropical cyclones is a relatively new field of research, with little focus on coastal zones. Focusing on the coastal zones for improved hurricane seasonal activity simulations can be applied to allow both the coastal population to better prepare for upcoming seasons and policy makers to budget for potential damages.

5.2 Overall conclusions

First, 15 years of global data is dynamically downscaled to a 12 km horizontal grid spacing coastal domain and put through a tropical cyclone detection and tracking algorithm. The number of storms and hurricanes detected with the first set of criteria has high error caused by the criteria values only having been tested for the most active year of simulation.

Many combinations of criteria are tested, and a map of error is used to find the set with the lowest error. This criteria still does not produce an accurate amount of hurricanes or major hurricanes. This may be due to biases in the dynamical model, or because 12km grid spacing may still be too coarse. The wind speed and central sea level pressure data for the detected storms are corrected for intensity by matching the 5^{th} and 95^{th} percentiles to the observed 5^{th} and 95^{th} percentiles. Once this is done, the wind speed and sea level pressure are also corrected through Atkinson and Holliday (1997) wind-pressure relationship. These new values match the observed extent of maxima wind and minima pressure, but not the full spread seen in the observations. The number of hurricanes is improved by the intensity correction, but the trend in the number of major hurricanes still needs improvement.

The dynamical tropical cyclone data is further improved through statistical regression. First, statistical regression is conducted only for observed climate predictors. To choose the correct combination of predictors, 768 combinations are tested using backwards stepwise technique for total storm, hurricane, and major hurricane numbers separately. The predictors that are included the most are run through stepwise technique again, to narrow down the predictors for use in combined statistical–dynamical regression tests and to create a purely statistical log-linear regression for comparison. Three, five, and seven predictor-response combinations are tested for total storm, hurricane, and major hurricane regressions respectively. These combinations included the predictors used in the statistical models and created from the dynamical data, along with response variables representing the natural log of the coastal number and the ratio of coastal numbers to full basin numbers. Each of these

tests, through backward stepwise technique, removed the improved dynamically detected storm, hurricane, and major hurricane number, showing the dynamical model simulated number of storms, hurricanes, and major hurricanes are not skillful. The best statistical-dynamical total storm model uses log-linear regression with the upper level warm anomaly from the dynamical model (DTKD), the northern hemispheric surface temperature anomaly (NGST), the sea level pressure in the Main Development Region (MDRSLP), Southern Oscillation Index (SOI), and Pacific/North American index (PNA) as predictors. The best statistical-dynamical hurricane model uses log-linear regression with mean sea level pressure from the dynamical model (DMSLP), Eastern Pacific Oscillation index (EPO), and the total observed hurricane numbers in the North Atlantic (TH) as the predictors. These two models are more skillful than the dynamical model and the statistical model for total storm and hurricane numbers. Two major hurricane statistical-dynamical models have the same mean absolute error, but they do not outperform the purely statistical model. However, the difference in error between these two types of major hurricane models is not large. To get a better representation of the statistical-dynamical downscaling of total storm, hurricane, and especially major hurricane frequency skills, more work needs to be done to expand the data set.

5.3 Future work

To improve upon this study, several things need to be done. The difference between the CFSR analysis data and the CFSR 6 hour forecast data should be calculated to find any

systematic errors that may have been introduced into the model. The same should be done for GFS final analysis and the CFSR data to analyze any discontinuity within the data used. More dynamical model bias detection and correction should be conducted to find why the error for some years of simulation is greater than others. A track and cyclone size analysis with landfall could be produced with the results of this thesis to produce more landfall risk analysis with extent of damage. To add statistical significance, the years of dynamical downscaling should extended back to 1980. Residual tests and other statistical tests need to be applied to the statistical models created in this thesis. Adding to the array of dynamical variables to test as predictors would improve the statistical-dynamical model ability to represent both types of model. With these results, future climate projections can be conducted using Global Climate Model dynamical output as predictors.

REFERENCES

Atkinson, G. D., and C. R. Holliday, 1977: Tropical cyclone minimum sea level pressure/maximum sustained wind relationship for the western North Pacific. *Mon. Wea. Rev.*, **105,** 421–427. doi:10.1175/1520-0493(1977)105<0421:TCMSLP>2.0.CO;2

Bengtsson, L., M. Botzet, and M. Esch, 1996: Will greenhouse gas-induced warming over the next 50 years lead to higher frequency and greater intensity of hurricanes? Tellus Series A-Dynamic Meteorology and Oceanography, 48, 57-73, doi:10.1034/j.1600-0870.1996.00004.x.

Bengtsson, L., K. Hodges, and E. Roeckner, 2006: Storm tracks and climate change. J.Clim., 19, 3518-3543, doi:10.1175/JCLI3815.1.

Bengtsson, L., K. I. Hodges, M. Esch, N. Keenlyside, L. Kornblueh, J. Luo, and T. Yamagata, 2007: How may tropical cyclones change in a warmer climate? Tellus Series A-Dynamic Meteorology and Oceanography, 59, 539-561, doi:10.1111/j.1600-0870.2007.00251.x.

Camargo, S. J., S. E. Zebiak, 2002: Improving the Detection and Tracking of Tropical Cyclones in Atmospheric General Circulation Models. Wea. Forecasting, 17, 1152-1153, doi:http://dx.doi.org/10.1175/1520-0434(2002)017<1152:ITDATO>2.0.CO;2.

Camargo, S.J., H. Li, and L. Sun, 2007. Feasibility study for downscaling seasonal tropical cyclone activity using the NCEP Regional Spectral Model. *International Journal of Climatology*, 27, 311-325. doi: 10.1002/joc.1400

Caron, L. P., C. G. Jones, and K. Winger, 2011: Impact of resolution and downscaling technique in simulating recent Atlantic tropical cyclone activity. Clim. Dyn. 37:869-892 DOI:10.1007/s00382-010-0846-7

Castro, C. L., R. A. Pielke Sr., and G. Leoncini (2005), Dynamical downscaling: Assessment of value retained and added using the Regional Atmospheric Modeling System (RAMS), J. Geophys. Res., 110, D05108, doi:10.1029/2004JD004721.

Chen, J., Zhang, X. J. and Brissette, F. P. (2014), Assessing scale effects for statistically downscaling precipitation with GPCC model. Int. J. Climatol., 34: 708–727. doi: 10.1002/joc.3717

Elsner, J. B., J. P. Kossin, and T. H. Jagger, 2008: The increasing intensity of the strongest tropical cyclones. Nature, 455, 92-95, doi:10.1038/nature07234.

Elsner, J. B., G. Villarini, 2011: Statistical models for tropical cyclone activity. (myweb.fsu.edu/jelsner/PDF/SMTCA.pdf)

Emanuel, K., 1987: The Dependence of Hurricane Intensity on Climate. Nature, 326, 483-485, doi:10.1038/326483a0.

Emanuel, K., 2006: Climate and Tropical Cyclone Activity: A New Model Downscaling Approach. *J. Climate*, **19**, 4797–4802. doi:10.1175/JCLI3908.1

Feser, F., H. von Storch, 2008: A dynamical downscaling case study for typhoons in SE Asia using a regional climate model. Mon. Wea. Rev., 136, 1806-1815. doi:10.1175/2007MWR2207.1

Ghosh, S. K., 2007: Approaches to Model Output Statistics (MOS). Client: MESO Inc. Project3: Construct different approaches to model output statistics (MOS) (June-August, 2007). Statistical consulting.

Goldenberg, S., C. Landsea, A. Mestas-Nunez, and W. Gray, 2001: The recent increase in Atlantic hurricane activity: Causes and implications. Science, 293, 474-479, doi:10.1126/science.1060040.

Gombos, Daniel, Ross N. Hoffman, James A. Hansen, 2012: Ensemble Statistics for Diagnosing Dynamics: Tropical Cyclone Track Forecast Sensitivities Revealed by Ensemble Regression. *Mon. Wea. Rev.*, **140**, 2647–2669. doi: http://dx.doi.org/10.1175/MWR-D-11-00002.1

Gray, W., 1968: Global View of Origin of Tropical Disturbances and Storms. Mon.Weather Rev., 96, 669-&, doi:10.1175/1520-0493(1968)096<0669:GVOTOO>2.0.CO;2.

Gray, W., C. Landsea, P. Mielke, and K. Berry, 1992: Predicting Atlantic Seasonal Hurricane Activity 6-11 Months in Advance. Weather and Forecasting, 7, 440-455, doi:10.1175/1520-0434(1992)007<0440:PASHAM>2.0.CO;2.

Henderson-Sellers, A., H. Zhang, G. Berz, K. Emanuel, W. Gray, C. Landsea, G. Holland, J. Lighthill, S-L. Shieh, P. Webster, and K. McGuffie, 1998: Tropical Cyclones and Global Climate Change: A Post-IPCC Assessment. Bull. Amer. Meteor. Soc., 79, 19-38, doi:http://dx.doi.org/10.1175/1520-0477(1998)079<0019:TCAGCC>2.0.CO;2.

Hoyos, C., P. Agudelo, P. Webster, and J. Curry, 2006: Deconvolution of the factors contributing to the increase in global hurricane intensity. Science, 312, 94-97, doi:10.1126/science.1123560.

Kishtawal, C. M., N. Jaiswal, R. Singh, and D. Niyogi, 2012: Tropical cyclone intensification trends during satellite era (1986-2010). Geophys.Res.Lett., 39, L10810, doi:10.1029/2012GL051700.

Klotzbach, P., W. Gray, 2008: Multidecadal variability in North Atlantic tropical cyclone activity. J.Clim., 21, 3929-3935, doi:10.1175/2008JCLI2162.1.

Knutson, T., R. Tuleya, and Y. Kurihara, 1998: Simulated increase of hurricane intensities in a CO2-warmed climate. Science, 279, 1018-1020, doi:10.1126/science.279.5353.1018.

Knutson, T. R., R. E. Tuleya, 1999: Increased hurricane intensities with CO2-induced warming as simulated using the GFDL hurricane prediction system. Clim.Dyn., 15, 503-519, doi:10.1007/s003820050296.

Knutson, T. R., J. J. Sirutis, S. T. Garner, I. M. Held, and R. E. Tuleya, 2007: Simulation of the Recent Multidecadal Increase of Atlantic Hurricane Activity Using an 18-km-Grid Regional Model. BAMS, , 1549-1550-1565, doi:DOI:10.1175/BAMS-88-10-1549.

Knutson, T. R., J. L. McBride, J. Chan, K. Emanuel, G. Holland, C. Landsea, I. Held, J. P. Kossin, A. K. Srivastava, and M. Sugi, 2010: Tropical cyclones and climate change. Nat.Geosci., 3, 157-163, doi:10.1038/NGEO779.

Landsea, C., R. Pielke, A. Mestas-Nunez, and J. Knaff, 1999: Atlantic basin hurricanes: Indices of climatic changes. Clim.Change, 42, 89-129, doi:10.1023/A:1005416332322.

Larow, T., Y. Lim, D. Shin, E. Chassignet, and S. Cocke, 2008: Atlantic basin seasonal hurricane simulations. J.Clim., 21, 3191-3206, doi:10.1175/2007JCLI2036.1.

LaRow, T., H. Wang, and I-S. Kang, 2013: Seasonal Forecasting of Tropical Cyclones. http://www.usclivar.org/working-groups/hurricane/science/seasonal_forecasting_of_tropical_cyclones

Li, X., S. Yang, H. Wang, X. Jia, and A. Kumar, 2013: A dynamical-statistical forecast model for the annual frequency of western Pacific tropical cyclones based on the NCEP Climate Forecast System version 2. J. Geophys. Res. Atmos., 118, 12,061–12,074, doi:10.1002/2013JD020708.

Lee, S., Y. Cheng, 2011: An examination of ENSO's effect on the monthly and seasonal climate of Hong Kong from a statistical perspective. Acta Meteorologica Sinica, 25, 1, 34-50, doi:10.1007/ s13351-011-0003-1

Muller, R., G. Stone, 2001: A climatology of tropical storm and hurricane strikes to enhance vulnerability prediction for the southeast US coast. J.Coast.Res., 17, 949-956. doi:http://www.jstor.org/stable/4300254

National Centers for Environmental Prediction/National Weather Service/NOAA/U.S. Department of Commerce, 2000: NCEP FNL Operational Model Global Tropospheric Analyses, continuing from July 1999. Research Data Archive at the National Center for Atmospheric Research, Computational and Information Systems Laboratory, Boulder, CO. [Available online at http://rda.ucar.edu/datasets/ds083.2.] Accessed 13 12 2013

Oouchi, K., J. Yoshimura, H. Yoshimura, R. Mizuta, S. Kusunoki, and A. Noda, 2006: Tropical cyclone climatology in a global-warming climate as simulated in a 20 km-mesh global atmospheric model: Frequency and wind intensity analyses. J.Meteorol.Soc.Jpn., 84, 259-276, doi:10.2151/jmsj.84.259.

Peng, S., L. Xie, B. Liu, and F. Semazzi, 2010: Application of Scale-Selective Data Assimilation to Regional Climate Modeling and Prediction. Mon.Weather Rev., 138, 1307-1318, doi:10.1175/2009MWR2974.1.

Peilke Jr, R., C. Landsea, 1998: Normalized Hurricane Damages in the United States: 1925-95. Wea. Forecasting, 13, 621-631, doi:http://dx.doi.org/10.1175/1520-0434(1998)013<0621:NHDITU>2.0.CO;2.

Pielke, R., C. Landsea, M. Mayfield, J. Laver, and R. Pasch, 2005: Hurricanes and global warming. Bull.Am.Meteorol.Soc., 86, 1571-1571, doi:10.1175/BAMS-86-11-1571.

Saha, S., et al. 2010. *NCEP Climate Forecast System Reanalysis (CFSR) 6-hourly Products, January 1979 to December 2010*. Research Data Archive at the National Center for Atmospheric Research, Computational and Information Systems Laboratory. http://dx.doi.org/10.5065/D69K487J. Accessed[§] 07 MAR 2014.

Saha, S., and coauthors, 2010. The *NCEP Climate Forecast System Reanalysis.* Bull. Amer. Meteor. Soc. 91, 1015.1057. doi: 10.1175/2010BAMS3001.1

Skamarock, W. C., J. B. Klemp, 2008: A time-split nonhydrostatic atmospheric model for weather research and forecasting applications. Journal of Computational Physics, 227, 3465-3485, doi:http://dx.doi.org/10.1016/j.jcp.2007.01.037.

Sugi, M., A. Noda, H. Murakami, and J. Yoshimura (2009), A reduction in global tropical cyclone frequency due to global warming, SOLA, 5, 164–167, doi:10.2151/sola.2009-042.

Villarini, G., G. Vecchi, T. Knutson, M. Zhao, and J. Smith, 2011: North Atlantic Tropical Storm Frequency Response to Anthropogenic Forcing: Projections and Sources of Uncertainty. J.Clim., 24, 3224-3238, doi:10.1175/2011JCLI3853.1.

Villarini, G., G. Vecchi, and J. Smith, 2010: Modeling the Dependence of Tropical Storm Counts in the North Atlantic Basin on Climate Indices. Mon.Weather Rev., 138, 2681-2705, doi:10.1175/2010MWR3315.1.

Vitart, F., T. N. Stockdale, 2001: Seasonal Forecasting of Tropical Storms Using Coupled GCM Integrations. Mon. Wea. Rev., 129, 2521-2522-2537, doi:http://dx.doi.org/10.1175/1520-0493(2001)129<2521:SFOTSU>2.0.CO;2.

Walsh, K., M. Fiorino, C. Landsea and K. McInnes, 2007: Objectively-determined resolution-dependent threshold criteria for the detection of tropical cyclones in climate models and reanalyses. Journal of Climate, 20, 2307-2314. doi: 10.1175/JCLI4074.1

Wang, C., H. Liu, S-K. Lee, and R. Atlas, 2011: Impact of the Atlantic warm pool on United States landfalling hurricanes. Geophys.Res.Lett., 38, doi:10.1029/2011GL049265.

Wang, C. and S-K. Lee, 2008: Global warming and United States landfalling hurricanes. Geophys.Res.Lett., 35, L02708, doi:10.1029/2007GL032396.

Weinkle, J., R. Maue, and R. Pielke Jr., 2012: Historical Global Tropical Cyclone Landfalls. J.Clim., 25, 4729-4735, doi:10.1175/JCLI-D-11-00719.1.

Xie, L., B. Liu, and S. Peng, 2010: Application of scale-selective data assimilation to tropical cyclone track simulation. Journal of Geophysical Research-Atmospheres, 115, D17105, doi:10.1029/2009JD013471.

Xie, L., L. J. Pietrafesa, and K. Wu, 2002: Interannual and decadal variability of landfalling tropical cyclones in the southeast coastal states of the united states. Adv.Atmos.Sci., 19, 677-686, doi:10.1007/s00376-002-0007-y.

Xu, Z., Z-L. Yang, 2012: An Improved Dynamical Downscaling Method with GCM Bias Corrections and Its Validation with 30 Years of Climate Simulations. *J. Climate,* **25**, 6271–6286. doi: http://dx.doi.org/10.1175/JCLI-D-12-00005.1

Zandbergen, P. A., 2009: Exposure of US counties to Atlantic tropical storms and hurricanes, 1851-2003. Nat.Hazards, 48, 83-99, doi:10.1007/s11069-008-9250-6.

Zhang, S., M. Zhao, S.-J. Lin, X. Yang, and W. Anderson (2014), Retrieval of tropical cyclone statistics with a high-resolution coupled model and data, Geophys. Res. Lett., 41, 652–660, doi:10.1002/2013GL058879.

Zhao, M., I. M. Held, S.-J. Lin, and G. A. Vecchi, 2009: Simulations of global hurricane climatology, interannual variability and response to global warming using a 50 km resolution gcm. J. Climate, 22, 6653-6678, doi: 10.1175/2009JCLI3049.1